

## A.6 CRITICALITY EVALUATION

The Advanced NUHOMS<sup>®</sup> System is designed to meet 10CFR 72.124 [A6.1] criticality safety limits during worst case wet loading/unloading operations with the use of fixed neutron absorbing materials (poisons) in the flooded Dry Shielded Canister (24PT4-DSC). The design assures criticality safety under all normal, off-normal and accident conditions associated with wet fuel loading/unloading, transfer and storage.

The results of the detailed analyses demonstrate that the Advanced NUHOMS<sup>®</sup> System is criticality safe under normal, off-normal and accident conditions considering a variety of mechanical uncertainties.

The bounding criticality model used in the analysis is a fully flooded 24PT4-DSC loaded into a flooded (fresh water) NUHOMS<sup>®</sup> OS197H Transfer Cask (TC). No burnup is credited in this evaluation, thus misloading with fresh fuel is bounded.

Specular boundary conditions are specified on all four sides of a square enveloping the outer cask diameter. This provides for an infinite array of OS197H casks. The AHSM storage configuration is bounded by this configuration. The canister is dry under all conditions of storage. The reactivity of this system is highly dependent on the internal moderator (fresh water) density, with the maximum reactivity occurring at maximum internal moderator density. All actual conditions of loading and unloading are bounded because an infinite array of flooded casks is more reactive than a single dry or flooded 24PT4-DSC and cask.

For all Hypothetical Accident Condition (HAC) cases, the TC neutron shield and neutron shield panel is assumed to be stripped away and replaced within water.

Boral<sup>®</sup> areal density credited is 75% of the specified design density.

Two alternate options for the poison rodlets are evaluated. For the borated stainless steel rod option, with 1.75 wt. % boron, 100% credit is taken in the criticality analysis. For the alternate option of a stainless steel tube filled with B<sub>4</sub>C with a minimum required linear B<sub>4</sub>C content of 0.70 g/cm, 64% credit is taken in the criticality analysis.

## A.6.1 Discussion and Results

Criticality control in the 24PT4-DSC is provided by the basket structural components that maintain the relative position of the spent fuel assemblies under all normal and accident conditions and by fixed neutron absorbing materials. The fixed neutron absorbers are present in the form of Boral<sup>®</sup> plates provided around the DSC guidesleeves and poison rodlets which are inserted in the guide tubes of certain assemblies in the basket. The structural analysis of the basket is presented in Chapter A.3.

The 24PT4-DSC is designed to ensure nuclear criticality safety during worst case wet loading operations. There is no credible scenario for fresh water inleakage in the 24PT4-DSC during transfer or storage. However, the wet loading scenario, assuming fresh water (unborated) in the 24PT4-DSC is used to envelope all storage and transfer scenarios. A high integrity confinement boundary tested to demonstrate it is leaktight per ANSI N14.5 [A6.11] is provided to exclude the possibility of flooding the 24PT4-DSC cavity during the transfer operations and storage period. Prior to these operations, the 24PT4-DSC is vacuum dried, backfilled with helium, double seal welded, and helium leak tested to assure weld integrity.

Spent fuel loading configurations and the spent fuel parameters are discussed in Section A.6.2. Computer models of the 24PT4-DSC are discussed in Section A.6.3. The criticality evaluation is presented in Section A.6.4. The 24PT4-DSC was evaluated for the following conditions that bound normal conditions and the accident conditions listed in Chapter A.11:

- varied water density including flooding of the basket, with fresh water (water density evaluated includes steam which may be generated during loading and unloading operations),
- variations in material tolerances,
- variations in fuel assembly position in guidesleeves,
- fresh water in the fuel pellet – clad annulus, and
- postulated failures for damaged fuel payloads.

The various effects are evaluated individually, and are combined as required to demonstrate compliance with the requirement of 10CFR 72.124 that "before a criticality accident is possible, at least two unlikely, independent, and concurrent or sequential changes have occurred in the conditions essential to nuclear criticality safety."

The criticality analyses are performed using the CSAS25 (KENO V.a) module of SCALE 4.4 PC [A6.3] using the 44-group ENDF/B-V cross-section library. A series of benchmark calculations were performed with the SCALE 4.4 PC/CSAS25 [A6.3] package using the 44-group cross-section library as presented in Section A.6.5. The minimum value of the Upper Subcritical Limit (USL) is determined to be 0.9411.

The results of the limiting criticality configurations are summarized in Table A.6.1-1.

**Table A.6.1-1**  
**Summary of Limiting Criticality Evaluations<sup>(1)</sup> for the CE 16x16 Fuel Assembly**

| <b>.025 g/cm<sup>2</sup> <sup>10</sup>B Configuration</b>  | <b>Maximum Initial Enrichment <sup>235</sup>U</b>   | <b>K<sub>KENO</sub></b> | <b>σ</b> | <b>K<sub>eff</sub></b> | <b>USL</b> |
|--|---|-------------------------|----------|------------------------|------------|
| 0.025 g/cm <sup>2</sup> <sup>10</sup> B, 24 intact assemblies  | 4.10 wt. %  | 0.9361                  | 0.0011   | 0.9383                 | 0.9411     |
| 0.025 g/cm <sup>2</sup> <sup>10</sup> B, 4 damaged assemblies + 20 intact assemblies, no poison rodlets                            | 4.10 wt. %  | 0.9337                  | 0.0012   | 0.9361                 | 0.9411     |
| 0.025 g/cm <sup>2</sup> <sup>10</sup> B, 12 damaged assemblies + 12 intact assemblies, no poison rodlets                           | 3.70 wt. % damaged assys;<br>4.1 wt. % intact assys | 0.9369                  | 0.0012   | 0.9393                 | 0.9411     |
| 0.025 g/cm <sup>2</sup> <sup>10</sup> B, 12 damaged assemblies + 12 intact assemblies, 1 poison rodlet per undamaged fuel assembly | 4.10 wt. %  | 0.9315                  | 0.0013   | 0.9341                 | 0.9411     |

| <b>0.068 g/cm<sup>2</sup> <sup>10</sup>B Configuration</b>  | <b>Maximum Initial Enrichment <sup>235</sup>U</b>    | <b>K<sub>KENO</sub></b> | <b>σ</b> | <b>K<sub>eff</sub></b> | <b>USL</b> |
|---|--|-------------------------|----------|------------------------|------------|
| 0.068 g/cm <sup>2</sup> <sup>10</sup> B, 24 intact assemblies   | 4.85 wt. %   | 0.9365                  | 0.0012   | 0.9389                 | 0.9411     |
| 0.068 g/cm <sup>2</sup> <sup>10</sup> B, 4 damaged assemblies + 20 intact assemblies, no poison rodlets                             | 4.85 wt. %   | 0.9360                  | 0.0011   | 0.9382                 | 0.9411     |
| 0.068 g/cm <sup>2</sup> <sup>10</sup> B, 12 damaged assemblies + 12 intact assemblies, no poison rodlets                            | 4.10 wt. % damaged assys;<br>4.85 wt. % intact assys | 0.9367                  | 0.0012   | 0.9391                 | 0.9411     |
| 0.068 g/cm <sup>2</sup> <sup>10</sup> B, 12 damaged assemblies + 12 intact assemblies, 5 poison rodlets per undamaged fuel assembly | 4.85 wt. %   | 0.9354                  | 0.0012   | 0.9378                 | 0.9411     |

(1) See Figure A.6.4-13 for location of damaged fuel assemblies and poison rodlets within the 24PT4-DSC.

## A.6.2 Spent Fuel Loading

This section provides a summary of the maximum spent fuel loading and spent fuel parameters for the 24PT4-DSC. The allowable contents are listed in Chapter A.2 and in the Functional and Operating Limits of the Technical Specifications.

Each 24PT4-DSC is designed to accommodate up to 12 damaged fuel assemblies (see Section A.6.4.7) in lieu of intact assemblies. The required placement of the damaged fuel assemblies is in the twelve outermost fuel assembly locations as specified in Figure A.2.1-4 (Zones A and/or B only). Damaged fuel includes assemblies with known or suspected cladding defects greater than hairline cracks or pinhole leaks or an assembly with partial and/or missing rods (i.e., extra water holes). Damaged fuel assemblies shall be placed in failed fuel cans which will replace basket guidesleeves.

The fuel parameters used in the criticality calculations for CE 16x16 fuel assemblies are listed in Table A.6.2-1.

**Table A.6.2-1  
Fuel Parameters for Criticality Analysis of the CE 16x16 Fuel Assemblies**

|                                     |                                |
|-------------------------------------|--------------------------------|
| Maximum Initial Enrichment          | 4.85 weight % <sup>235</sup> U |
| Number of Rods                      | 236 fuel rods                  |
| Number of Guide Tubes               | 5 guide tubes                  |
| Fuel Rod Material (sintered pellet) | UO <sub>2</sub>                |
| Pellet Diameter (nominal, inches)   | 0.3255                         |
| Pellet Density (% theoretical)      | 97                             |
| Clad Material                       | Zircaloy-4                     |
| Clad OD (nominal, inches)           | 0.382                          |
|                                     |                                |
| Active Fuel Length (inches)         | 150                            |
| Rod Pitch (inches)                  | 0.506                          |
| Guide Tube ID (in)                  | 0.90                           |
| Guide Tube OD (in)                  | 0.98                           |

Design parameters for Boral<sup>®</sup> and poison rodlets are listed in Table A.6.3-2.

The KENO V.a model incorporates borated stainless steel (1.75 wt. % Boron) poison rodlets for storage of damaged fuel in specific configurations. An option is allowed to fabricate the poison rodlets from B<sub>4</sub>C filled thin wall stainless steel tubing incorporating an equivalent amount of <sup>10</sup>B. The equivalent linear B<sub>4</sub>C content per rodlet is calculated by:

- 1) The modeled boron density (1.75 wt. % x 7.60 g/cm<sup>3</sup>) of the borated stainless steel is multiplied by the cross sectional area of minimum borated steel rod (0.71875 inches OD) = 0.348 g/cm boron.
- 2) To convert to the B<sub>4</sub>C equivalent linear weight, divide by the boron weight fraction of B<sub>4</sub>C (0.7828) = 0.445 g/cm B<sub>4</sub>C.
- 3) Divide this result by 0.64 to account for 64% credit taken for the <sup>10</sup>B content in the criticality analysis.

This results in a minimum required linear B<sub>4</sub>C content of 0.70g/cm.

## A.6.3 Model Specification

### A.6.3.1 Description of Criticality Analysis Model

Criticality analyses were performed using the KENO V.a and the 44 neutron group library based on ENDF-B Version 5 cross-section data that are part of the SCALE 4.4 code package [A6.3]. Validation and benchmarking of these codes is discussed in Section A.6.5.

SCALE 4.4 [A6.3] is an extensive computer code package which has many applications, including cross section processing, criticality studies, and heat transfer analyses. The package is comprised of many functional modules, which can be run independently of each other. Control Modules were created to combine certain functional modules in order to make the input requirements less complex. For the purpose of criticality analysis, only four functional modules and one control module are used. These Modules are CSAS25, which includes the three dimensional criticality code KENO V.a and the preprocessing codes BONAMI-S, NITAWL-II and XSDRNPM-S.

KENO V.a, in conjunction with a suitable working library of nuclear cross section data, is used to calculate the multiplication factor,  $k_{\text{eff}}$ , of systems of fissile material. It can also compute lifetime and generation time, energy dependent leakages, energy and region-dependent absorptions, fissions, fluxes, and fission densities. KENO V.a utilizes a three-dimensional Monte-Carlo computation scheme. KENO V.a is capable of modeling complex geometries including facilities for handling arrays, arrays of arrays, and holes.

SCALE 4.4 is set up so that any number of cross-section libraries may be used with the preprocessing functional and control modules. For the purpose of this analysis, only the 44-group ENDF/B V library is used.

The preprocessing codes used for this analysis are the functional modules BONAMI-S, NITAWL-II and XSDRNPM-S. They are consolidated into the control module CSAS25. BONAMI-S has the function of performing Bondarenko calculations for resonance self-shielding. The cross sections and Bondarenko factor data are pulled from an AMPX master library. The output is placed into a master library as well. Dancoff approximations allow for different fuel lattice cell geometries. The main function of NITAWL-II is to change the format of the master cross-section libraries to one that the criticality code (KENO V.a) can access. It also provides the Nordheim Integral Treatment for resonance self-shielding. XSDRNPM-S provides cell-weighted cross sections based on the specified unit cell.

The criticality analysis, using the above computer codes, is performed in compliance with 10CFR 71 [A6.2] and bounds the 10CFR 72 [A6.1] requirements. Transportation regulations (10CFR 71) distinguish between "damaged" and "undamaged" packages. The undamaged condition is denoted "NOC" for Normal Operating Condition and the damaged condition is denoted "HAC" for Hypothetical Accident Condition. The conditions of a damaged package are established by tests that simulate the effects of a cask drop during handling, fire, extremes of summer heat, winter cold and rain. Specifically for criticality analysis, the HAC case eliminates the neutron shield and neutron shield panels and fills the space with moderator.

The KENO V.a model consists of 304 axial layers stacked into an array. The layers consist of partial spacer disk or partial moderator regions of various lengths along the active fuel region as shown in Figure A.6.3-1 and Figure A.6.3-2. The length of the active fuel is modeled as 150.12 inches but with specular boundary conditions applied it is considered as infinitely long. The 24PT4-DSC model contains 28 spacer disk regions, each 1.25 inches thick, surrounded by a total of 29 non-disk regions. The center to center spacing of the spacer disk intervals varies over a range from 4 inches to 5.63 inches. An infinite array of casks is created by specifying specular reflection on the  $\pm x$  and  $\pm y$  axis and is used for all cases.

Figure A.6.3-2 shows the KENO V.a model in an exploded view. UNIT 33 is a 0.25 inch slice through the cask at the 24PT4-DSC spacer disk level. UNIT 34 is a 0.25 inch slice through the moderator region between spacer disks. Units 35 and 36 are the same as UNIT 34 except the length of the slice is increased from 0.25 inches to 4.43 inches and 5.63 inches, respectively.

Figure A.6.3-3 shows the structure of the cask at the 24PT4-DSC spacer disk level (UNIT 33), while Figure A.6.3-4 highlights the structure of the cask at the moderator region between spacer disks (UNIT 34). Note that the difference between the two is that UNIT 33 has a spacer disk (steel surrounding fuel assemblies) and UNIT 34 has steel support rods in addition to water surrounding fuel assemblies. The fuel assemblies are identified in Figure A.6.3-3 and Figure A.6.3-4 by the position numbers (1-24) which are used to refer to their unique locations. UNIT numbers 1-8, 101-108, and 201-208 are used to represent the active fuel assemblies in both the spacer disk region and in the moderator region differing only in the UNIT heights. The fuel assemblies are inserted into the model using KENO's HOLE capability.

A detail of the guidesleeve and fuel assembly is shown in Figure A.6.3-5. The KENO V.a cases model the square tube, Boral<sup>®</sup> sheets (4 per tube for the inner fuel assembly locations and 2 per tube for the outer fuel assembly locations), and a stainless steel oversleeve wrapper, not shown, which holds the Boral<sup>®</sup> sheets in place. Note that the absorber sheets on the outer periphery of the basket (12 sheets total) are not needed due to neutron leakage through the cask walls.

The analyses performed are based on a completely flooded 24PT4-DSC. Slots are provided at the bottom of the guidesleeves and openings are provided at the bottom and sides (near the bottom) of the failed fuel cans to ensure uniform draining and filling of all areas of the 24PT4-DSC. The failed fuel can openings are screened to contain potentially loose pellets or debris.

The models developed are conservative. Major conservatisms in the models are:

- No cases have been made to model fission products, absorber materials (<sup>10</sup>B, Gadolinia or Erbia, etc.) in the burnable poison rods, or axial and radial variations in initial fuel enrichment. Instead, fuel assemblies have been modeled as if they were composed of only a single enrichment unirradiated fuel. This results in a very large margin of conservatism in the calculated  $k_{eff}$ .
- Only 75% credit for the boron in the Boral<sup>®</sup> panels is taken in the criticality evaluation.
- Poison rodlets are placed only in the intact assemblies located in Zone C of Figure A.2.1-4.

The major assumptions made in the calculations are:

- No credit is taken for soluble boron in the spent fuel pool. All moderation is assumed to be from pure water. No credit is taken for neutron absorption in water impurities.
- Omission of spacer grids, spacers, and hardware in the fuel assembly. This is conservative because this material results in parasitic neutron absorption and displaces moderating material reducing the fuel assembly  $k_{eff}$ .
- The maximum fuel pin enrichment is modeled as uniform everywhere throughout the assembly. Natural Uranium blankets, Erbia Rods, and axial or radial enrichment zones are modeled as fully enriched uranium. It is assumed that the fuel assemblies are of uniform enrichment everywhere. All fuel rods are assumed to be filled with 100% moderator in the fuel/cladding gap to account for the possibility of water being entrained in the fuel pin and because it has a slight positive effect on reactivity.
- The fuel assemblies are conservatively modeled as infinitely long.
- The fuel pellet stack density was conservatively modeled at 97% of theoretical density with no allowance for dishing and chamfer, although this assumption conservatively increases the total fuel content in the model.
- The burnable absorber rod material is modeled as pure  $(^{11}\text{B})_4\text{C}$  only. Modeling the poison as  $(^{11}\text{B})_4\text{C}$  is appropriate since the net effect is to substitute material with a very small thermal absorption cross section for the material, which in reality would contain  $^{10}\text{B}$  for a fresh fuel assembly. ( $^{11}\text{B} = 1.10000\text{E-}01$  atms/bn-cm and  $\text{C} = 2.75000\text{E-}02$  atms/bn-cm)
- The worst case position tolerance was assumed for all spacer disk cutout locations. This is achieved by utilizing the maximum tolerance on the spacer disk hole dimensions and minimum possible tolerance on the ligament widths. The ligament represents the steel region between spacer disk cutouts. This arrangement effectively moves all the guidesleeve assembly units further inwards thereby minimizing the inter-assembly separation distance. Further, the values utilized in the criticality models for fuel assembly placement are slightly lower than the actual positions bringing the fuel assemblies even closer together. This is the worst case condition for criticality since inter-assembly moderation is minimized, thereby reducing the effectiveness of the neutron absorber plates.
- The fuel is assumed to be intact with no gross damage or missing rods for the intact fuel analyses. Damaged and missing rods are addressed in the damaged fuel analyses.
- Reconstituted fuel assemblies are considered intact unless otherwise specified as damaged fuel assemblies.
- It is assumed for the criticality analyses for all Hypothetical Accident Condition (HAC) cases, the TC neutron shield and stainless steel neutron shield panels are stripped away and replaced with moderator.

- The least material condition (LMC) was assumed for the guidesleeves and wrappers. This minimizes neutron absorption in the steel sheets and poison plates. The “least material condition” means use of those feature dimensions that minimize the amount of material in the part.
- Both the bottom of the bottom spacer disk and the bottom of the guidesleeve and Boral<sup>®</sup> panel start at the same axial level. The fuel assembly is completely covered by the Boral<sup>®</sup> panels over the entire active fuel length for the intact fuel analyses.
- The Boral<sup>®</sup> material is modeled as Al/<sup>10</sup>B material sandwiched between two thin sheets of pure Al. The Aluminum in the poison material is assumed to have a theoretical density of 70%. This assumption is conservative, as less material leads to less neutron absorption, although aluminum is such a weak absorber that this assumption is within the uncertainty of the Monte Carlo method itself.

The following additional assumptions were made for the damaged fuel analyses:

- The worst case gross damage resulting from a cask-drop accident is assumed to be either a single-ended or double-ended rod shear with fresh water intrusion.
- The rod pitch is allowed to vary from its nominal fuel rod pitch.
- The single-ended fuel rod shear cases assume that sixteen fuel rods (one assembly face) shear in one place and are displaced to new locations. The fuel pellets are conservatively assumed to remain in the fuel rods. The possibility of fuel rods and/or rod fragments being lodged above or below the Boral<sup>®</sup> panel height is addressed in the damaged fuel analyses. This was addressed by considering a 16x16 array of bare fuel rods 5.25” long above the active fuel. Additional analyses of one row and two rows of rods displaced 6” above the Boral<sup>®</sup> panels were performed to address possible repositioning of the fuel during a drop. These results were bounded by the results of the optional pitch study with one row of rods missing.
- The double-ended fuel rod shear cases assume that sixteen fuel rods (one assembly face) shear in two places and the intact fuel rod pieces are separated from the parent fuel rods. The fuel pellets are conservatively assumed to remain in the fuel rods.
- The bounding case crediting poison rodlets was analyzed for a rodlet 2” shorter than the active fuel. This analysis resulted in a change in keff that was within the statistical uncertainty of the base case.

Table A.6.3-1 and Table A.6.3-2 summarize the 24PT4-DSC materials and dimensions that were assumed in these analyses.

The fuel parameters used in the criticality calculations for CE 16x16 Fuel Assemblies are listed in Table A.6.2-1. The assembly fuel pin loading pattern is given in Figure A.6.3-5. The analysis methodology and modeling provide an accurate representation of actual cask configurations with the exception of conservatisms employed and the use of conservative simplifying assumptions.

### A.6.3.2 Neutron Absorber Panel Material Efficacy

The absorber panel material used in the 24PT4-DSC was chosen due to its desirable neutron attenuation, low density, and minimal thickness. It has been used for applications and in environments comparable to those found in spent fuel storage and transportation since the early 1950s (the U.S. Atomic Energy Commission's AE-6 Water-Boiler Reactor). In the 1960s, it was used as a poison material to ship irradiated fuel rods from Canada's Chalk River laboratories to Savannah River. More than 12,000 British Nuclear Fuels, Ltd. (BNFL) flasks containing the material have been used to transport fuel to BNFL's reprocessing plant in Sellafield.

The neutron absorber panels are composed of boron carbide and 1100 alloy aluminum. Boron carbide provides the necessary content of the neutron absorbing  $^{10}\text{B}$  isotope in a chemically inert, heat resistant, highly crystalline and extremely hard form. Boron carbide contained in the panels does not react under these conditions. The boron carbide core is tightly held within an 1100 aluminum alloy matrix and further protected by solid 1100 aluminum alloy cladding plates. Although 1100 alloy aluminum is a chemically reactive material; it behaves much like an inert material when properly applied. Proper application includes due consideration to the formation of a highly protective aluminum oxide layer and allowance for creation of the reaction by-product hydrogen.

Aluminum reacts with water to produce hydrogen ( $\text{H}_2$ ) and an impervious tightly adhering layer of hydrated aluminum oxide ( $\text{Al}_2\text{O}_3 \cdot 3\text{H}_2\text{O}$ ) called bayerite which protects the surface from further attack.

When the 24PT4-DSC basket is initially submerged in the spent fuel pool, aluminum in the panels will react with water to form a small amount of hydrogen gas and a stable bayerite layer on all surfaces of the panel. The bayerite layer formed on the panel during pool immersion persists through 24PT4-DSC drying, sealing, storage, and eventual shipping, preventing further corrosion or hydrogen production.

Leaching of the boron carbide along the unsealed edges of the panels is expected to occur to an insignificant degree. There are three reasons why this is anticipated to be insignificant. First, the panel core is a sintered  $\text{Al}/\text{B}_4\text{C}$  material. Only the boron carbide particles exposed by saw cut are available for leaching. Second, the immersion environment is relatively benign and the time is brief (a few hours or days). The material has been commonly used in the United States spent fuel racks for many years and, in fact, has gained a reputation for not leaching. And third, direct experimental observations of accelerated aging tests performed at the University of Michigan [A6.10] showed no indications of boron degradation. The test specimens were exposed to high neutron and gamma irradiation in a reactor pool environment for over nine years. Subsequent neutron radiography showed no signs of reduced neutron attenuation anywhere on the test specimens.

Depletion of the  $^{10}\text{B}$  in the neutron poison plates is evaluated below. Although the license period of the cask is 20 years, actual storage time could be much longer. Using an estimated scalar flux of  $5.0 \times 10^5 \text{ n/cm}^2\text{-s}$  at the center of the basket, and the thermal neutron cross section for  $^{10}\text{B}$  of 3837 barn [A6.9], the fraction of the original  $^{10}\text{B}$  depleted after 1000 years would be:

$$5 \times 10^5 \text{ n/cm}^2\text{-s} \times (3837 \times 10^{-24} \text{ cm}^2) \times 3.156 \times 10^7 \text{ s/year} \times (1000 \text{ year}) = 1.1 \times 10^{-6}$$

which is negligible. Therefore, the continued efficacy of the neutron poison is assured.

**Table A.6.3-1  
Geometric Parameters Used in the Criticality Analysis**

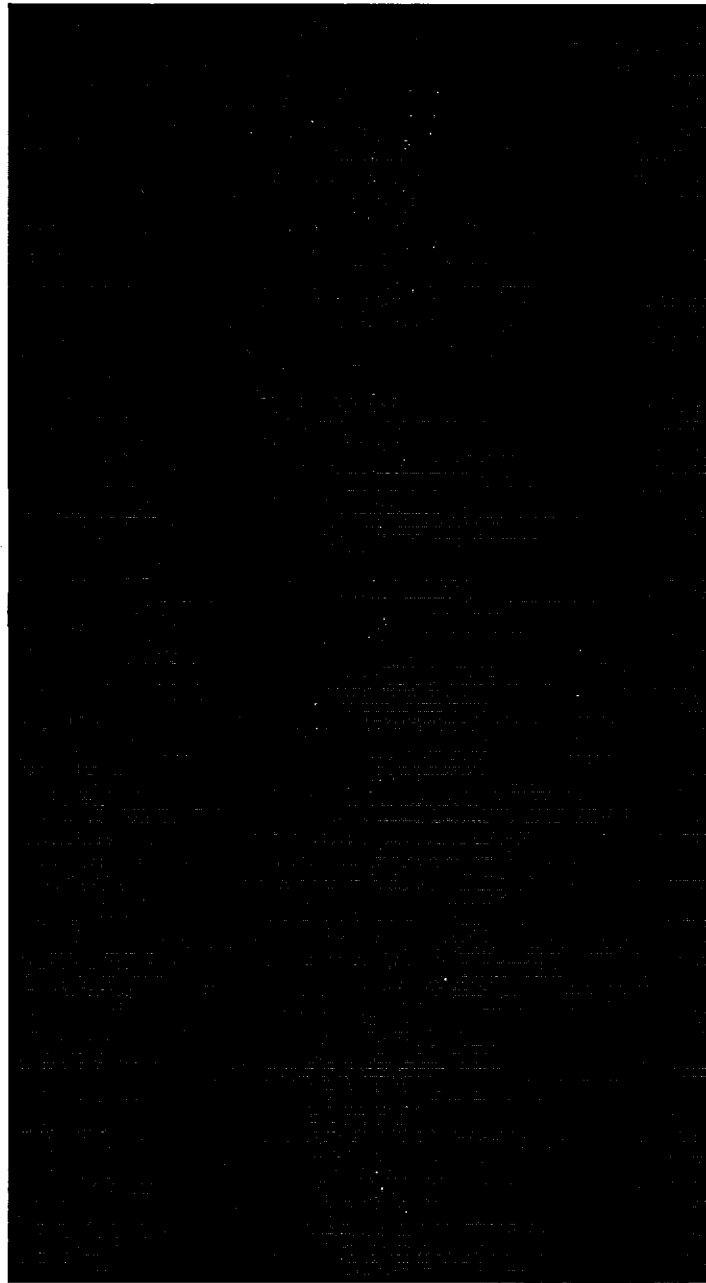


**Table A.6.3-1  
Geometric Parameters Used in the Criticality Analysis**

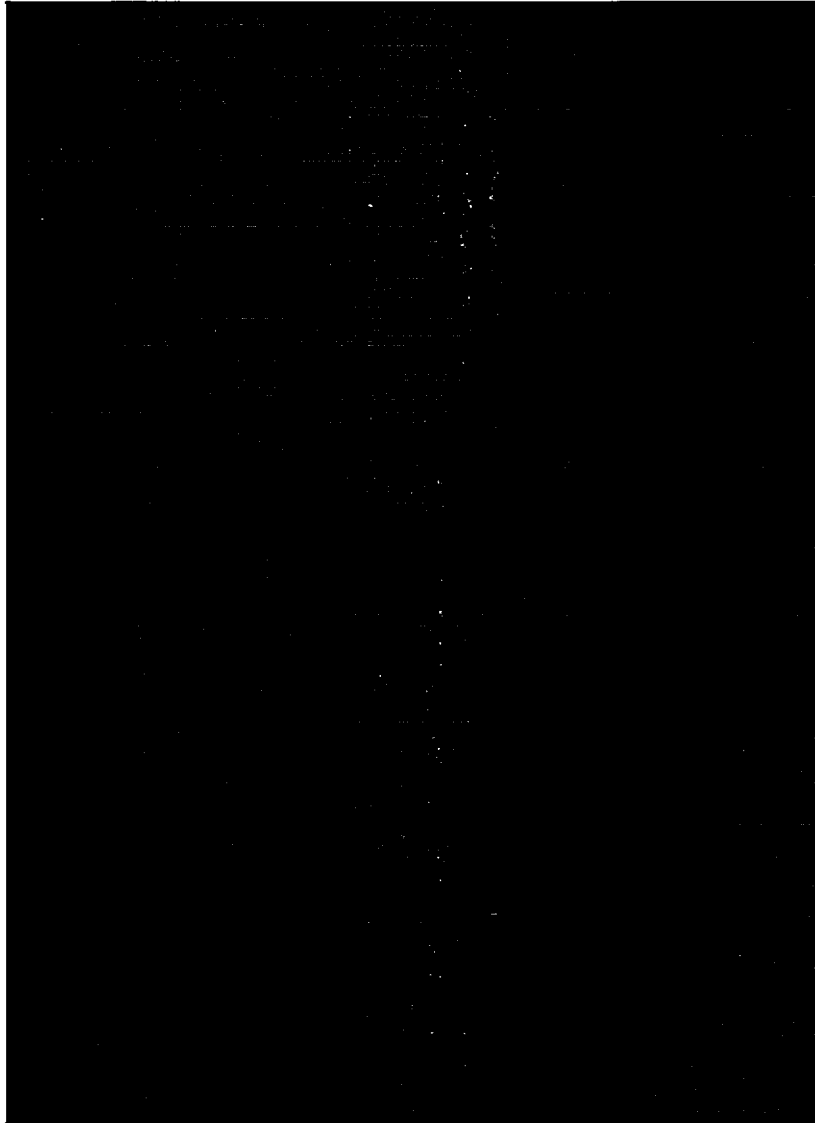


**Table A.6.3-1**  
**Geometric Parameters Used in the Criticality Analysis**



**Table A.6.3-2  
Design Parameters for Poison Material**

| <b>Boral<sup>®</sup> (75% <sup>10</sup>B) Material Density</b> |                                   |                        |
|--|-----------------------------------|------------------------|
| Aluminum   | 70% theoretical density           |                        |
| <sup>10</sup> B (0.068 g/cm <sup>2</sup> )                     | 0.092957 g/cm <sup>3</sup> (max)  |                        |
|  | 0.098425 g/cm <sup>3</sup> (min)  |                        |
|  | 0.095613 g/cm <sup>3</sup> (nom)  |                        |
| <sup>10</sup> B (0.025 g/cm <sup>2</sup> )                     | 0.034175 g/cm <sup>3</sup> (max)  |                        |
|  | 0.036186 g/cm <sup>3</sup> (min)  |                        |
|  | 0.0352152 g/cm <sup>3</sup> (nom) |                        |
| <b>Poison Rodlet Design Parameters</b>                         |                                   |                        |
| <b>Borated Stainless Steel Rod</b>                             |                                   |                        |
| Material Density   | 7.60 g/cm <sup>3</sup>            |                        |
| Composition (By Weight)  | SS304 (98.25%)                    |                        |
|  | Boron (1.75%)                     |                        |
| Rodlet Outer Diameter  | 0.78125 inches (max)              |                        |
|  | 0.71875 inches (min)              |                        |
|  | 0.75000 inches (nom)              |                        |
| Rodlet Length  | 171 inches                        |                        |
| <b>B<sub>4</sub>C Filled Stainless Steel Tube</b>              |                                   |                        |
| Tube   | OD                                | 0.750 ± .005           |
|  | Wall thickness                    | 0.035 ± .002           |
| Material Density   | Tube                              | 7.60 g/cm <sup>3</sup> |
|  | B <sub>4</sub> C                  | 0.70 g/cm              |
| Rodlet length  | 171 inches                        |                        |

EACH MODERATOR REGION  
BETWEEN SPACER DISCS  
IS MODELED AS A STACK  
OF UNITS 34, 35, OR 36  
AS APPROPRIATE TO MODEL  
EACH REGION

EACH SPACER DISC IS MODELED  
AS A STACK OF 5 - 0.25" THICK  
UNIT 33's

28 SPACER DISCS

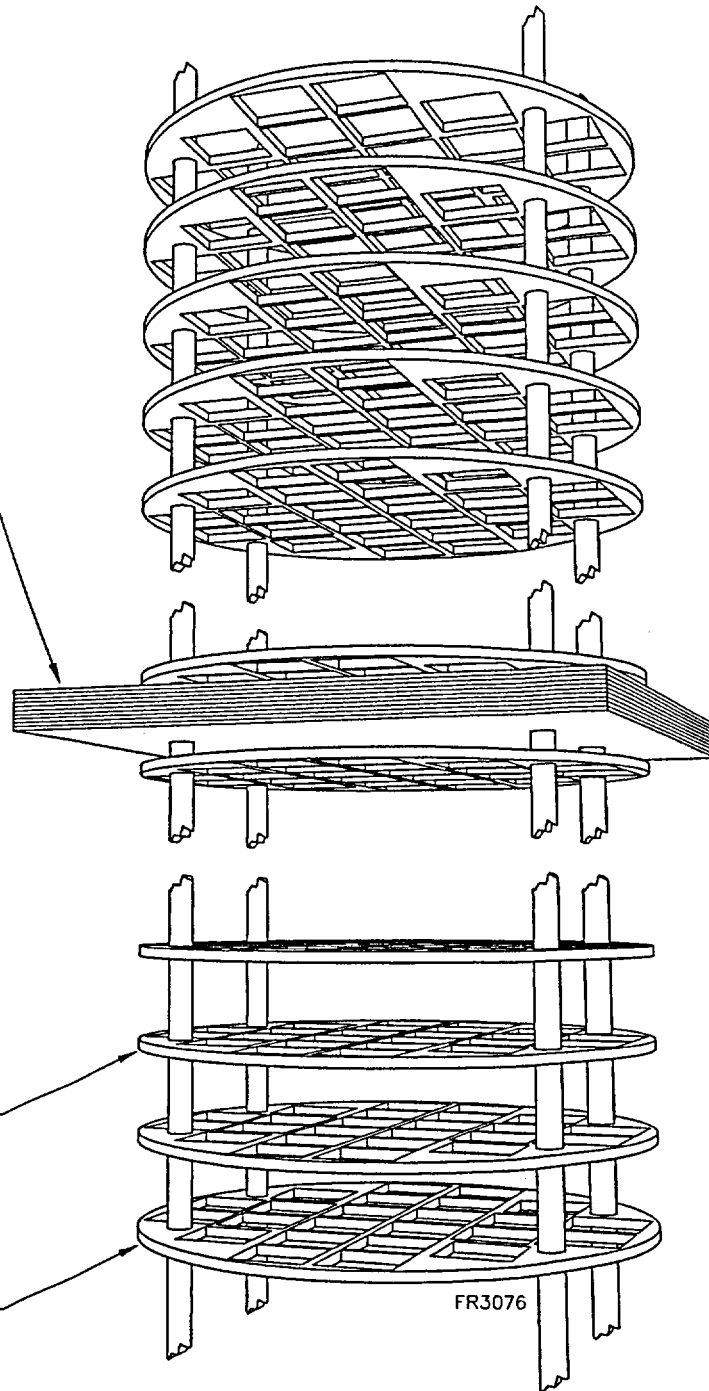


**Figure A.6.3-1**  
**KENO V.a Model of the 24PT4-DSC Basket**

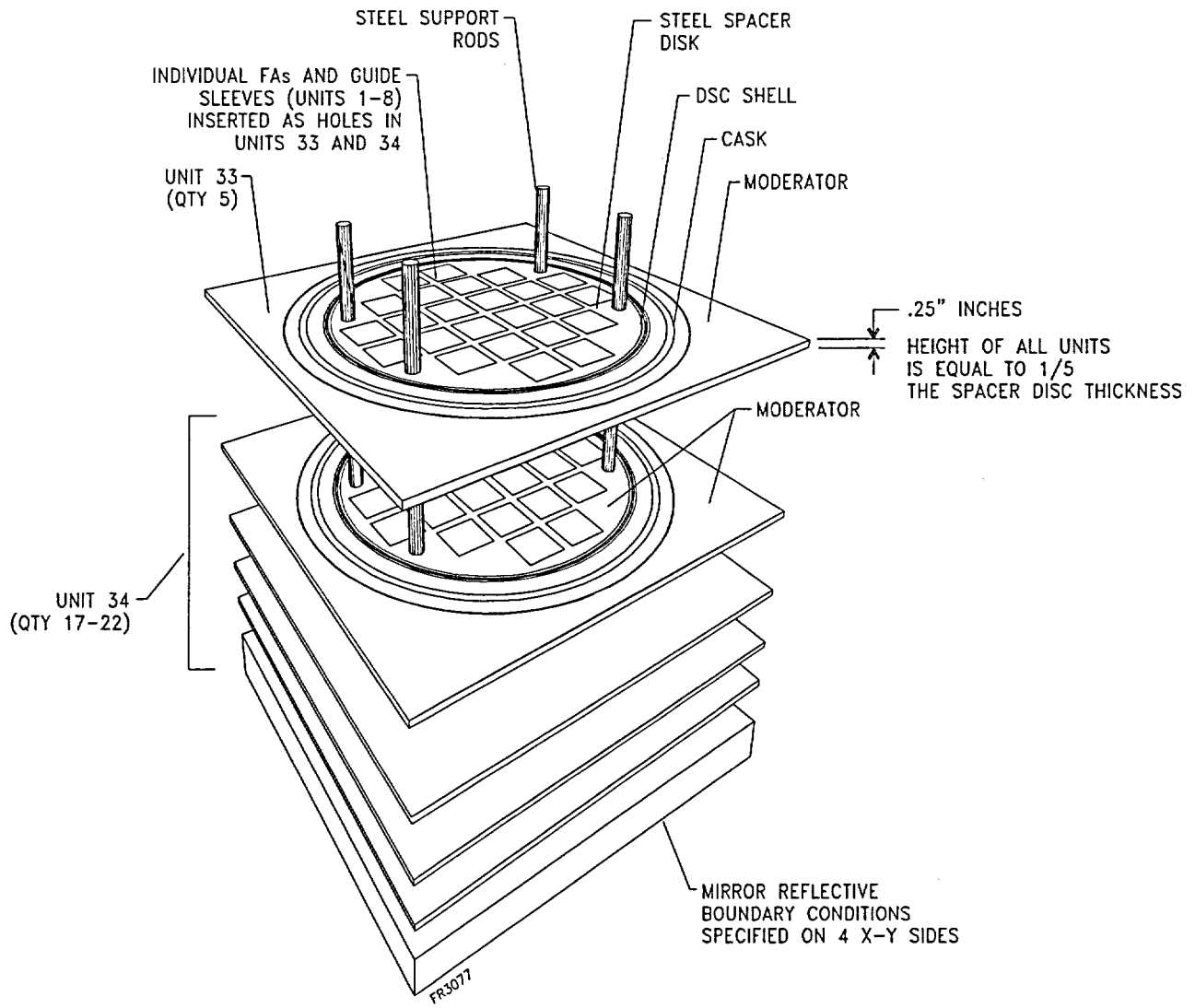


**Figure A.6.3-2**  
**Exploded View of KENO V.a Model**

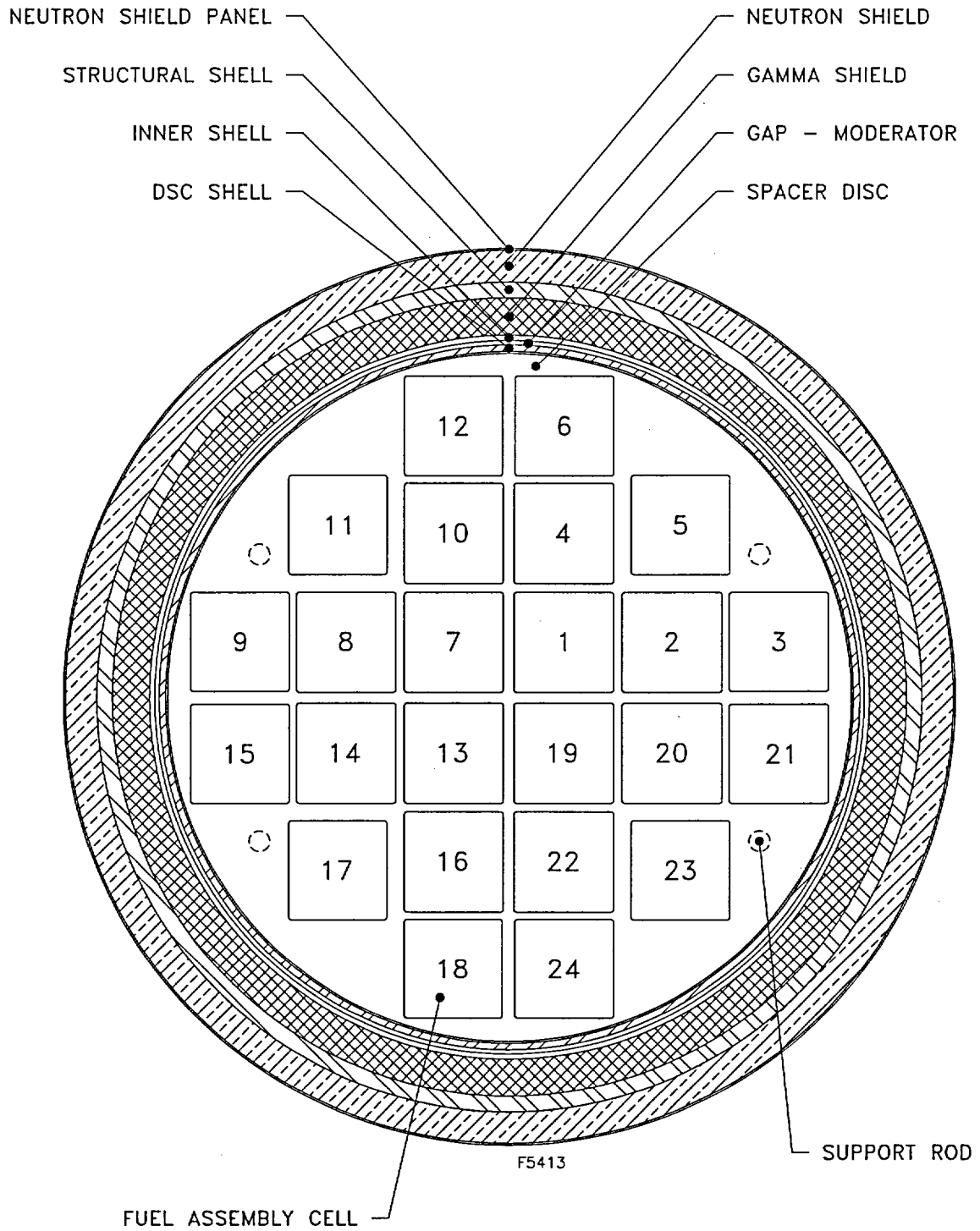


**Figure A.6.3-3**  
**Structure of KENO V.a Model – UNIT 33**

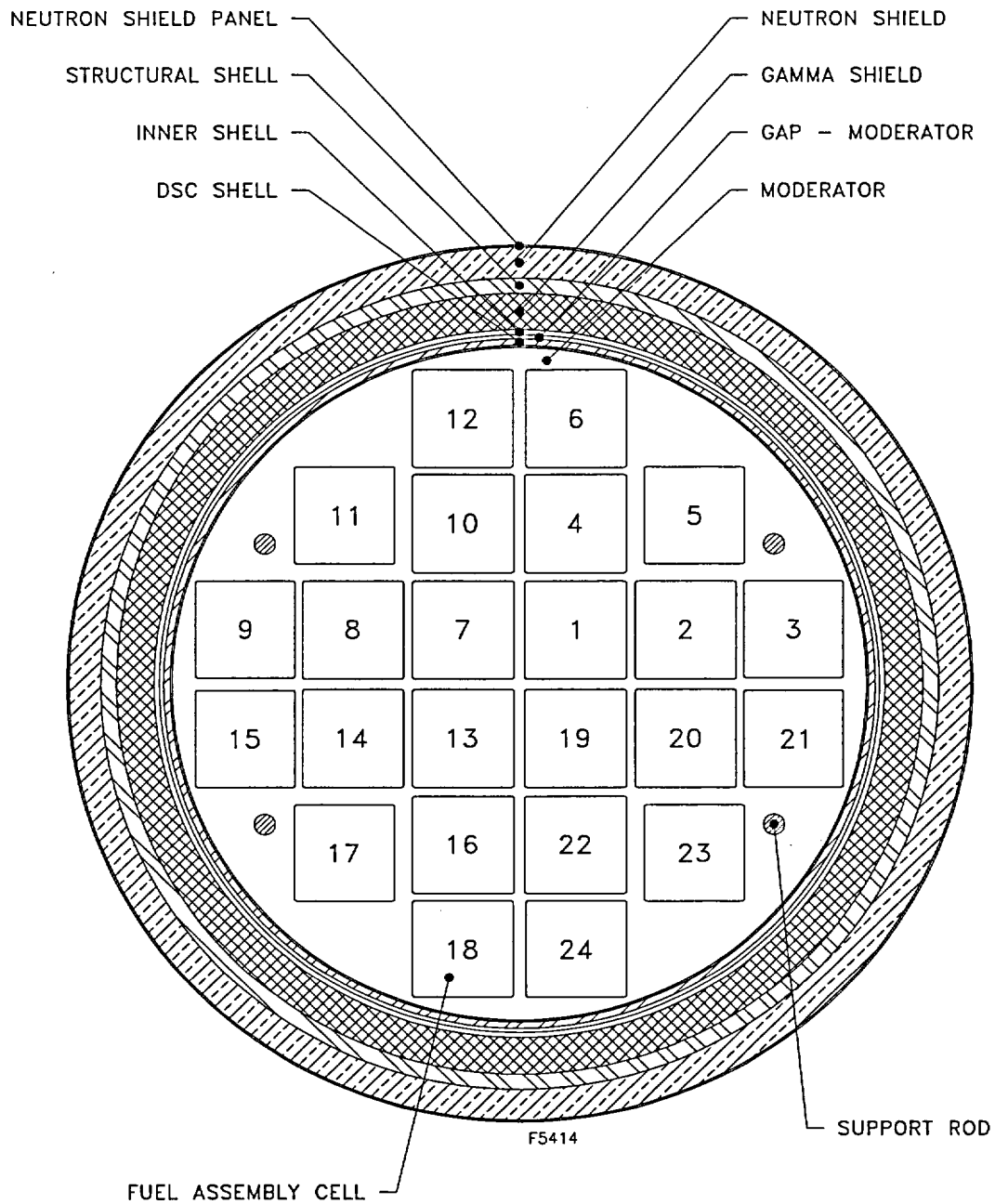


**Figure A.6.3-4**  
**Structure of KENO V.a Model – UNIT 34**



**Figure A.6.3-5**  
**Cross Section of the CE 16x16 Fuel Assembly**

## A.6.4 Criticality Calculation

This section contains descriptions of the calculational methods used to determine the nuclear reactivity for the maximum fuel loading intended to be stored in the 24PT4-DSC.

### A.6.4.1 Calculational Method

The effective neutron multiplication factor ( $k_{\text{eff}}$ ) was calculated using the CSAS25 module of the SCALE 4.4 Code with the 44-group ENDF/B-V cross-section library [A6.3]. The control module CSAS25 includes the three dimensional criticality code KENO V.a and the preprocessing codes BONAMI-S, NITAWL-II and XSDRNPM-S.

All the input decks were run with 500 generations with 1000 neutrons per generation. Five neutron generations were omitted before collecting the results. These values provided for a well converged solution.

Section A.6.6.2 contains a listing of select KENO V.a input files.

### A.6.4.2 Normal Operating Conditions (NOC)

The following parametric studies were performed for a Boral<sup>®</sup> sheet with  $0.025 \text{ g/cm}^2 \text{ }^{10}\text{B}$  areal density at a maximum fuel enrichment of 4.2 wt. %  $^{235}\text{U}$  (except as noted) to determine the worst case geometry. This fuel to poison plate combination is designed to be similar in reactivity to the combination of  $0.068 \text{ g/cm}^2 \text{ }^{10}\text{B}$  areal density at a maximum fuel enrichment of 4.85 wt. %  $^{235}\text{U}$  and therefore, the results from the parametric studies are applicable to all the fuel to poison plate combinations discussed in this chapter.

1. Most Reactive Fuel Pellet OD assuming 236 fuel rods in the fuel assembly.
2. Most Reactive Fuel Clad Thickness using the worst case model from Step 1.
3. Most Reactive Fuel Rod OD using the worst case model from Step 2.
4. Most Reactive Fuel Assembly using the worst case model from Step 3 and varying the absorber rod configurations for an enrichment of 4.1 wt. %  $^{235}\text{U}$ .
5. Boral<sup>®</sup> Sheet Thickness using the worst case model from Step 4.

The following studies were performed for both a Boral<sup>®</sup> sheet with  $0.025 \text{ g/cm}^2 \text{ }^{10}\text{B}$  areal density at a maximum fuel enrichment of 4.1 wt. %  $^{235}\text{U}$  and  $0.068 \text{ g/cm}^2 \text{ }^{10}\text{B}$  areal density at a maximum fuel enrichment of 4.85 wt. %  $^{235}\text{U}$  using the worst case geometry as determined in Step 6:

6. Most Reactive Fuel Assembly Position using the worst case model from Step 5 (both the fuel/poison design are investigated).
7. Internal Moderator Density Varying.

## 8. External Moderator Density Varying.

A parametric study on the reactivity effect of the tolerance on the spacer grid was not performed because it is unlikely that biases at a specific location on all 11 spacer grids would be the same magnitude and in the same direction. Therefore only the nominal pitch was used in the criticality calculations.

### A.6.4.2.1 Fuel Pellet OD Study

The first series of analyses determined the most reactive fuel pellet outer diameter (OD). The maximum fuel enrichment of 4.2 wt. %  $^{235}\text{U}$  and a poison plate  $^{10}\text{B}$  loading of  $0.01875\text{ g/cm}^2$  are used in the model. (Note that the  $0.01875\text{ g/cm}^2$  used in the model is 75% of the  $0.025\text{ g/cm}^2$  for a maximum lattice average enrichment of 4.2 wt. %  $^{235}\text{U}$ ). All models use nominal rod pitch, 100% internal and external moderator density, 100% moderator flooded fuel-cladding gap and specular boundary conditions. The most reactive configuration is the nominal pellet diameter (see Table A.6.4-1).

### A.6.4.2.2 Fuel Cladding Thickness Study

The second set of analysis evaluates the effect of fuel clad thickness on the system reactivity. The model starts with the nominal fuel pellet OD case from above and the poison plate thickness is modeled with nominal dimensions. All models assume nominal rod pitch, 100% internal and external moderator density, 100% moderator flooded fuel-cladding gap and specular boundary conditions. The most reactive configuration is the minimum cladding thickness (see Table A.6.4-1).

### A.6.4.2.3 Fuel Cladding OD Study

The third set of analyses evaluates the sensitivity of the system reactivity on fuel cladding OD. The model starts with the nominal fuel pellet OD and the minimum fuel cladding thickness input file from above. All models assume nominal rod pitch, 100% internal and external moderator density, 100% moderator flooded fuel-cladding gap and specular boundary conditions. The most reactive configuration is the minimum clad diameter (see Table A.6.4-1).

### A.6.4.2.4 Burnable Absorber Rod Study

The fourth set of analyses evaluates the sensitivity of the system reactivity to burnable absorber rods included in the fuel assemblies. Note that the  $^{10}\text{B}$  in the poison rods is modeled as  $^{11}\text{B}$ . The poison rod loading patterns are provided in Figure A.6.4-1. The model starts with the nominal fuel pellet OD, the minimum fuel cladding thickness and the minimum clad OD input deck from above except that the fuel enrichment is based on the design basis value of 4.10 wt. %  $^{235}\text{U}$ . All models assume nominal rod pitch, 100% internal and external moderator density, 100% moderator flooded fuel-cladding and poison-cladding gap and specular boundary conditions. The most reactive configuration is the zero poison rod configuration (see Table A.6.4-1).

### A.6.4.2.5 Boral<sup>®</sup> Sheet Thickness Study

The fifth set of analyses evaluates the effect of poison plate thickness on the system reactivity. The model starts with the most reactive dimensions determined above and the poison plate thickness is varied from 0.224 to 0.236 inches. In order to maintain the minimum  $^{10}\text{B}$  areal density the gram density of the poison plate material is adjusted in the model. All models assume nominal rod pitch, 100% internal and external moderator density, 100% moderator flooded fuel-cladding gap and specular boundary conditions. The most reactive configuration is the minimum Boral<sup>®</sup> plate thickness (see Table A.6.4-1).

#### A.6.4.2.6 Assembly Position Study

The sixth series of analyses evaluates the effect of the assembly to assembly pitch on the system reactivity. These models represent the most reactive intact fuel models determined above with the assembly-to-assembly pitch varied.

There are four assembly position model types which study how fuel assembly positions within the guidesleeves may affect the system's  $k_{\text{eff}}$ . Type 1 models the system with all fuel assemblies shifted radially inwards toward the center of the canister. All the fuel assemblies in the middle of the guidesleeves (Type 2) are the same as the worst case model determined in the previous step. Type 3 models all fuel assemblies shifted radially outwards, and Type 4 models all fuel assemblies shifted to the upper left corner of the guidesleeves. Examples of the assembly positions within the guidesleeve are presented in Figure A.6.4-2 through Figure A.6.4-4. All models use the nominal rod pitch, 100% internal and external moderator density, 100% moderator flooded fuel-cladding gap and specular boundary conditions. This study is performed on both the fuel enrichment / poison loading combination designs of 4.10 wt. %  $^{235}\text{U}$  / 0.025 g  $^{10}\text{B}/\text{cm}^2$  and 4.85 wt. %  $^{235}\text{U}$  / 0.068 g  $^{10}\text{B}/\text{cm}^2$  to ensure that the relative reactivities are about the same. The results showed that the most reactive assembly position is with the assemblies shifted inwards toward the center of the canister.

#### A.6.4.2.7 Moderator Varying Studies

The seventh set of analyses evaluates the effect of internal and external moderator density on reactivity. The model starts with the most reactive models from above. The internal moderator is varied from 100 to 0 percent full density. The results confirm that the most reactive condition occurs at full internal moderator density.

A second set of runs are also performed which increase the  $^{10}\text{B}$  loading from 0.025 g/cm<sup>2</sup> to 0.068 g/cm<sup>2</sup> (less 25%) and an initial fuel enrichment of 4.85 wt. %  $^{235}\text{U}$ .

The external moderator density uses the most reactive case with internal moderator (full density) density and the external internal moderator is varied from 100 to 0 percent full density. The results show that the system reactivity is not affected by external moderator density. The variation in the results is due entirely to the statistical uncertainties in KENO V.a.

#### A.6.4.3 Hypothetical Accident Conditions (HAC)

The HAC models duplicate the NOC moderator variation models developed in Section A.6.4.2.7 (both the 0.025/4.1 and 0.068/4.85 casks) outlined above. The only difference between the

models is the elimination of the neutron shield and neutron shield panel around the cask. Therefore, in the KENO V.a model, external water replaces both the neutron shield and the stainless steel cylinder around the neutron shield (neutron shield panel).

#### A.6.4.4 Damaged Fuel Models

There are several mechanisms by which a fuel rod may be breached. These mechanisms may occur while the fuel is loaded in the reactor core, in the spent fuel pool and during transport. In addition, the type and extent of fuel rod breach can be broken down into several categories. For this calculation the method by which the fuel rod is breached is not as important as the extent of the resultant damage. The worst case gross damage resulting from a cask-drop accident is assumed to be either a single-ended or double-ended rod shear with fresh water intrusion. It is possible that the fuel rod pitch may vary. Therefore, this will be evaluated by varying the fuel rod pitch from a minimum pitch of 0.380" to a maximum of 0.551" (limited to the inner guidesleeve opening). All pitch variations assume a uniform rod pitch throughout the entire fuel matrix.

The single-ended fuel rod shear cases assume that a fuel rod shears in one place and is displaced to a new location. The fuel pellets are assumed to remain in the fuel rod. This case will be evaluated by displacing one row of rods (16 rods) from the base fuel assembly matrix at small increments towards the side of the guidesleeves. The base fuel assembly matrix will be at nominal pitch and positioned in the upper left corner of the 24PT4-DSC fuel assembly sleeve to maximize the separation distance between the fuel array and the sheared row of fuel rods. A smaller rod pitch for the base fuel assembly matrix was not chosen because it has been shown from the pitch cases that decreasing the rod pitch decreases reactivity. Increasing the base fuel assembly rod pitch will increase reactivity, however, the resulting model is similar to and is bounded by the rod pitch varying cases presented above and therefore will not be duplicated here.

The double-ended fuel rod shear cases assume that the fuel rod shears in two places and the intact fuel rod piece is separated from the parent fuel rod. Three resulting conditions are exhibited by the occurrence of a double-ended rod shear. These are, the fuel rod piece can remain in place, it can be displaced in the same plane, or it can be displaced to a different plane. The "remain in place" situation results in no deviation from the base fuel assembly matrix, and is therefore considered trivial and will not be evaluated separately. The fuel rod piece displaced in the same plane is equivalent to the single-ended rod shear case discussed above and will not be reevaluated in these cases. The fuel rod piece displaced in a different plane results in two possibilities: an added rod or a removed rod. As in the single-ended shear cases, the base fuel assembly matrix will be positioned in the upper left corner of the 24PT4-DSC guidesleeve to allow room for a row of displaced fuel rods. One row of 16 fuel rods of different lengths will be removed from a section of the assembly and added to another to determine if the system exhibits any trends. The nominal rod pitch of 0.506" is used for the base fuel matrix just as in the single-ended shear rod cases.

It is postulated that during a cask drop accident the neutron shield and its neutron shield panel may be torn away from the cask and replaced with moderator. After all of the previous results are tabulated, an analysis is performed to determine to what degree the multiplication factor,  $k_{eff}$ ,

is affected by the removal of the cask neutron shield panel and subsequent replacement with moderator.

The first step is to determine the most reactive damaged fuel assembly geometry. This was completed using the  $0.068 \text{ g/cm}^2 \text{ }^{10}\text{B}$  areal density with 4.85% enriched fuel. All 24 assembly locations were filled with damaged fuel assemblies. The intent of these calculations was to determine the most reactive geometry, not meet the USL. The following is a breakdown of runs made in this analysis:

- Optimum Rod Pitch Study including enough missing fuel rods in an assembly to demonstrate that the worst case fuel geometry has been determined.
- Single-ended Shear Study.
- Double-ended Shear Study.
- Worst Configuration External Moderator Density Varying.
- Worst Single-ended and Double-ended Shear Configuration modeled with Bare Damaged Rods and External Moderator Density Varying.
- Rows of bare rods added to a fuel assembly to bound any possible relocation of fuel pellets.
- Addition of sheared rods below the poison sheet height.

With the selection of the most reactive damaged fuel assembly geometry, the next set of analyses determined the maximum  $k_{\text{eff}}$  for various damaged fuel assembly loading configurations in the 24PT4-DSC. Cases are run for both Boral<sup>TM</sup> sheets with areal densities of  $0.025 \text{ g/cm}^2$  and  $0.068 \text{ g/cm}^2$ . For both sets of cases, the maximum acceptable  $^{235}\text{U}$  enrichment are determined for 12 damaged fuel assemblies loaded around the outside assembly locations and for only 4 damaged fuel assemblies loaded in the assembly locations on the diagonal using the most reactive damaged fuel assembly geometry. The following set of analyses are performed:

- Maximum enrichment for the  $0.068 \text{ g/cm}^2 \text{ }^{10}\text{B}$  areal density, 4 damaged fuel assemblies loaded in the diagonal assembly positions, undamaged fuel in the remaining locations.
- Maximum enrichment for  $0.068 \text{ g/cm}^2 \text{ }^{10}\text{B}$  areal density, 12 damaged fuel assemblies loaded around the outside of the 24PT4-DSC, undamaged fuel in the remaining locations.
- Maximum enrichment for  $0.025 \text{ g/cm}^2 \text{ }^{10}\text{B}$  areal density, 4 damaged fuel assemblies loaded in the diagonal assembly positions, undamaged fuel in the remaining locations.
- Maximum enrichment for  $0.025 \text{ g/cm}^2 \text{ }^{10}\text{B}$  areal density, 12 damaged fuel assemblies loaded around the outside of the 24PT4-DSC, undamaged fuel in the remaining locations.

#### A.6.4.4.1 Rod Pitch Study

The first set of damaged fuel analyses involved a study on the effect of the fuel rod pitch on system reactivity. KENO V.a models with rod pitches ranging from 0.380 inches to 0.551 inches are created. All models assume 100% internal and external moderator density, 100% moderator flooded fuel-cladding gap and specular boundary conditions. Results of this analysis show that the maximum pitch of 0.551" (limited by the inner diameter of the guidesleeve) was the most reactive fuel rod pitch.

Once the most reactive pitch was determined, a series of calculations were performed that added or subtracted fuel rods from the base assembly to determine the limiting fuel assembly geometry. The removal of fuel rods was restricted to those in the interior locations of the 16x16 lattice. The selection of the rod loading patterns is aimed at maximizing the reactivity and those that are investigated are representative. All combinations of fuel rod positions are not investigated here. It is expected that the reactivities of other cases (not investigated) with the same number of rods but with different loading patterns are within statistical uncertainty. All models assume a rod pitch of 0.551 inches.

In addition to the postulated damaged assembly mechanisms, a damaged fuel assembly arrangement in the form of a rod storage basket is also analyzed. Rod storage baskets are typically used to store damaged fuel rods. A representative and conservative 9x9 arrangement of fuel in this basket is analyzed with two different rod pitches - 0.551 inches and 1.033 inches (corresponding to a grid-sleeve ID of 8.65 inches). All models assume 100% internal and external moderator density, 100% moderator flooded fuel-cladding gap and specular boundary conditions.

#### A.6.4.4.2 Single-ended Rod Shear Study

The next set of analyses performed are the single-end rod shear study. The Single-ended Rod Shear Study depicts a 16x16 fuel assembly with its last row of rods torn away from the rest of the assembly. The displacement of the dislocated row of torn rods vary radially from fuel assembly up to 0.4738 inches (next to the side of the guidesleeve).

To model this in KENO, a 15x16 fuel assembly array is created along with a 1x16 row of fuel rods. The 15x16 array is pushed up against the upper left hand corner of the guidesleeve to allow for the most room for the displacement of the dislocated 1x16 row of fuel rods. The displaced row of rods is then shifted toward the side of the guidesleeve by varying increments. The amount of fuel remains the same, i.e. no new fuel is added to the system. Nominal rod pitch of 0.506 inches is used for the base 15x16 fuel assembly. The rod pitch studies outlined above show that a decrease in the fuel rod pitch results in a decrease in system reactivity, therefore for the single-ended rod shear study runs, rod pitch is modeled at nominal value. Results of this study show that the most reactive Single-ended shear case occurs with the sheared row of fuel rods moved 0.55" away from the rest of the fuel assembly.

A graphical representation of the single-ended shear models is provided in Figure A.6.4-5. The  $\Delta$  shown is used to show the separation of the sheared rows distance from the base assembly. All

models assume 100% internal and external moderator density, 100% moderator flooded fuel-cladding gap and specular boundary conditions.

#### A.6.4.4.3 Double-ended Rod Shear Study

The three Double-ended Rod Shear cases model a row (1x16 array) of dislocated rods severed at different sections axially and then displacing to other sections of the 24PT4-DSC in order to define a conservative bounding condition for fuel rod location subsequent to a double-ended rod shear. The first run models an outer row of fuel breaking off at the top third of an assembly and then displacing itself to the second third of the assembly, creating a 15x16 assembly at the top third, a 16x16 assembly with an additional 1x16 row of fuel rods at the middle third and a standard 16x16 assembly at the bottom third of the canister. Similar scenarios except with the movement of one exterior row of 1/4 and 1/2 of the fuel assembly length are also modeled. Results of the double-ended rod shear study show that the movement of one exterior row of 1/2 of the fuel assembly length is the most reactive.

The same rod pitch assumptions made for the Single-ended Shear runs also apply here. The base 16x16 fuel rod matrices are shifted to the top left hand corner. All models assume nominal rod pitch, 100% internal and external moderator density, 100% moderator flooded fuel-cladding gap and specular boundary conditions. A graphical representation of the model including the sheared views along the length of the fuel assembly is shown in Figure A.6.4-6.

#### A.6.4.4.4 Most Reactive Configurations

Out of all the damaged fuel runs completed above, the rod pitch of 0.551" with 16 missing rods has the highest reactivity of  $0.9847 \pm 0.0012$ . A set of external moderator varying runs are made with this same configuration.

Additionally, a series of bare rod (replacement of cladding with moderator) external moderator varying runs are performed using the most reactive single-ended shear case and double-ended shear case. These two cases are modified to reflect the desired external moderator density as well as replacing the sheared row's cladding with internal moderator.

##### A.6.4.4.4.1 External Moderator Varying for Rod Pitch Case

Mixture 9, which is the mixture ID number for the system's external moderator, is changed for each external moderator case being modeled to cover densities from 0.0001 to 1.0000 g/cm<sup>3</sup>.

##### A.6.4.4.4.2 External Moderator for Single-ended Shear Case

The effect of bare sheared rod is investigated to determine the most reactive single sheared configuration. UNIT 31, UNIT 131, and UNIT231 are created to model the bare damaged rods. It is similar to UNIT 29 with the exception of the cladding material being replaced with internal moderator. The single row of damaged fuel pins are also modified and linked to the appropriate bare fuel cards. The most reactive single shear case is based on a separation distance of 0.55" with cladded damaged rods. Mixture 9, which is the mixture ID for the system's external

moderator, is changed for each external moderator case being modeled. These cases cover moderator densities from 0.0001 to 1.0000 g/cm<sup>3</sup>.

#### A.6.4.4.4.3 External Moderator for Double-ended Shear Case

The effect of bare sheared rod is investigated to determine the most reactive double sheared configuration. UNIT 329 is created to model the bare damaged rods. It is similar to UNIT 29 with the exception of the cladding material being replaced with internal moderator. The most reactive double shear case is based on "1/2 shear" with bare damaged rods. Mixture 9, which is the mixture ID for the system's external moderator, is changed for each external moderator case being modeled. These cases cover moderator densities from 0.0001 to 1.0000 g/cm<sup>3</sup>.

#### A.6.4.4.5 Bare Rods and Loose Fuel Pellets Added to a Fuel Assembly

In order to ensure that the worst case geometry is identified by the above cases, two further cases are run. Rows of bare fuel rods were added to intact fuel assemblies to bound the possible movement of loose fuel pellets. To model this in KENO, a 16x16 fuel assembly array is created along with a 1x17 and a 16x1 row of fuel rods. The 16x16 array is pushed up against the lower left hand corner of the guidesleeve to allow for the most amount of room for the placement of the dislocated 1x17 row and 16x1 row of bare fuel rods to create a 17x17 array, as shown in Figure A.6.4-7.

Another scenario that was modeled was the accumulation of fuel pellets in the 5.25-inch space between the top of the poison sheet and the bottom of the 24PT4-DSC lid. It is assumed that the fuel pellets stay stacked on top of each other and also retain the 16x16 lattice configuration. To achieve this, a 16x16 array of bare fuel rods was added in the 5.25 inches of uncovered space to the most reactive normal fuel geometry (fuel assembly in the inward most position).

This analysis bounds a loading configuration where loose pellets, from any on-site source (e.g., other reactor fuel sharing the same fuel pool), may be stored in a failed fuel can as long as the fuel pellet enrichment are within the parameters specified in Table A.6.2-1 and the total UO<sub>2</sub> in the failed fuel can does not exceed that associated with a CE 16x16 fuel assembly.

#### A.6.4.4.6 Worst Case Damaged Reactivity

The most reactive damaged fuel assembly geometry is determined to be the fuel rod pitch of 0.551" with 16 missing rods, 100% internal and external moderator density, 100% moderator flooded fuel-cladding gap and specular boundary conditions. The next set of analyses are performed to determine the maximum  $k_{eff}$  for various damaged fuel assembly loading patterns. Cases are run for both Boral<sup>®</sup> sheets with areal densities of 0.025 g/cm<sup>2</sup> and 0.068 g/cm<sup>2</sup>. For both sets of cases, the maximum acceptable <sup>235</sup>U enrichment is determined for 12 damaged fuel assemblies loaded around the outside assembly locations and for only 4 damaged fuel assemblies loaded in the assembly locations on the diagonal. The following set of analyses were performed:

- Maximum enrichment for the 0.068 g/cm<sup>2</sup> <sup>10</sup>B areal density and 4 damaged fuel assemblies loaded in the diagonal assembly positions.

- Maximum enrichment for  $0.068 \text{ g/cm}^2 \text{ }^{10}\text{B}$  areal density and 12 damaged fuel assemblies loaded around the outside of the 24PT4-DSC.
- Maximum enrichment for  $0.025 \text{ g/cm}^2 \text{ }^{10}\text{B}$  areal density and 4 damaged fuel assemblies loaded in the diagonal assembly positions.
- Maximum enrichment for  $0.025 \text{ g/cm}^2 \text{ }^{10}\text{B}$  areal density and 12 damaged fuel assemblies loaded around the outside of the 24PT4-DSC.

The normal fuel assembly geometry represents the most reactive intact fuel models with the assemblies shifted radially inwards toward the center of the 24PT4-DSC assuming 100% internal and external moderator density, 100% moderator flooded fuel-cladding gap and specular boundary conditions. For the configurations with both intact and damaged fuel assemblies loaded in a single 24PT4-DSC, modifications in the KENO V.a input files are necessary to represent both the fuel lattices accurately. The fuel lattice data for the damaged fuel assemblies are provided through the "more data" card while those for the intact fuel assemblies are provided through the usual "squarepitch card". This is due to the limitation of KENO V.a to handle only one "squarepitch card." The resonance absorption details in the damaged fuel lattice is input to the model via the Dancoff factor. Since, this is an input value, it is necessary that the value utilized should be correct if not conservative. The Dancoff factor for damaged fuel assemblies is obtained from previous KENO V.a output files for fuel that matches the geometry of the damaged fuel. The maximum enrichment models are then generated by loading the appropriate damaged fuel assembly into the location necessary for the cases being investigated.

Examples of a slice through the 24PT4-DSC are presented in Figure A.6.4-8 and Figure A.6.4-9. All normal fuel assembly models assume nominal rod pitch and all models assume 100% internal and external moderator density, 100% moderator flooded fuel-cladding gap and specular boundary conditions for the normal assemblies.

For the 12 damaged assembly model, the maximum enrichments determined above will be less than the desired values of 4.85 and 4.10 wt. %  $^{235}\text{U}$  for the boron-10 areal densities of  $0.068$  and  $0.025 \text{ g/cm}^2$ , respectively. For these cases, poison rodlets, composed of either Borated Stainless Steel or  $\text{B}_4\text{C}$  encased in a thin walled stainless steel tube, are added to each undamaged fuel assembly in order to increase the allowable damaged fuel enrichment for both  $0.025$  (4.1  $^{235}\text{U}$  wt. %) and  $0.068 \text{ }^{10}\text{B}$  areal density (4.85  $^{235}\text{U}$  wt. %). The worst case damaged fuel model was modified to include the 5 guide tubes per assembly. The poison rodlets are then inserted into the guide tubes to provide enough negative reactivity to reach the desired enrichment levels, as shown in Figure A.6.4-10. The required number of poison rodlets for each undamaged fuel assembly for the two poison plate designs are determined in this study.

The worst case damaged reactivity models described above are for a cask with NOC geometry, i.e., the neutron shield and stainless steel skin are present. To examine the effects on  $k_{\text{eff}}$  of removing the neutron shield and pushing the casks closer together, the cases with the poison rodlet are also run for this condition.

#### A.6.4.5 Fuel Assembly Replacement

An analysis is conducted to demonstrate that the removal of the four center fuel assembly locations in the 24PT4-DSC is bounded by the USL. The worst case normal geometry was modified to remove the four center fuel assemblies. The models generated have the same geometry as presented previously except that up to four of the center fuel assembly locations are empty, as shown in Figure A.6.4-11.

#### A.6.4.6 Assembly Reconstitution

Reconstituted fuel assemblies are those in which the damaged fuel pins are replaced with solid stainless steel pins or fuel pins with the same or lower enrichment and are considered as intact fuel assemblies. There are five models to study the effects of fuel rod reconstitution on the  $k_{\text{eff}}$  of the system on the worst case normal (intact) fuel geometry. KENO V.a models with rod pitches ranging 2 to 10 replacement stainless steel rods were created. An example of 10 reconstituted rods included in a fuel assembly is shown in Figure A.6.4-12. All models use 100% internal and 100% external moderator densities.

#### A.6.4.7 Criticality Results

The results for each case are presented in the following sections. These results are compared to the upper subcritical limit ( $USL=0.9411$ ) to determine the limiting  $k_{\text{eff}}$  for the 24PT4-DSC for normal and accident conditions and determine the acceptability of the criticality analysis.

The worst case geometry is selected based on a series of parametric studies (see Section A.6.4.2). The result for the effect of fuel pellet OD show that there was no significant statistical variation between the results for different fuel pellet diameters analyzed and therefore the nominal fuel pellet OD was selected as the worst case. Based on the results of the clad thickness evaluation the balance of the calculations used the minimum fuel clad thickness because it represented the more reactive condition. The fuel clad OD analysis showed that there was no significant statistical variation between the results. Therefore, the fuel clad was modeled with the minimum fuel clad OD. Results of the analysis to determine the effect of the burnable poison rods on the fuel assembly reactivity showed that it is conservative to model fuel assemblies as consisting completely of fuel rods with no integral burnable poison rods. The analysis of the effect of the Boral<sup>®</sup> plate thickness showed that there was no significant statistical variation between the results. Therefore, since the minimal thickness was slightly more reactive, it was selected as the worst case. The results of the assembly position study showed that the most reactive assembly position is with the assemblies shifted radially inwards toward the center of the canister. The worst case model was then the combination of the results of the above studies.

The maximum  $k_{\text{eff}}$  for NUHOMS<sup>®</sup> 24PT4-DSC system loaded with 24 CE 16x16 Fuel Assemblies using the  $0.068 \text{ g/cm}^2$   $^{10}\text{B}$  areal density was determined to be  $0.9365 \pm 0.0012$  ( $0.9389 \text{ w/2 } \sigma$ ) with a  $^{235}\text{U}$  maximum enrichment of 4.85 wt. %, an internal moderation at  $1.0 \text{ g/cm}^3$ ,  $0.3 \text{ g/cm}^3$  external moderation, and pure water in the fuel-cladding gap. The maximum  $k_{\text{eff}}$  for NUHOMS<sup>®</sup> 24PT4-DSC system loaded with 24 CE 16x16 Fuel Assemblies using the  $0.025 \text{ g/cm}^2$   $^{10}\text{B}$  areal density was determined to be  $0.9361 \pm 0.0011$  ( $0.9383 \text{ w/2 } \sigma$ ) with a  $^{235}\text{U}$

maximum enrichment of 4.1 wt. %, an internal moderation at 1.0 g/cm<sup>3</sup>, 1.0 g/cm<sup>3</sup> external moderation, and pure water in the fuel-cladding gap.

The most reactive damaged fuel assembly configuration was determined based on the results of the pitch variation calculations. These results indicate that the most reactive damaged fuel assembly configuration consisted of a 16X16 fuel lattice arranged with a pitch of 0.551" and 16 rods missing. A few other damaged configurations are also investigated including the single and double shear configurations and the rod storage basket with a 9x9 lattice at maximum pitch. An examination of the damaged configuration study indicates that the difference in reactivity between the most reactive configuration and all the other configuration is at least 0.02 in delta-k<sub>eff</sub> units. Even though, missing rod configurations greater than 20 were not investigated, it is expected that the k<sub>eff</sub> will be lower for these arrangements. Therefore, the fuel assembly represented by a 16x16 arrangement of CE fuel pins with 16 missing rods forms the design basis fuel assembly to represent the damaged fuel.

Results of worst case damaged fuel analyses show that for the loading of 4 damaged fuel assemblies on the diagonal, the maximum enrichment for both the 0.025 g/cm<sup>2</sup> <sup>10</sup>B areal density and for 0.068 g/cm<sup>2</sup> <sup>10</sup>B areal density is the same as the normal fuel assembly; 4.1 wt. % <sup>235</sup>U and 4.85 wt. % <sup>235</sup>U, respectively. The loading of 12 damaged fuel assemblies around the outer perimeter of the 24PT4-DSC shows that the maximum fuel pin enrichment in the damaged fuel assemblies must be limited to 3.7 wt. % <sup>235</sup>U for the 0.025 g/cm<sup>2</sup> <sup>10</sup>B areal density and 4.1 wt. % <sup>235</sup>U for 0.068 g/cm<sup>2</sup> <sup>10</sup>B areal density.

The maximum k<sub>eff</sub> for NUHOMS<sup>®</sup> 24PT4-DSC system loaded with 4 CE 16x16 Damaged Fuel Assemblies using the 0.068 g/cm<sup>2</sup> <sup>10</sup>B areal density was determined to be 0.9360±0.0011 (0.9382 w/2σ) with an <sup>235</sup>U maximum enrichment of 4.85 wt. %, an internal moderation at 1.0 g/cm<sup>3</sup>, 1.0 g/cm<sup>3</sup> external moderation, and pure water in the fuel-cladding gap. The maximum k<sub>eff</sub> for NUHOMS<sup>®</sup> 24PT4-DSC system loaded with 4 CE 16x16 Damaged Fuel Assemblies using the 0.025 g/cm<sup>2</sup> <sup>10</sup>B areal density was determined to be 0.9337±0.0012 (0.9361 w/2 σ) with an <sup>235</sup>U maximum enrichment of 4.1 wt. %, an internal moderation at 1.0 g/cm<sup>3</sup>, 1.0 g/cm<sup>3</sup> external moderation, and pure water in the fuel-cladding gap.

The maximum k<sub>eff</sub> for NUHOMS<sup>®</sup> 24PT4-DSC system loaded with 12 CE 16x16 Damaged Fuel Assemblies using the 0.068 g/cm<sup>2</sup> <sup>10</sup>B areal density was determined to be 0.9367±0.0012 (0.9391 w/2σ) with an <sup>235</sup>U maximum enrichment of 4.1 wt. %, an internal moderation at 1.0 g/cm<sup>3</sup>, 1.0 g/cm<sup>3</sup> external moderation, and pure water in the fuel-cladding gap. The maximum k<sub>eff</sub> for NUHOMS<sup>®</sup> 24PT4-DSC system loaded with 12 CE 16x16 Damaged Fuel Assemblies using the 0.025 g/cm<sup>2</sup> <sup>10</sup>B areal density was determined to be 0.9369±0.0012 (0.9393 w/2 σ) with an <sup>235</sup>U maximum enrichment of 3.7 wt. %, an internal moderation at 1.0 g/cm<sup>3</sup>, 1.0 g/cm<sup>3</sup> external moderation, and pure water in the fuel-cladding gap.

The discussion in the preceding paragraph did not include the use of poison rodlets in the assembly guide tubes. In order to load fuel at the highest enrichment (of 4.10 wt. % <sup>235</sup>U) for the 0.025 g/cm<sup>2</sup> Boral<sup>®</sup> poison cases, a single poison rodlet in the center guide tube of the fuel assemblies was determined to be sufficient. Similarly, to load fuel at the highest enrichment (of 4.85 wt. % <sup>235</sup>U) for the 0.068 g/cm<sup>2</sup> Boral<sup>®</sup> poison cases, five poison rodlets in each intact fuel assembly (maximum rodlets per assembly) was determined to be sufficient. These poison rodlet

cases were run with both NOC and HAC cask geometry. The values obtained for  $k_{\text{eff}}$  demonstrate that replacing the neutron shield skin with moderator has relatively minimal effect on the system reactivity.

These calculations show that the system  $k_{\text{eff}}$  remains about the same if one fuel assembly is removed from the above configuration (11 intact fuel assemblies with five poison rodlets each and 12 damaged fuel assemblies). This is due to the fact that the removal of the highly absorbing poison rodlets from the system approximately compensates for the effect of removing fissile material (an intact fuel assembly). However, all these were carried out at full moderator density conditions. Several calculations involving dry damaged fuel assemblies were also performed. The results indicate that the most reactive "dry" fuel is the one with 4 damaged fuel assemblies, with an enrichment of 4.10 wt. %  $^{235}\text{U}$ , a Boral<sup>®</sup> poison loading of 0.025 g/cm<sup>2</sup> and the  $k_{\text{eff}}$  for this case is  $0.4356 \pm 0.0005$  ( $0.4366$  w/ $2\sigma$ ).

The calculations also show that the system  $k_{\text{eff}}$  decreases as the separation between adjacent assemblies increases. Thus, removing an assembly from the 24PT4-DSC results in an effective increase in the assembly separation decreasing the system eigenvalue. Also, since the assemblies are inside the guidesleeve and the Boral<sup>®</sup> plates, when an assembly is replaced by water, there will be a flux trap where fast neutrons enter the tube. The neutrons thermalize, but on average, do not escape because of the highly preferential thermal neutron flux trap made by the guidesleeve and the  $1/v$  Boral<sup>®</sup> plate absorbers. Thus, the system  $k_{\text{eff}}$  decreases with the removal of fuel assemblies. In addition, the reconstitution of fuel rods with up to 10 stainless steel rods reduces the amount of reactive material in the fuel assembly thereby reducing the system  $k_{\text{eff}}$ . Fuel assemblies with reconstituted rods are considered intact fuel assemblies and are bounded by the results of the intact fuel calculations since they are shown to be less reactive. Results of all the cases run are presented in the following tables.

#### A.6.4.8 Summary and Conclusions

In summary, the criticality analysis for the Advanced NUHOMS<sup>®</sup> 24PT4-DSC system demonstrates that the maximum  $k_{\text{eff}}$  value is below the USL of 0.9411 for a variety of loading configurations under normal, off-normal and hypothetical accident conditions. The criticality of the system is analyzed utilizing two types of Boral<sup>®</sup> loadings in the basket, a normal loading of 0.025 g  $^{10}\text{B}/\text{cm}^2$  and a high loading of 0.068 g  $^{10}\text{B}/\text{cm}^2$ . The allowable storage configurations for both  $^{10}\text{B}$  loadings for the various fuel assembly types are summarized below:

##### A.6.4.8.1 Summary of 24PT4-DSC Limits with Normal $^{10}\text{B}$ Loading of 0.025 g/cm<sup>2</sup>

###### Limits for Intact Fuel (no damaged fuel assemblies)

- Intact fuel assemblies (including reconstituted fuel assemblies) can be stored in all 24 fuel assembly locations. Empty locations are allowed.
- The maximum permissible initial fuel enrichment of the fuel assemblies is 4.10 wt. %  $^{235}\text{U}$ .

### General Limits for Damaged Fuel

- There is no limit on the number of damaged rods in a single fuel assembly. Also, there is no limit on the number of missing rods that constitute a damaged fuel assembly.
- Damaged fuel assemblies can only be stored in the Type A spacer hole positions. These are the fuel assembly positions along the outer periphery of the 24PT4-DSC basket. A maximum of 12 damaged fuel assemblies can be stored per 24PT4-DSC.

### Limits for Damaged Fuel without Poison Rodlets

- A maximum of four damaged fuel assemblies at an initial enrichment of 4.10 wt. %  $^{235}\text{U}$  can be stored in the four corner locations (positions #5, #11, #17 and #23, see Figure A.6.4-2) along with intact fuel assemblies. The remaining intact fuel assemblies are also limited to an initial enrichment of 4.10 wt. %  $^{235}\text{U}$ .
- For the case of 5 to 12 damaged fuel assemblies, the initial enrichment of the damaged fuel assemblies is limited to 3.70 wt. %  $^{235}\text{U}$ . The remaining intact fuel assemblies are limited to an initial enrichment of 4.10 wt. %  $^{235}\text{U}$ .

### Limits for Damaged Fuel with Poison Rodlets (5 to 12 damaged fuel assemblies)

- For the case of 5 to 12 damaged fuel assemblies, if a poison rodlet is inserted into the center position of each intact fuel assembly, the maximum permissible fuel enrichment of each damaged fuel assembly is 4.10 wt. %  $^{235}\text{U}$ . The maximum enrichment of the intact fuel assemblies is also 4.10 wt. %  $^{235}\text{U}$ . Empty intact fuel assembly locations are permissible. Poison rodlets are not required for intact assemblies in Zone A or B positions (see Figure A.6.4-13), if present.

### A.6.4.8.2 Summary of 24PT4-DSC Limits with High $^{10}\text{B}$ Loading of 0.068 g/cm<sup>2</sup>

#### Limits for Intact Fuel (no damaged fuel assemblies)

- Intact fuel assemblies (including reconstituted fuel assemblies) can be stored in all 24 fuel assembly locations. Empty locations are allowed.
- The maximum permissible initial fuel enrichment of the fuel assemblies is 4.85 wt. %  $^{235}\text{U}$ .

### General Limits for Damaged Fuel

- There is no limit on the number of damaged rods in a single fuel assembly. Also, there is no limit on the number of missing rods that constitute a damaged fuel assembly.
- Damaged fuel assemblies can only be stored in the Type A spacer hole positions. These are the fuel assembly positions along the outer periphery of the 24PT4-DSC basket. A maximum of 12 damaged fuel assemblies can be stored per 24PT4-DSC.

### Limits for Damaged Fuel without Poison Rodlets

- A maximum of four damaged fuel assemblies at an initial enrichment of 4.85 wt. %  $^{235}\text{U}$  can be stored in the peripheral locations (positions #5, #11, #17 and #23, see Figure A.6.4-2) along with intact fuel assemblies. The remaining intact fuel assemblies are also limited to an initial enrichment of 4.85 wt. %  $^{235}\text{U}$ .
- For the case of 5 to 12 damaged fuel assemblies, the initial enrichment of the damaged fuel assemblies is limited to 4.10 wt. %  $^{235}\text{U}$ . The remaining intact fuel assemblies are limited to an initial enrichment of 4.85 wt. %  $^{235}\text{U}$ .

### Limits for Damaged Fuel with Poison Rodlets (5 to 12 damaged fuel assemblies)

- For the case of 5 to 12 damaged fuel assemblies, if 5 poison rodlets are inserted into each intact inner fuel assembly, the maximum permissible fuel enrichment of each damaged fuel assembly is 4.85 wt. %  $^{235}\text{U}$ . The maximum enrichment of the intact fuel assemblies is also 4.85 wt. %  $^{235}\text{U}$ . Empty intact fuel assembly locations are permissible. Poison rodlets are not required for intact assemblies in Zone A or B positions (see Figure A.6.4-13), if present.

**Table A.6.4-1**  
**Parametric Study Results – <sup>10</sup>B Areal density of 0.025 g/cm<sup>2</sup>**

| <b>Fuel Pellet OD</b>         |               |                        |  |
|-------------------------------|---------------|------------------------|--|
| <b>k<sub>KENO</sub></b>       | <b>1 σ</b>    | <b>k<sub>eff</sub></b> | <b>Description</b>                                 |
| <b>0.9323</b>                 | <b>0.0012</b> | <b>0.9347</b>          | <b>nominal pellet OD</b>                           |
| 0.9297                        | 0.0011        | 0.9319                 | maximum pellet OD                                  |
| 0.9317                        | 0.0012        | 0.9341                 | minimum pellet OD                                  |
|                               |               |                        |  |
| <b>Cladding Thickness</b>     |               |                        |  |
| <b>k<sub>KENO</sub></b>       | <b>1 σ</b>    | <b>k<sub>eff</sub></b> | <b>Description</b>                                 |
| 0.9323                        | 0.0012        | 0.9347                 | nominal clad thickness                             |
| <b>0.9360</b>                 | <b>0.0012</b> | <b>0.9384</b>          | <b>minimum clad thickness</b>                      |
| 0.9281                        | 0.0011        | 0.9303                 | maximum clad thickness                             |
|                               |               |                        |  |
| <b>Cladding OD</b>            |               |                        |  |
| <b>k<sub>KENO</sub></b>       | <b>1 σ</b>    | <b>k<sub>eff</sub></b> | <b>Description</b>                                 |
| 0.9360                        | 0.0012        | 0.9384                 | nominal clad OD                                    |
| 0.9351                        | 0.0011        | 0.9373                 | maximum clad OD                                    |
| <b>0.9362</b>                 | <b>0.0012</b> | <b>0.9386</b>          | <b>minimum clad OD</b>                             |
|                               |               |                        |  |
| <b>Burnable Absorber Rods</b> |               |                        |  |
| <b>k<sub>KENO</sub></b>       | <b>1 σ</b>    | <b>k<sub>eff</sub></b> | <b>Description</b>                                 |
| 0.9290                        | 0.0012        | 0.9314                 | 16 Poison Rods with water in the gap               |
| 0.9273                        | 0.0013        | 0.9299                 | 16 Poison Rods without water in the gap            |
| 0.9265                        | 0.0013        | 0.9291                 | 12 Poison Rods with water in the gap               |
| 0.9286                        | 0.0013        | 0.9312                 | 8 Poison Rods with water in the gap                |
| 0.9323                        | 0.0012        | 0.9347                 | 4 Poison Rods with water in the gap                |
| <b>0.9331</b>                 | <b>0.0013</b> | <b>0.9357</b>          | <b>0 Poison Rods with water in the gap</b>         |
|                               |               |                        |  |
| <b>Boral Plate Thickness</b>  |               |                        |  |
| <b>k<sub>KENO</sub></b>       | <b>1 σ</b>    | <b>k<sub>eff</sub></b> | <b>Description</b>                                 |
| 0.9297                        | 0.0011        | 0.9319                 | nominal Boral <sup>®</sup> plate thickness         |
| 0.9328                        | 0.0012        | 0.9352                 | maximum Boral <sup>®</sup> plate thickness         |
| <b>0.9331</b>                 | <b>0.0013</b> | <b>0.9357</b>          | <b>minimum Boral<sup>®</sup> plate thickness</b>   |
|                               |               |                        |  |
| <b>Assembly Position</b>      |               |                        |  |
| <b>k<sub>KENO</sub></b>       | <b>1 σ</b>    | <b>k<sub>eff</sub></b> | <b>Description</b>                                 |
| <b>0.9361</b>                 | <b>0.0011</b> | <b>0.9383</b>          | <b>radially inward (minimum Boral<sup>®</sup>)</b> |
| 0.9331                        | 0.0013        | 0.9357                 | centered (minimum Boral <sup>®</sup> )             |
| 0.9227                        | 0.0011        | 0.9249                 | radially outward (nominal Boral <sup>®</sup> )     |
| 0.9258                        | 0.0012        | 0.9282                 | upper left corner (nominal Boral <sup>®</sup> )    |

**Note:** Bold type identifies bounding analysis.

**Table A.6.4-2**  
**NOC Moderator Varying Results – <sup>10</sup>B Areal density of 0.068 g/cm<sup>2</sup>**

| <b>Internal Moderator Varying</b> |               |                        |                                 |
|-----------------------------------|---------------|------------------------|---------------------------------|
| <b>k<sub>KENO</sub></b>           | <b>1 σ</b>    | <b>k<sub>eff</sub></b> | <b>Description</b>              |
| 0.4219                            | 0.0005        | 0.4229                 | H <sub>2</sub> O: 0.0001 g/cc   |
| 0.5078                            | 0.0007        | 0.5092                 | H <sub>2</sub> O: 0.1 g/cc      |
| 0.5692                            | 0.0009        | 0.5710                 | H <sub>2</sub> O: 0.2 g/cc      |
| 0.6258                            | 0.0009        | 0.6276                 | H <sub>2</sub> O: 0.3 g/cc      |
| 0.6855                            | 0.0011        | 0.6877                 | H <sub>2</sub> O: 0.4 g/cc      |
| 0.7351                            | 0.0011        | 0.7373                 | H <sub>2</sub> O: 0.5 g/cc      |
| 0.7857                            | 0.0012        | 0.7881                 | H <sub>2</sub> O: 0.6 g/cc      |
| 0.8264                            | 0.0013        | 0.8290                 | H <sub>2</sub> O: 0.7 g/cc      |
| 0.8687                            | 0.0013        | 0.8713                 | H <sub>2</sub> O: 0.8 g/cc      |
| 0.9032                            | 0.0011        | 0.9054                 | H <sub>2</sub> O: 0.9 g/cc      |
| 0.9359                            | 0.0013        | 0.9385                 | H <sub>2</sub> O: 1.0 g/cc      |
|                                   |               |                        |                                 |
| <b>External Moderator Varying</b> |               |                        |                                 |
| <b>k<sub>KENO</sub></b>           | <b>1 σ</b>    | <b>k<sub>eff</sub></b> | <b>Description</b>              |
| 0.9325                            | 0.0013        | 0.9351                 | H <sub>2</sub> O: 0.0001 g/cc   |
| 0.9337                            | 0.0013        | 0.9363                 | H <sub>2</sub> O: 0.05 g/cc     |
| 0.9351                            | 0.0011        | 0.9373                 | H <sub>2</sub> O: 0.1 g/cc      |
| 0.9345                            | 0.0013        | 0.9371                 | H <sub>2</sub> O: 0.2 g/cc      |
| 0.9348                            | 0.0013        | 0.9374                 | H <sub>2</sub> O: 0.3 g/cc      |
| 0.9348                            | 0.0011        | 0.9370                 | H <sub>2</sub> O: 0.4 g/cc      |
| 0.9357                            | 0.0014        | 0.9385                 | H <sub>2</sub> O: 0.5 g/cc      |
| <b>0.9361</b>                     | <b>0.0012</b> | <b>0.9385</b>          | <b>H<sub>2</sub>O: 0.6 g/cc</b> |
| 0.9342                            | 0.0013        | 0.9368                 | H <sub>2</sub> O: 0.7 g/cc      |
| 0.9336                            | 0.0014        | 0.9364                 | H <sub>2</sub> O: 0.8 g/cc      |
| 0.9355                            | 0.0011        | 0.9377                 | H <sub>2</sub> O: 0.9 g/cc      |
| 0.9359                            | 0.0013        | 0.9385                 | H <sub>2</sub> O: 1.0 g/cc      |

**Table A.6.4-3**  
**NOC Moderator Varying Results -  $^{10}\text{B}$  Areal density of  $0.025 \text{ g/cm}^2$**

| <b>Internal Moderator Varying</b> |               |                  |                                 |
|-----------------------------------|---------------|------------------|---------------------------------|
| $k_{\text{KENO}}$                 | $1 \sigma$    | $k_{\text{eff}}$ | Description                     |
| 0.4437                            | 0.0005        | 0.4447           | H <sub>2</sub> O: 0.0001 g/cc   |
| 0.5477                            | 0.0007        | 0.5491           | H <sub>2</sub> O: 0.1 g/cc      |
| 0.6099                            | 0.0008        | 0.6115           | H <sub>2</sub> O: 0.2 g/cc      |
| 0.6667                            | 0.0010        | 0.6687           | H <sub>2</sub> O: 0.3 g/cc      |
| 0.7179                            | 0.0010        | 0.7199           | H <sub>2</sub> O: 0.4 g/cc      |
| 0.7645                            | 0.0012        | 0.7669           | H <sub>2</sub> O: 0.5 g/cc      |
| 0.8056                            | 0.0013        | 0.8082           | H <sub>2</sub> O: 0.6 g/cc      |
| 0.8446                            | 0.0012        | 0.8470           | H <sub>2</sub> O: 0.7 g/cc      |
| 0.8763                            | 0.0011        | 0.8785           | H <sub>2</sub> O: 0.8 g/cc      |
| 0.9082                            | 0.0013        | 0.9108           | H <sub>2</sub> O: 0.9 g/cc      |
| <b>0.9361</b>                     | <b>0.0011</b> | <b>0.9383</b>    | <b>H<sub>2</sub>O: 1.0 g/cc</b> |
|                                   |               |                  |                                 |
| <b>External Moderator Varying</b> |               |                  |                                 |
| $k_{\text{KENO}}$                 | $1 \sigma$    | $k_{\text{eff}}$ | Description                     |
| 0.9346                            | 0.0014        | 0.9374           | H <sub>2</sub> O: 0.0001 g/cc   |
| 0.9339                            | 0.0011        | 0.9361           | H <sub>2</sub> O: 0.05 g/cc     |
| 0.9341                            | 0.0011        | 0.9363           | H <sub>2</sub> O: 0.1 g/cc      |
| 0.9351                            | 0.0012        | 0.9375           | H <sub>2</sub> O: 0.2 g/cc      |
| 0.9351                            | 0.0012        | 0.9375           | H <sub>2</sub> O: 0.3 g/cc      |
| 0.9340                            | 0.0012        | 0.9364           | H <sub>2</sub> O: 0.4 g/cc      |
| 0.9341                            | 0.0011        | 0.9363           | H <sub>2</sub> O: 0.5 g/cc      |
| 0.9333                            | 0.0013        | 0.9359           | H <sub>2</sub> O: 0.6 g/cc      |
| 0.9341                            | 0.0011        | 0.9363           | H <sub>2</sub> O: 0.7 g/cc      |
| 0.9337                            | 0.0012        | 0.9361           | H <sub>2</sub> O: 0.8 g/cc      |
| 0.9351                            | 0.0012        | 0.9375           | H <sub>2</sub> O: 0.9 g/cc      |
| <b>0.9361</b>                     | <b>0.0011</b> | <b>0.9383</b>    | <b>H<sub>2</sub>O: 1.0 g/cc</b> |

**Table A.6.4-4**  
**HAC Moderator Varying Results - <sup>10</sup>B Areal density of 0.068 g/cm<sup>2</sup>**

| <b>Internal Moderator Varying</b> |               |                        |                                 |
|-----------------------------------|---------------|------------------------|---------------------------------|
| <b>k<sub>KENO</sub></b>           | <b>1 σ</b>    | <b>k<sub>eff</sub></b> | <b>Description</b>              |
| 0.4228                            | 0.0005        | 0.4238                 | H <sub>2</sub> O: 0.0001 g/cc   |
| 0.5069                            | 0.0007        | 0.5083                 | H <sub>2</sub> O: 0.1 g/cc      |
| 0.5689                            | 0.0009        | 0.5707                 | H <sub>2</sub> O: 0.2 g/cc      |
| 0.6288                            | 0.0011        | 0.6310                 | H <sub>2</sub> O: 0.3 g/cc      |
| 0.6824                            | 0.0010        | 0.6844                 | H <sub>2</sub> O: 0.4 g/cc      |
| 0.7391                            | 0.0012        | 0.7415                 | H <sub>2</sub> O: 0.5 g/cc      |
| 0.7860                            | 0.0014        | 0.7888                 | H <sub>2</sub> O: 0.6 g/cc      |
| 0.8310                            | 0.0013        | 0.8336                 | H <sub>2</sub> O: 0.7 g/cc      |
| 0.8689                            | 0.0012        | 0.8713                 | H <sub>2</sub> O: 0.8 g/cc      |
| 0.9031                            | 0.0013        | 0.9057                 | H <sub>2</sub> O: 0.9 g/cc      |
| <b>0.9361</b>                     | <b>0.0012</b> | <b>0.9385</b>          | <b>H<sub>2</sub>O: 1.0 g/cc</b> |
|                                   |               |                        |                                 |
| <b>External Moderator Varying</b> |               |                        |                                 |
| <b>k<sub>KENO</sub></b>           | <b>1 σ</b>    | <b>k<sub>eff</sub></b> | <b>Description</b>              |
| 0.9341                            | 0.0013        | 0.9367                 | H <sub>2</sub> O: 0.0001 g/cc   |
| 0.9345                            | 0.0013        | 0.9371                 | H <sub>2</sub> O: 0.05 g/cc     |
| 0.9343                            | 0.0012        | 0.9367                 | H <sub>2</sub> O: 0.1 g/cc      |
| 0.9321                            | 0.0012        | 0.9345                 | H <sub>2</sub> O: 0.2 g/cc      |
| <b>0.9365</b>                     | <b>0.0012</b> | <b>0.9389</b>          | <b>H<sub>2</sub>O: 0.3 g/cc</b> |
| 0.9352                            | 0.0013        | 0.9378                 | H <sub>2</sub> O: 0.4 g/cc      |
| 0.9323                            | 0.0014        | 0.9351                 | H <sub>2</sub> O: 0.5 g/cc      |
| 0.9322                            | 0.0015        | 0.9352                 | H <sub>2</sub> O: 0.6 g/cc      |
| 0.9353                            | 0.0012        | 0.9377                 | H <sub>2</sub> O: 0.7 g/cc      |
| 0.9353                            | 0.0011        | 0.9375                 | H <sub>2</sub> O: 0.8 g/cc      |
| 0.9353                            | 0.0013        | 0.9379                 | H <sub>2</sub> O: 0.9 g/cc      |
| 0.9361                            | 0.0012        | 0.9385                 | H <sub>2</sub> O: 1.0 g/cc      |

**Table A.6.4-5**  
**HAC Moderator Varying Results - <sup>10</sup>B Areal density of 0.025 g/cm<sup>2</sup>**

| <b>Internal Moderator Varying</b> |            |                        |                               |
|-----------------------------------|------------|------------------------|-------------------------------|
| <b>k<sub>KENO</sub></b>           | <b>1 σ</b> | <b>k<sub>eff</sub></b> | <b>Description</b>            |
| 0.4440                            | 0.0005     | 0.4450                 | H <sub>2</sub> O: 0.0001 g/cc |
| 0.5474                            | 0.0008     | 0.5490                 | H <sub>2</sub> O: 0.1 g/cc    |
| 0.6097                            | 0.0008     | 0.6113                 | H <sub>2</sub> O: 0.2 g/cc    |
| 0.6677                            | 0.0009     | 0.6695                 | H <sub>2</sub> O: 0.3 g/cc    |
| 0.7205                            | 0.0011     | 0.7227                 | H <sub>2</sub> O: 0.4 g/cc    |
| 0.7653                            | 0.0011     | 0.7675                 | H <sub>2</sub> O: 0.5 g/cc    |
| 0.8066                            | 0.0012     | 0.8090                 | H <sub>2</sub> O: 0.6 g/cc    |
| 0.8445                            | 0.0013     | 0.8471                 | H <sub>2</sub> O: 0.7 g/cc    |
| 0.8811                            | 0.0014     | 0.8839                 | H <sub>2</sub> O: 0.8 g/cc    |
| 0.9075                            | 0.0015     | 0.9105                 | H <sub>2</sub> O: 0.9 g/cc    |
| 0.9320                            | 0.0013     | 0.9346                 | H <sub>2</sub> O: 1.0 g/cc    |
|                                   |            |                        |                               |
| <b>External Moderator Varying</b> |            |                        |                               |
| <b>k<sub>KENO</sub></b>           | <b>1 σ</b> | <b>k<sub>eff</sub></b> | <b>Description</b>            |
| 0.9355                            | 0.0011     | 0.9377                 | H <sub>2</sub> O: 0.0001 g/cc |
| 0.9332                            | 0.0013     | 0.9358                 | H <sub>2</sub> O: 0.05 g/cc   |
| 0.9341                            | 0.0012     | 0.9365                 | H <sub>2</sub> O: 0.1 g/cc    |
| 0.9351                            | 0.0014     | 0.9379                 | H <sub>2</sub> O: 0.2 g/cc    |
| 0.9353                            | 0.0013     | 0.9379                 | H <sub>2</sub> O: 0.3 g/cc    |
| 0.9338                            | 0.0013     | 0.9364                 | H <sub>2</sub> O: 0.4 g/cc    |
| 0.9327                            | 0.0012     | 0.9351                 | H <sub>2</sub> O: 0.5 g/cc    |
| 0.9322                            | 0.0013     | 0.9348                 | H <sub>2</sub> O: 0.6 g/cc    |
| 0.9350                            | 0.0012     | 0.9374                 | H <sub>2</sub> O: 0.7 g/cc    |
| 0.9332                            | 0.0013     | 0.9358                 | H <sub>2</sub> O: 0.8 g/cc    |
| 0.9347                            | 0.0013     | 0.9373                 | H <sub>2</sub> O: 0.9 g/cc    |
| 0.9320                            | 0.0013     | 0.9346                 | H <sub>2</sub> O: 1.0 g/cc    |

**Table A.6.4-6**  
**Damaged Fuel, Rod Pitch Varying Results - <sup>10</sup>B Areal density of 0.068 g/cm<sup>2</sup>**

| <b>k<sub>KENO</sub></b> | <b>1 <math>\sigma</math></b> | <b>k<sub>eff</sub></b> | <b>Pitch (inches)</b> |
|-------------------------|------------------------------|------------------------|-----------------------|
| 0.7002                  | 0.0011                       | 0.7024                 | 0.380                 |
| 0.7900                  | 0.0012                       | 0.7924                 | 0.4200                |
| 0.8671                  | 0.0011                       | 0.8693                 | 0.4600                |
| 0.9268                  | 0.0012                       | 0.9292                 | 0.5000                |
| 0.9471                  | 0.0013                       | 0.9497                 | 0.5160                |
| 0.9550                  | 0.0014                       | 0.9578                 | 0.5260                |
| 0.9663                  | 0.0013                       | 0.9689                 | 0.5360                |
| 0.9741                  | 0.0013                       | 0.9767                 | 0.5460                |
| <b>0.9774</b>           | <b>0.0012</b>                | <b>0.9798</b>          | <b>0.5510</b>         |

**Table A.6.4-7**  
**Damaged Fuel, Rod Pitch Varying Results with Rod Addition or Subtraction**

| $k_{KENO}$                                  | $1 \sigma$    | $k_{eff}$     | Pitch (inches) | Rods Added or Subtracted |
|---|---------------|---------------|----------------|--------------------------|
| 0.9751                                      | 0.0011        | 0.9773        | 0.5510         | 20                       |
| 0.9759                                      | 0.0014        | 0.9787        | 0.5510         | 15                       |
| 0.9790                                      | 0.0013        | 0.9816        | 0.5510         | 14                       |
| 0.9796                                      | 0.0011        | 0.9818        | 0.5510         | 10                       |
| 0.9783                                      | 0.0011        | 0.9805        | 0.5510         | 5                        |
| 0.9785                                      | 0.0013        | 0.9811        | 0.5510         | 4                        |
| 0.9774                                      | 0.0012        | 0.9798        | 0.5510         | 0                        |
| 0.9773                                      | 0.0012        | 0.9797        | 0.5510         | -2                       |
| 0.9769                                      | 0.0012        | 0.9793        | 0.5510         | -4                       |
| 0.9771                                      | 0.0012        | 0.9795        | 0.5510         | -6                       |
| 0.9777                                      | 0.0013        | 0.9803        | 0.5510         | -8                       |
| 0.9774                                      | 0.0013        | 0.9800        | 0.5510         | -10                      |
| 0.9802                                      | 0.0012        | 0.9826        | 0.5510         | -12                      |
| 0.9804                                      | 0.0013        | 0.9830        | 0.5510         | -14                      |
| <b>0.9847</b>                               | <b>0.0012</b> | <b>0.9871</b> | <b>0.5510</b>  | <b>-16</b>               |
| 0.9798                                      | 0.0011        | 0.9820        | 0.5510         | -18                      |
| 0.9806                                      | 0.0011        | 0.9828        | 0.5510         | -20                      |
| <b>Cases for the 9x9 Rod Storage Basket</b> |               |               |                |                          |
| 0.7061                                      | 0.0013        | 0.7087        | 0.5510         | 0                        |
| 0.7930                                      | 0.0013        | 0.7956        | 1.0330         | 0                        |

**Table A.6.4-8  
Damaged Fuel, Single-ended Shear**

| $k_{KENO}$ | $1 \sigma$ | $k_{eff}$ |
|------------|------------|-----------|
| 0.9271     | 0.0013     | 0.9297    |
| 0.9396     | 0.0013     | 0.9422    |
| 0.9379     | 0.0011     | 0.9401    |
| 0.9413     | 0.0012     | 0.9437    |
| 0.9390     | 0.0013     | 0.9416    |
| 0.9422     | 0.0013     | 0.9448    |
| 0.9395     | 0.0011     | 0.9417    |
| 0.9421     | 0.0011     | 0.9443    |
| 0.9421     | 0.0014     | 0.9449    |
| 0.9415     | 0.0012     | 0.9439    |
| 0.9403     | 0.0013     | 0.9429    |
| 0.9414     | 0.0013     | 0.9440    |
| 0.9429     | 0.0013     | 0.9455    |

**Table A.6.4-9  
Damaged Fuel, Double-ended Shear**

| $k_{KENO}$ | $1 \sigma$ | $k_{eff}$ |
|------------|------------|-----------|
| 0.9423     | 0.0014     | 0.9451    |
| 0.9367     | 0.0013     | 0.9393    |
| 0.9352     | 0.0014     | 0.9380    |
| 0.9368     | 0.0013     | 0.9394    |
| 0.9349     | 0.0011     | 0.9371    |
| 0.9324     | 0.0012     | 0.9348    |

**Table A.6.4-10**  
**Damaged Fuel, Rod Pitch Cases – External Moderator Density Varying**

| $k_{KENO}$    | $1 \sigma$    | $k_{eff}$     | Description                     |
|---------------|---------------|---------------|---------------------------------|
| 0.9807        | 0.0012        | 0.9831        | H <sub>2</sub> O: 0.0001 g/cc   |
| 0.9805        | 0.0012        | 0.9829        | H <sub>2</sub> O: 0.05 g/cc     |
| 0.9829        | 0.0013        | 0.9855        | H <sub>2</sub> O: 0.1 g/cc      |
| 0.9800        | 0.0014        | 0.9828        | H <sub>2</sub> O: 0.2 g/cc      |
| 0.9808        | 0.0011        | 0.9830        | H <sub>2</sub> O: 0.3 g/cc      |
| 0.9823        | 0.0013        | 0.9849        | H <sub>2</sub> O: 0.4 g/cc      |
| 0.9836        | 0.0013        | 0.9862        | H <sub>2</sub> O: 0.5 g/cc      |
| 0.9808        | 0.0013        | 0.9834        | H <sub>2</sub> O: 0.6 g/cc      |
| 0.9816        | 0.0012        | 0.9840        | H <sub>2</sub> O: 0.7 g/cc      |
| 0.9813        | 0.0012        | 0.9837        | H <sub>2</sub> O: 0.8 g/cc      |
| 0.9800        | 0.0013        | 0.9826        | H <sub>2</sub> O: 0.9 g/cc      |
| <b>0.9847</b> | <b>0.0012</b> | <b>0.9871</b> | <b>H<sub>2</sub>O: 1.0 g/cc</b> |

**Table A.6.4-11**  
**Damaged Fuel, Single Shear Cases – External Moderator Density Varying**

| $k_{KENO}$    | $1 \sigma$    | $k_{eff}$     | Description                     |
|---------------|---------------|---------------|---------------------------------|
| 0.9415        | 0.0012        | 0.9439        | H <sub>2</sub> O: 0.0001 g/cc   |
| 0.9431        | 0.0012        | 0.9455        | H <sub>2</sub> O: 0.05 g/cc     |
| 0.9410        | 0.0011        | 0.9432        | H <sub>2</sub> O: 0.1 g/cc      |
| 0.9408        | 0.0011        | 0.9430        | H <sub>2</sub> O: 0.2 g/cc      |
| 0.9409        | 0.0013        | 0.9435        | H <sub>2</sub> O: 0.3 g/cc      |
| 0.9395        | 0.0013        | 0.9421        | <b>H<sub>2</sub>O: 0.4 g/cc</b> |
| 0.9394        | 0.0011        | 0.9416        | H <sub>2</sub> O: 0.5 g/cc      |
| 0.9408        | 0.0015        | 0.9438        | H <sub>2</sub> O: 0.6 g/cc      |
| 0.9412        | 0.0011        | 0.9434        | H <sub>2</sub> O: 0.7 g/cc      |
| <b>0.9426</b> | <b>0.0015</b> | <b>0.9456</b> | H <sub>2</sub> O: 0.8 g/cc      |
| 0.9426        | 0.0014        | 0.9454        | H <sub>2</sub> O: 0.9 g/cc      |
| 0.9429        | 0.0013        | 0.9455        | H <sub>2</sub> O: 1.0 g/cc      |

**Table A.6.4-12  
Damaged Fuel, Double Shear Cases – External Moderator Density Varying**

| $k_{KENO}$    | $1 \sigma$    | $k_{eff}$     | Description                     |
|---------------|---------------|---------------|---------------------------------|
| 0.9390        | 0.0012        | 0.9414        | H <sub>2</sub> O: 0.0001 g/cc   |
| 0.9394        | 0.0012        | 0.9418        | H <sub>2</sub> O: 0.05 g/cc     |
| 0.9411        | 0.0016        | 0.9443        | H <sub>2</sub> O: 0.1 g/cc      |
| 0.9387        | 0.0014        | 0.9415        | H <sub>2</sub> O: 0.2 g/cc      |
| 0.9405        | 0.0013        | 0.9431        | H <sub>2</sub> O: 0.3 g/cc      |
| 0.9420        | 0.0013        | 0.9446        | H <sub>2</sub> O: 0.4 g/cc      |
| 0.9389        | 0.0013        | 0.9415        | H <sub>2</sub> O: 0.5 g/cc      |
| 0.9384        | 0.0012        | 0.9408        | H <sub>2</sub> O: 0.6 g/cc      |
| 0.9390        | 0.0013        | 0.9416        | H <sub>2</sub> O: 0.7 g/cc      |
| 0.9410        | 0.0014        | 0.9438        | <b>H<sub>2</sub>O: 0.8 g/cc</b> |
| 0.9397        | 0.0011        | 0.9419        | H <sub>2</sub> O: 0.9 g/cc      |
| <b>0.9423</b> | <b>0.0014</b> | <b>0.9451</b> | H <sub>2</sub> O: 1.0 g/cc      |

**Table A.6.4-13  
Damaged Fuel, Bare Fuel Added**

| $k_{KENO}$    | $1 \sigma$    | $k_{eff}$     | Description  |
|---------------|---------------|---------------|--|
| <b>0.9564</b> | <b>0.0014</b> | <b>0.9592</b> | <b>extra bare rods added</b>   |
| 0.9353        | 0.0013        | 0.9379        | bare pellets added above the boral sheet height, 0.025 g/cm <sup>2</sup> <sup>10</sup> B |
| 0.9333        | 0.0015        | 0.9363        | bare pellets added above the boral sheet height, 0.068 g/cm <sup>2</sup> <sup>10</sup> B |

**Table A.6.4-14**  
**Summary of Maximum Enrichment for the Damaged Fuel Assemblies**

| $k_{KENO}$ | $1 \sigma$ | $k_{eff}$ | Description  | Enrich                      |
|------------|------------|-----------|--|-----------------------------|
| 0.9360     | 0.0011     | 0.9382    | 4 damaged assemblies,<br>NOC cask                        | 4.85 (Intact)<br>4.85 (Dam) |
| 0.9337     | 0.0012     | 0.9361    | 4 damaged assemblies,<br>NOC cask                        | 4.10 (Intact)<br>4.10 (Dam) |
| 0.9367     | 0.0012     | 0.9391    | 12 damaged assemblies,<br>NOC cask                       | 4.85 (Intact)<br>4.10 (Dam) |
| 0.9369     | 0.0012     | 0.9393    | 12 damaged assemblies,<br>NOC cask                       | 4.10 (Intact)<br>3.70 (Dam) |
| 0.9340     | 0.0014     | 0.9368    | 12 damaged assemblies w/<br>5 poison rodlet, NOC cask    | 4.85 (Intact)<br>4.85 (Dam) |
| 0.9315     | 0.0013     | 0.9341    | 12 damaged assemblies w/<br>1 poison rodlet, NOC cask    | 4.10 (Intact)<br>4.10 (Dam) |
| 0.9354     | 0.0012     | 0.9378    | 12 damaged assemblies w/<br>5 poison rodlet, HAC cask    | 4.85 (Intact)<br>4.85 (Dam) |
| 0.9279     | 0.0013     | 0.9305    | 12 damaged assemblies w/<br>1 poison rodlet, HAC cask    | 4.10 (Intact)<br>4.10 (Dam) |
| 0.9353     | 0.0016     | 0.9385    | 12 damaged, HAC, Assy # 1<br>missing, 5 poison rodlets   | 4.85 (Intact)<br>4.85 (dam) |
| 0.9339     | 0.0016     | 0.9371    | 12 damaged, HAC, Assy # 2<br>missing, 5 poison rodlets   | 4.85 (Intact)<br>4.85 (dam) |
| 0.9341     | 0.0014     | 0.9369    | 12 damaged, HAC, Assy # 3<br>missing, 5 poison rodlets   | 4.85 (Intact)<br>4.85 (dam) |
| 0.4356     | 0.0005     | 0.4366    | 4 damaged, NOC, dry case                                 | 4.10 (Intact)<br>4.10 (dam) |
| 0.4177     | 0.0006     | 0.4189    | 12 damaged, NOC dry case                                 | 4.10 (Intact)<br>3.70 (dam) |
| 0.4203     | 0.0005     | 0.4213    | 12 damaged, NOC, 1 poison<br>rodlet, dry case            | 4.10 (Intact)<br>4.10 (dam) |
| 0.4157     | 0.0005     | 0.4167    | 4 damaged, NOC, dry case                                 | 4.85 (Intact)<br>4.85 (dam) |
| 0.3954     | 0.0005     | 0.3964    | 12 damaged, NOC dry case                                 | 4.85 (Intact)<br>4.10 (dam) |
| 0.3961     | 0.0005     | 0.3971    | 12 damaged, NOC, 5 poison<br>rodlets at min OD, dry case | 4.85 (Intact)<br>4.85 (dam) |

**Table A.6.4-15  
Empty Fuel Assembly Locations**

| $k_{KENO}$ | $1\sigma$ | $k_{eff}$ | Description                |
|------------|-----------|-----------|----------------------------|
| 0.9359     | 0.0013    | 0.9385    | 0 empty assembly positions |
| 0.9228     | 0.0013    | 0.9254    | 1 empty assembly positions |
| 0.9140     | 0.0012    | 0.9164    | 2 empty assembly positions |
| 0.9045     | 0.0013    | 0.9071    | 3 empty assembly positions |
| 0.9010     | 0.0011    | 0.9032    | 4 empty assembly positions |

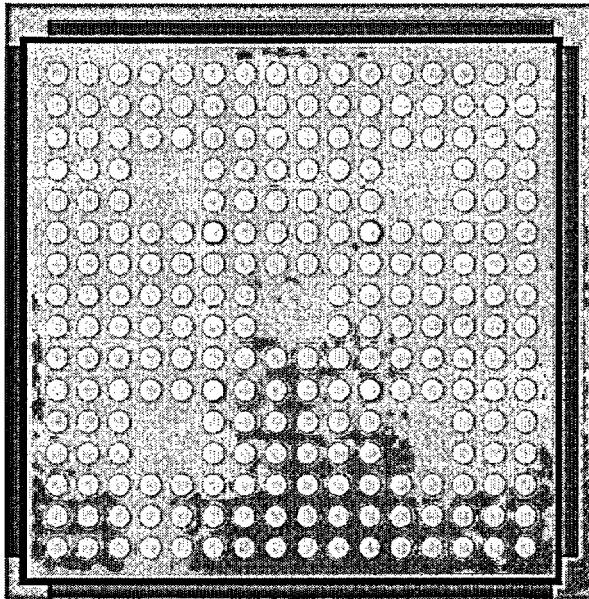
**Table A.6.4-16  
Reconstituted Fuel Assemblies**

| $k_{KENO}$ | $1\sigma$ | $k_{eff}$ | Description           |
|------------|-----------|-----------|-----------------------|
| 0.9359     | 0.0013    | 0.9385    | 0 reconstituted rods  |
| 0.9255     | 0.0011    | 0.9277    | 2 reconstituted rods  |
| 0.9226     | 0.0013    | 0.9252    | 4 reconstituted rods  |
| 0.9151     | 0.0013    | 0.9177    | 6 reconstituted rods  |
| 0.9092     | 0.0014    | 0.9120    | 8 reconstituted rods  |
| 0.9039     | 0.0012    | 0.9063    | 10 reconstituted rods |

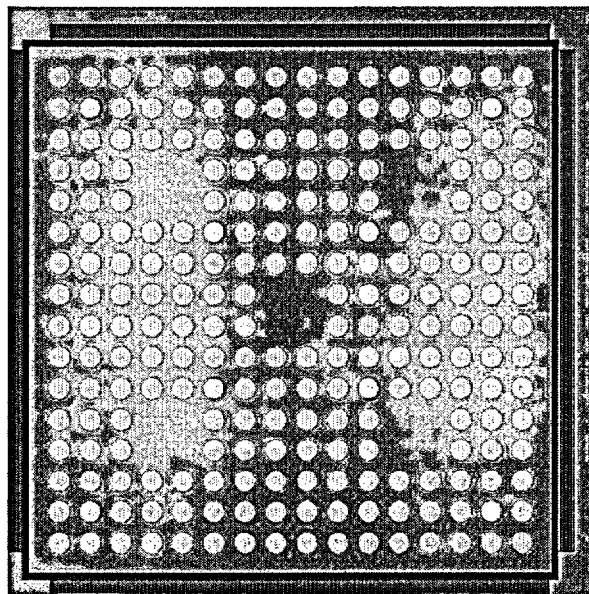
**Table A.6.4-17  
Storage Requirements by Fuel Enrichment**

|  |       |       |                                  |                                  |                                       |                                       |                                       |                                       |
|--|-------|-------|----------------------------------|----------------------------------|---------------------------------------|---------------------------------------|---------------------------------------|---------------------------------------|
| Intact Fuel Maximum Enrichment (%)                                     | 4.85  | 4.1   | 4.85                             | 4.1                              | 4.1                                   | 4.85                                  | 4.1                                   | 4.85                                  |
| Failed Fuel Maximum Enrichment (%)                                     | N/A   | N/A   | 4.85                             | 4.1                              | 3.7                                   | 4.1                                   | 4.1                                   | 4.85                                  |
| Maximum Number of Damaged Fuel Assemblies                              | N/A   | N/A   | 4<br>(Figure A.6.4-13)<br>Zone A | 4<br>(Figure A.6.4-13)<br>Zone A | 12<br>(Figure A.6.4-13)<br>Zone A & B |
| DSC Minimum Bora <sup>®</sup> Panel Areal Density (g/cm <sup>2</sup> ) | 0.068 | 0.025 | 0.068                            | 0.025                            | 0.025                                 | 0.068                                 | 0.025                                 | 0.068                                 |
| Minimum Number of Poison Rodlets Required <sup>(1)</sup>               | N/A   | N/A   | 0                                | 0                                | 0                                     | 0                                     | 1<br>(in center guide tube)           | 5<br>(in all five guide tubes)        |

Note: (1) For intact fuel assemblies located in Figure A.6.4-13, Zone C.

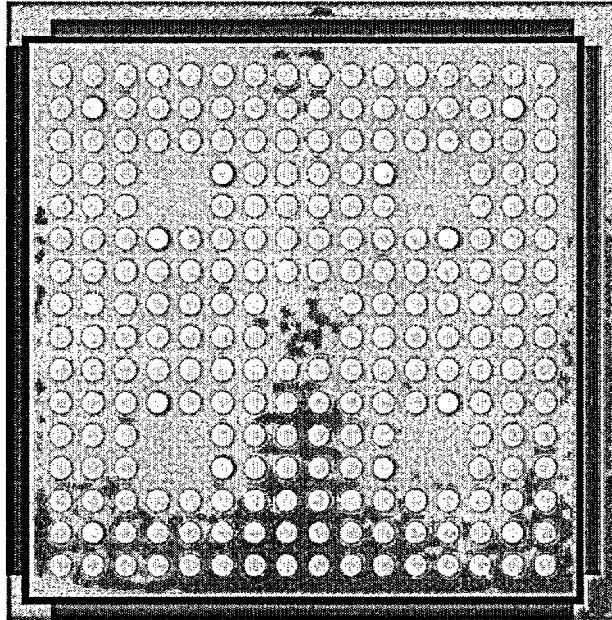


**4 Burnable Absorber Rods**

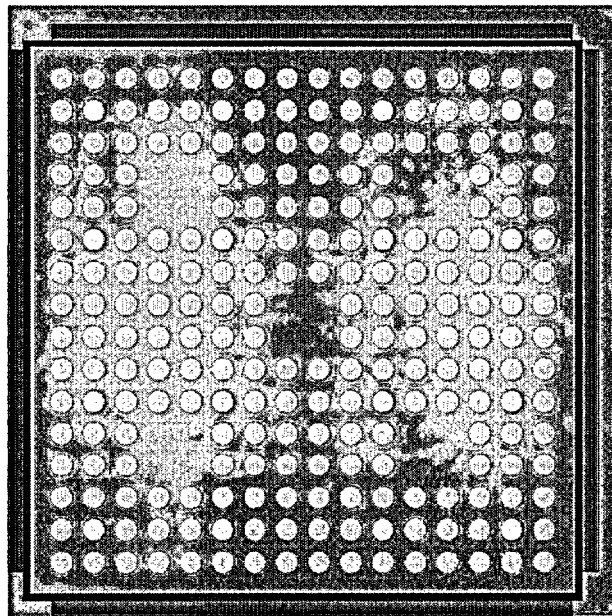


**8 Burnable Absorber Rods**

**Figure A.6.4-1**  
**Fuel Assembly Cross Section Showing the Burnable Absorber Rod Configuration**  
**(continued)**



**12 Burnable Absorber Rods**



**16 Burnable Absorber Rods**

**Figure A.6.4-1  
Fuel Assembly Cross Section Showing the Burnable Absorber Rod Configuration**

(concluded)

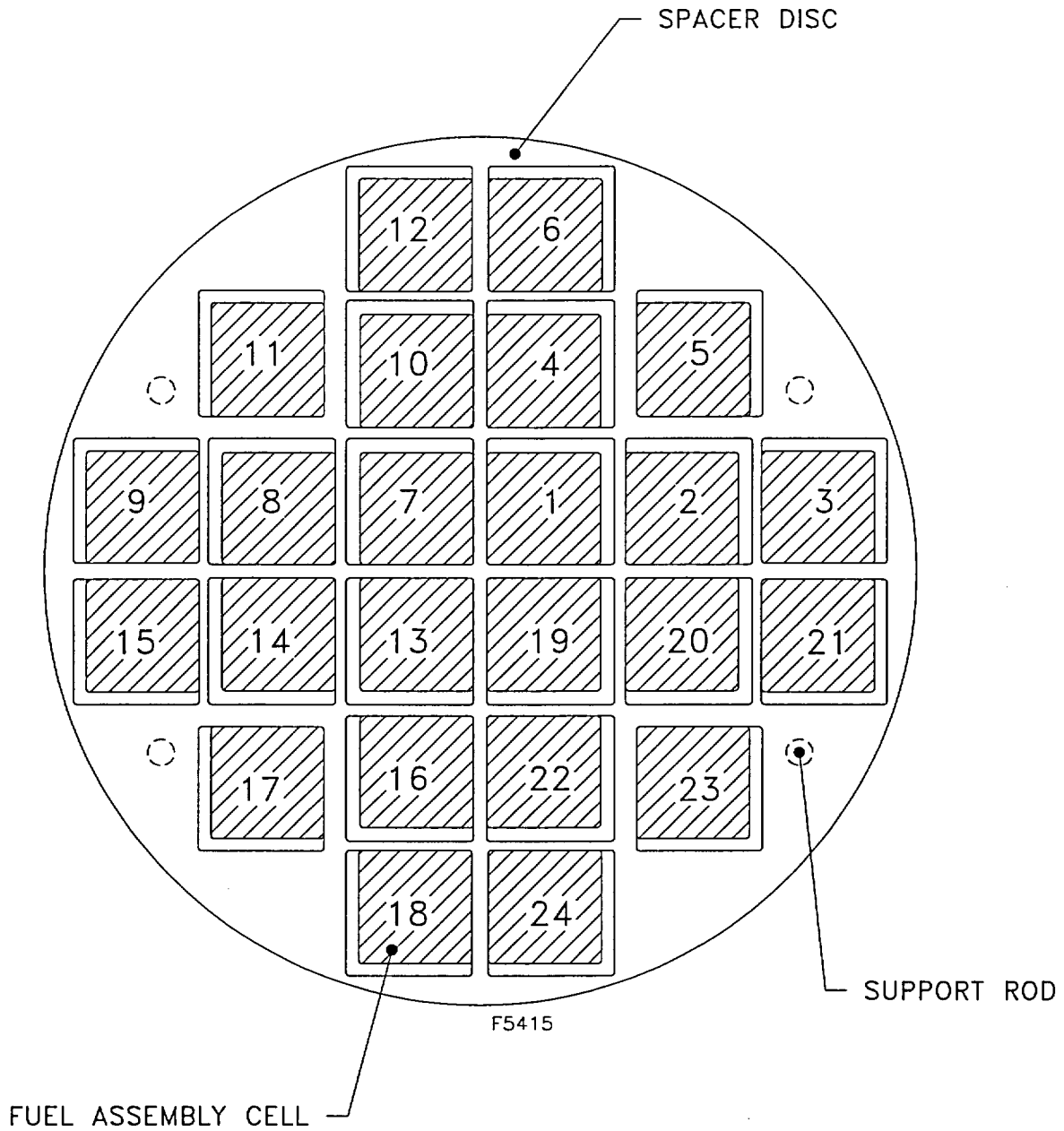


**Figure A.6.4-2**  
**Fuel Assemblies Located in the Inner Guidesleeve Corner Closest to the DSC Centerline (Assembly in Case)**

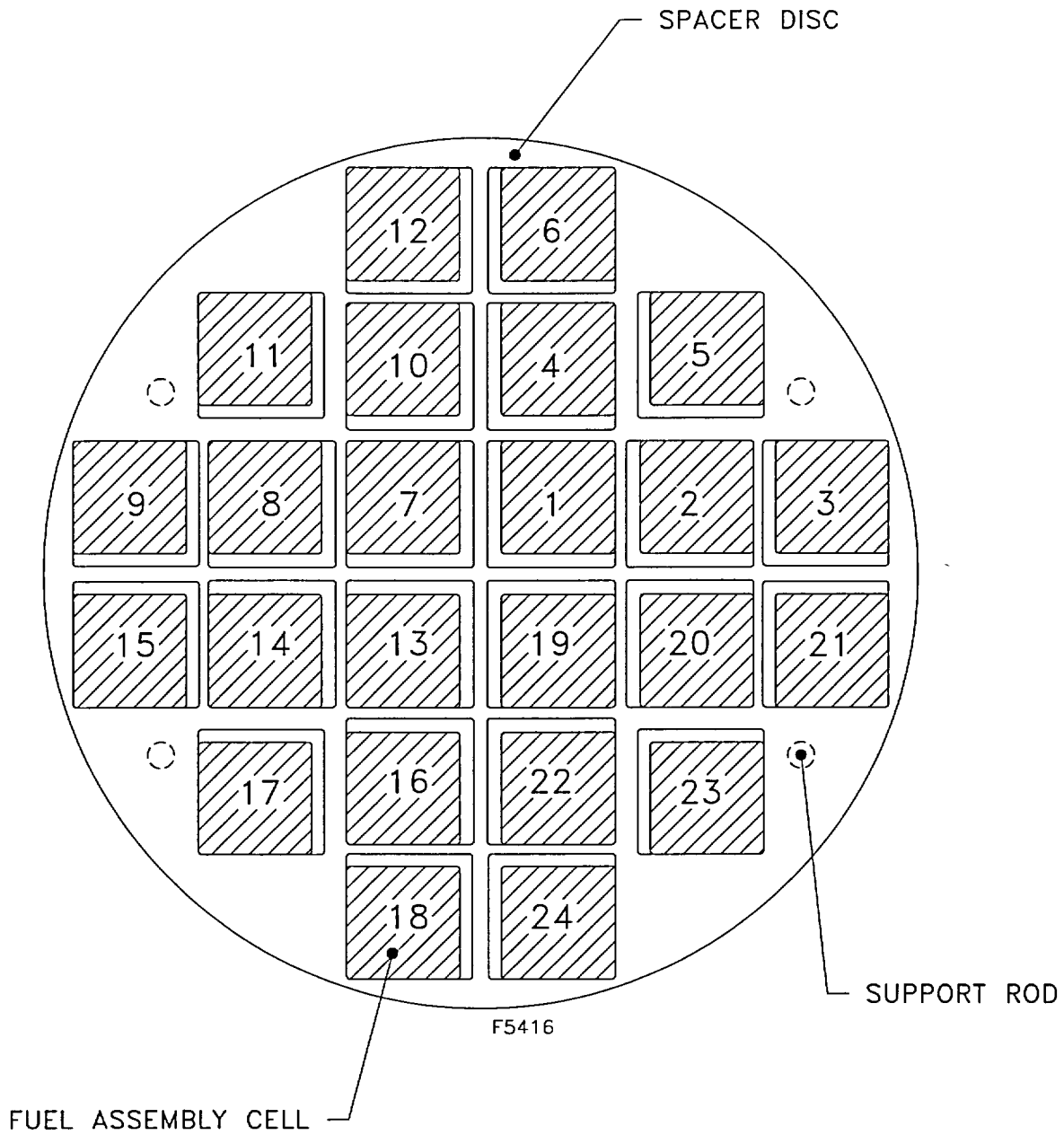


**Figure A.6.4-3**  
**Fuel Assemblies Moved Radially Outwards from the Center**  
**of the 24PT4-DSC (Assembly Out Case)**

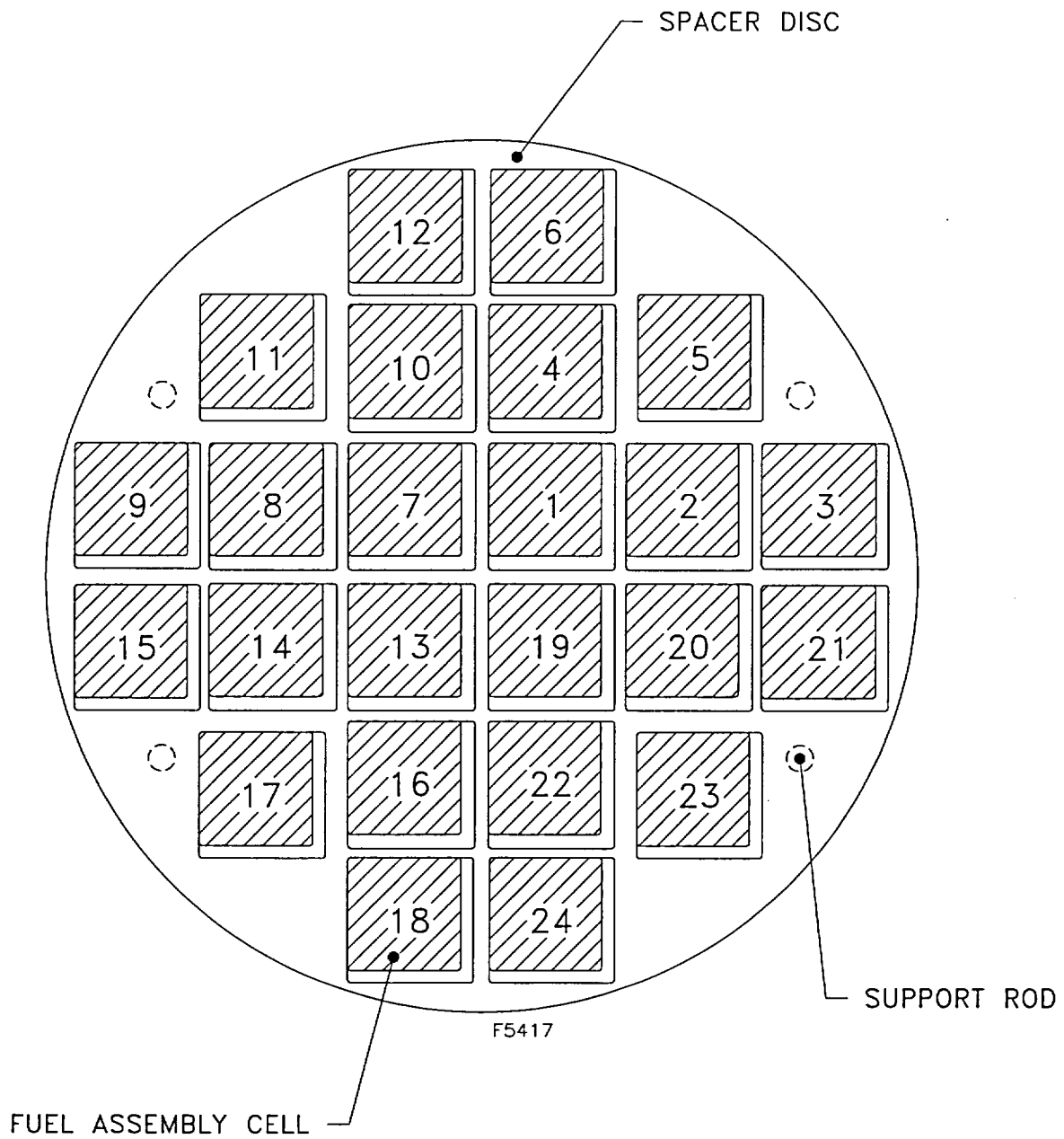


**Figure A.6.4-4**  
**Fuel Assemblies Moved Towards the Upper Left Corner of Each**  
**Guidesleeve Assembly Upper Left Corner Case**

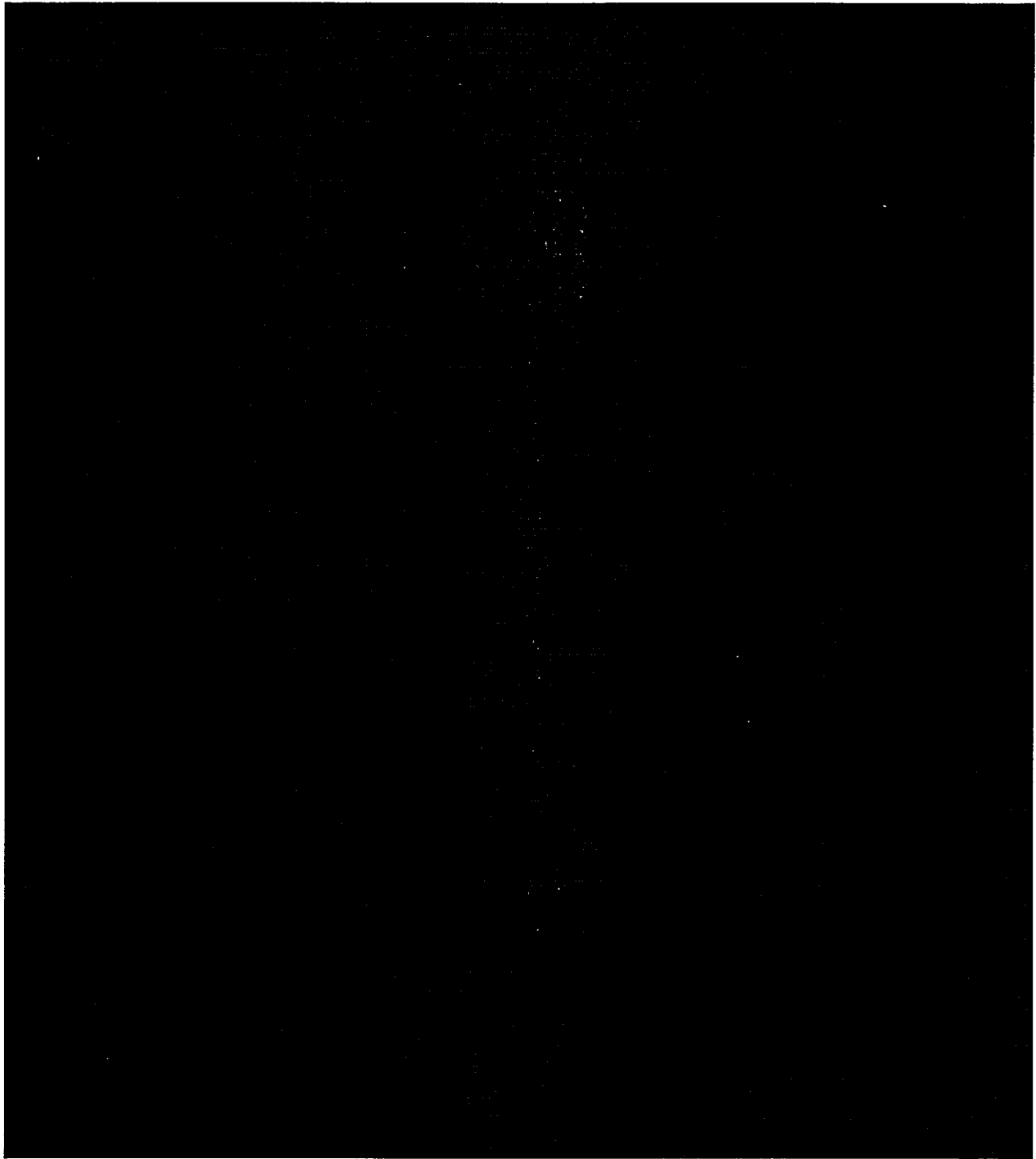


**Figure A.6.4-5**  
**Single-ended Shear Model**

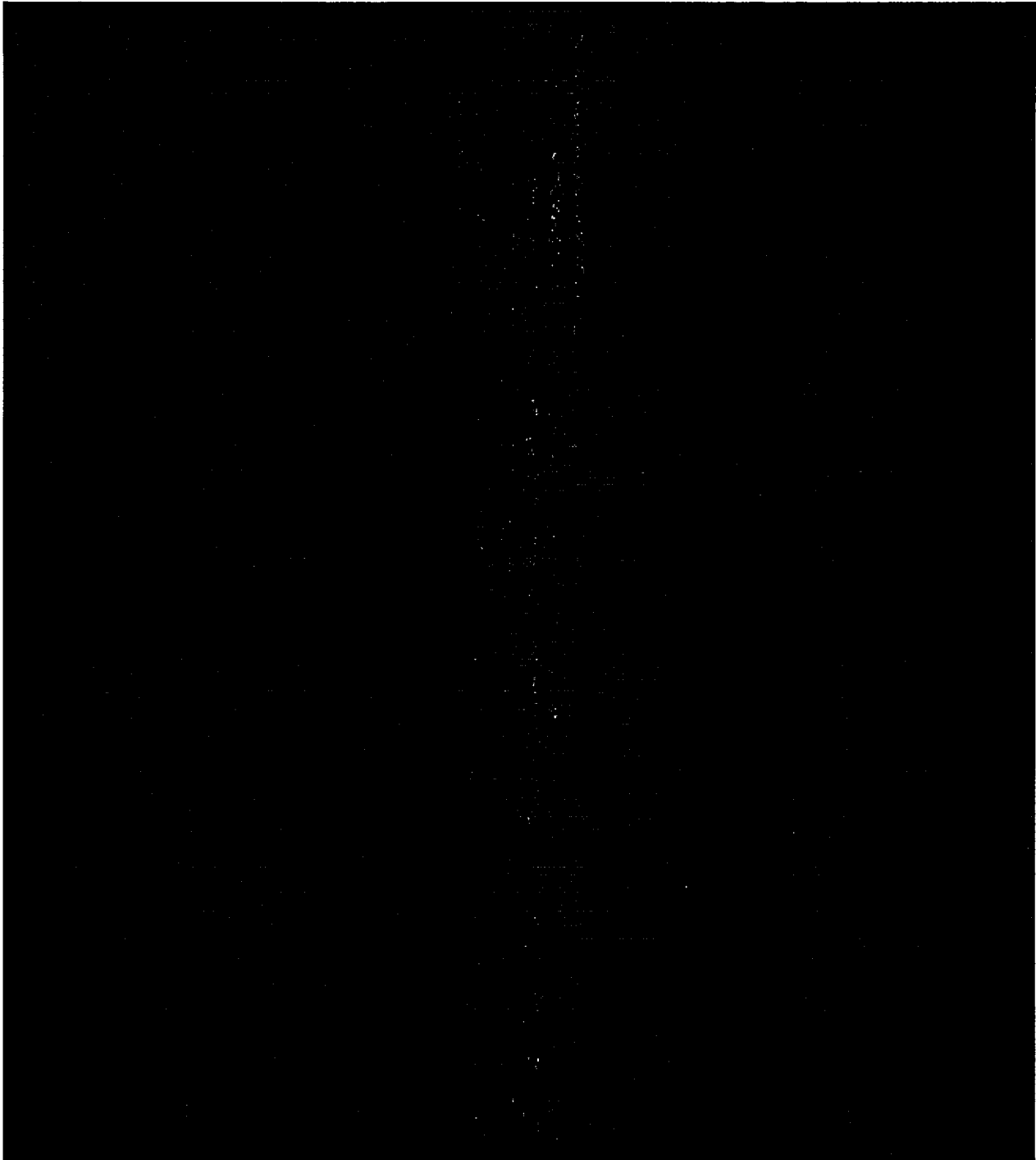


**Figure A.6.4-6**  
**Double-ended Shear Model**

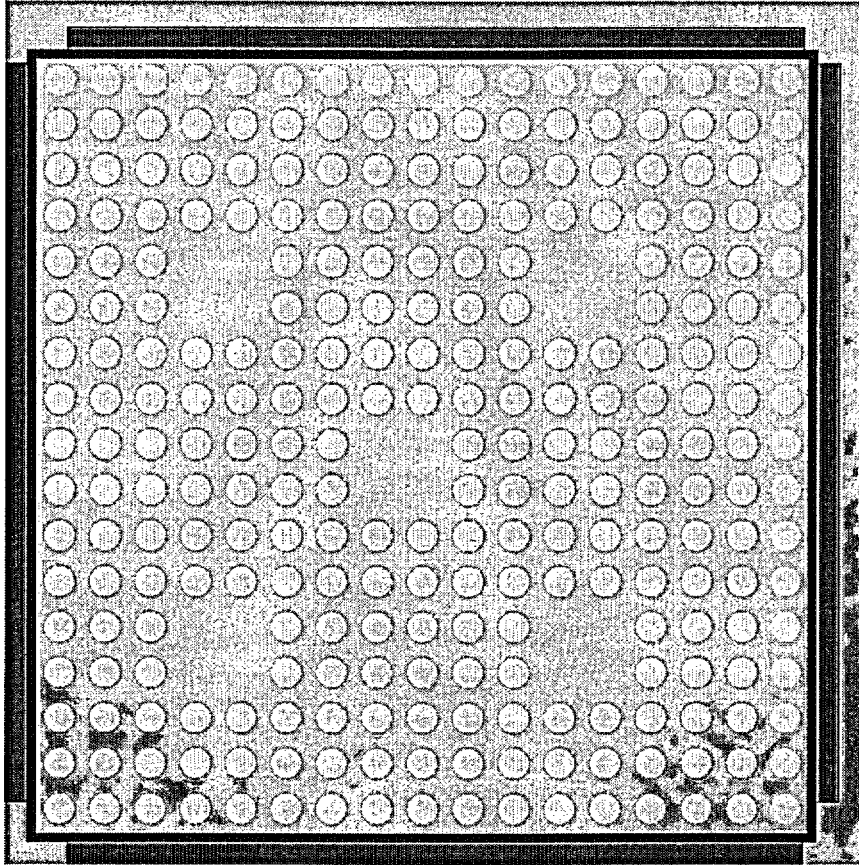


**Figure A.6.4-7**  
**Geometry with Bare Fuel Rods Added**

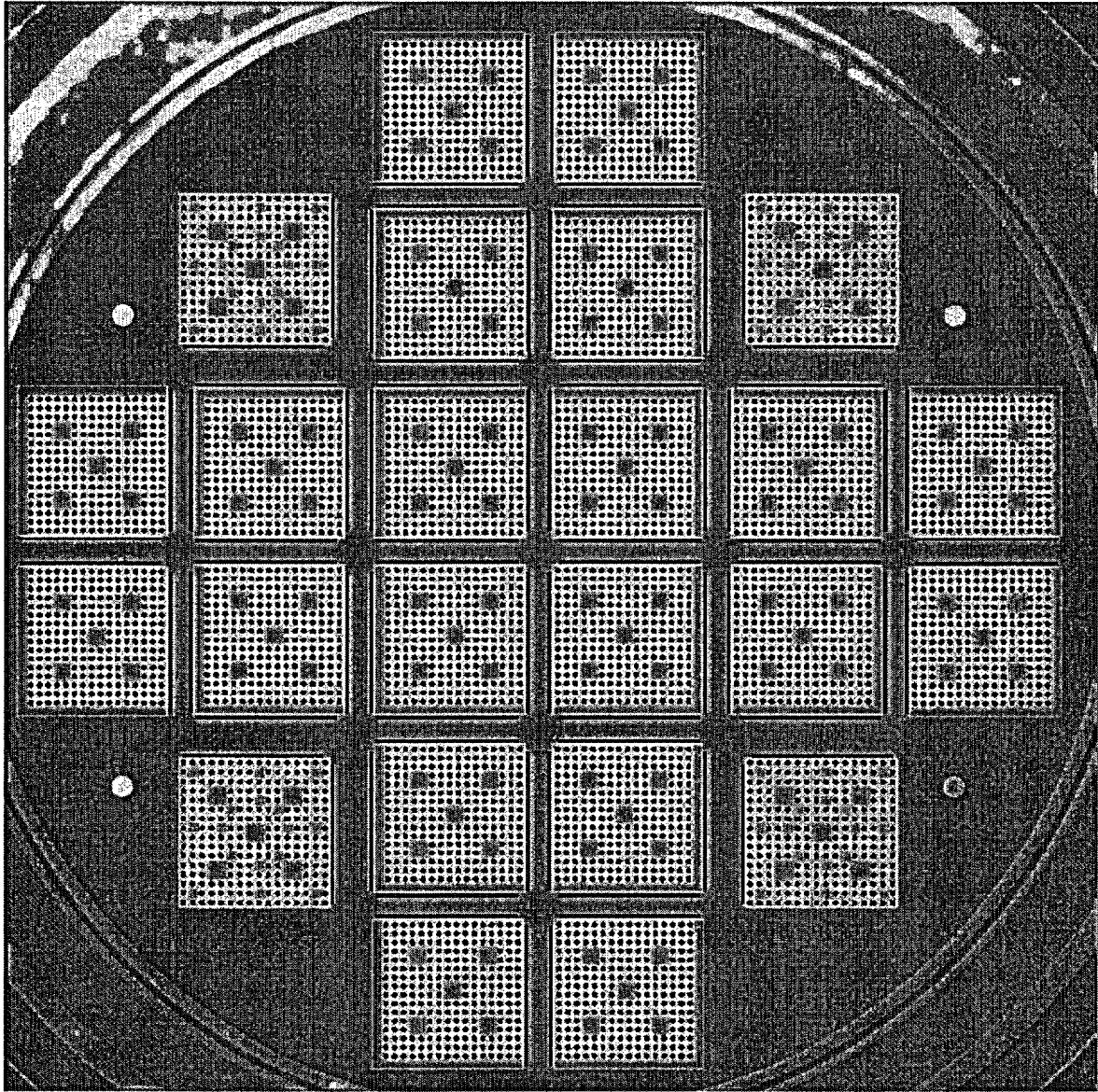


**Figure A.6.4-8**  
**Loading Pattern for 4 Damaged Fuel Assemblies**

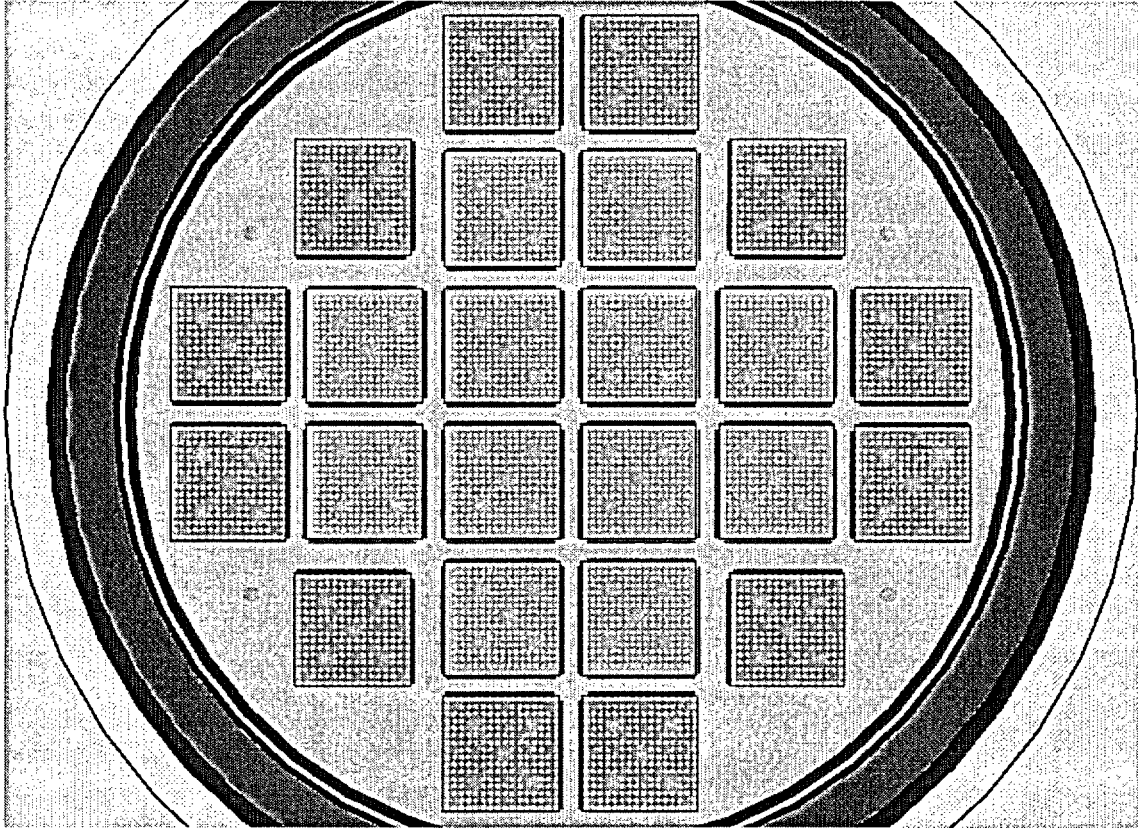


**Figure A.6.4-9**  
**Loading Pattern for 12 Damaged Fuel Assemblies**

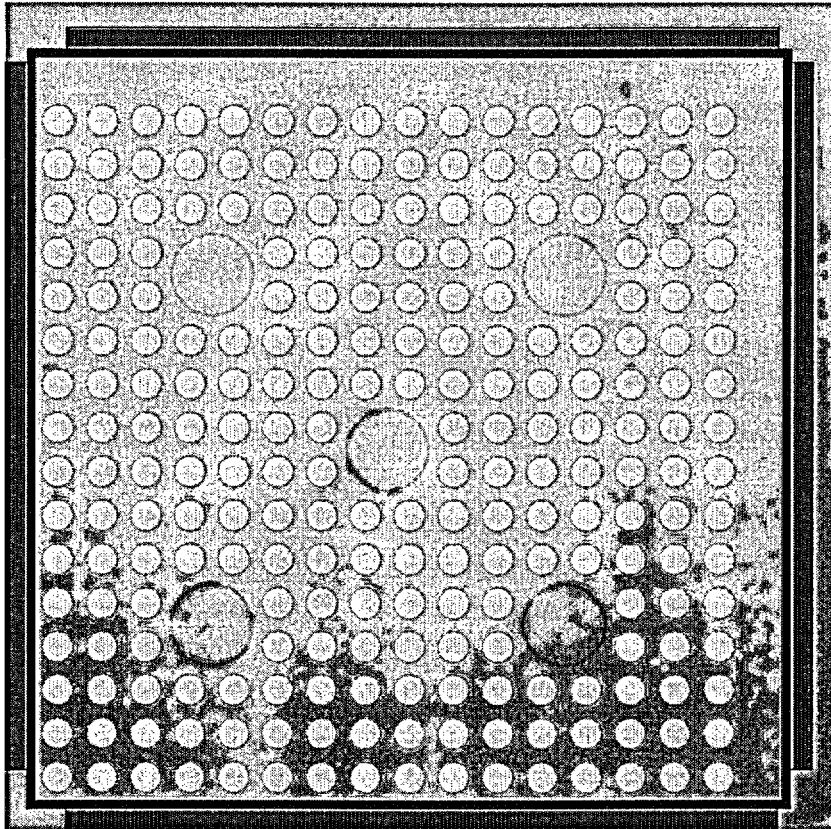


**Figure A.6.4-10**  
**Fuel Assembly with Guide Tubes and Poison Rodlets**

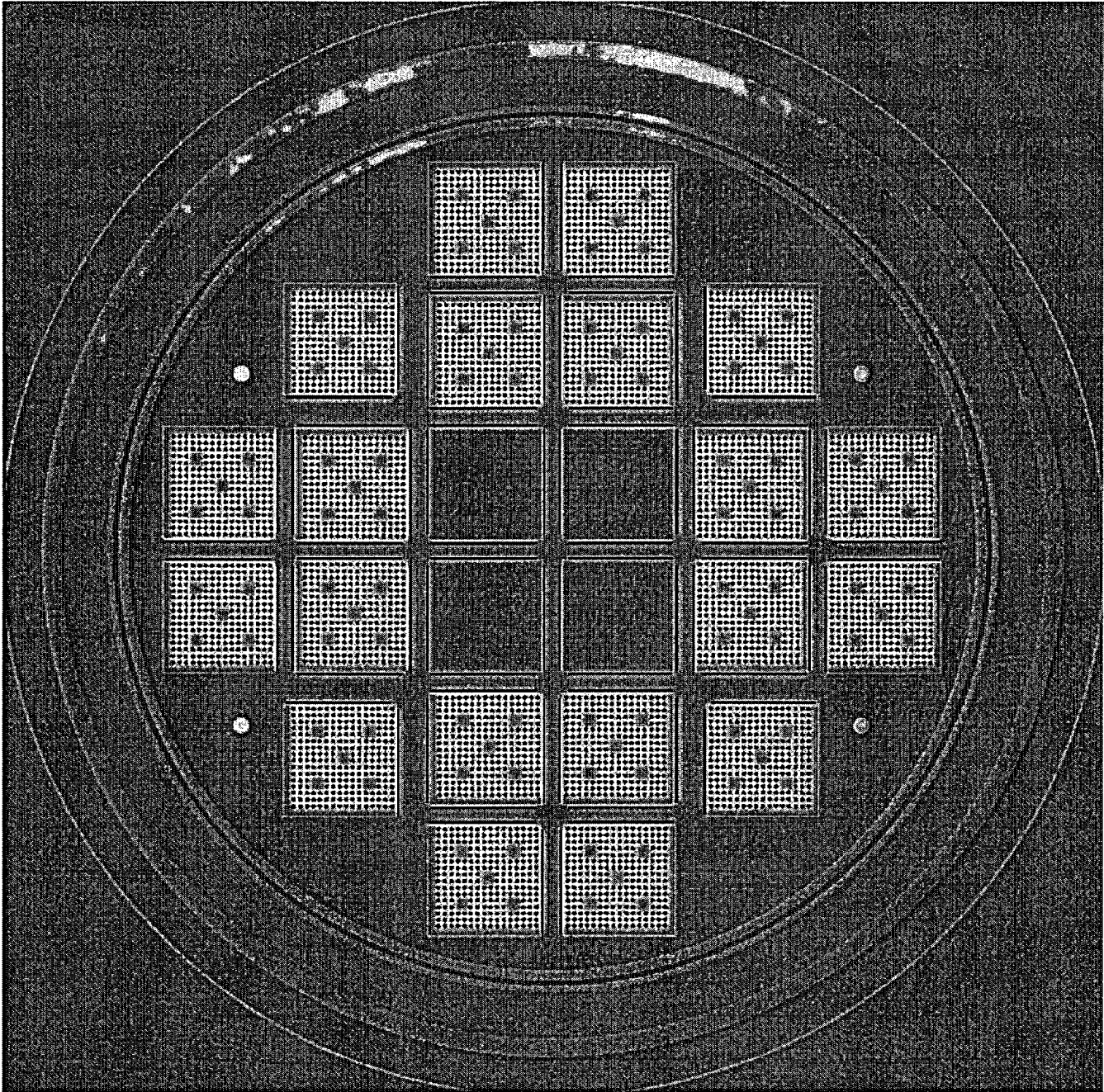


**Figure A.6.4-11**  
**Example of 4 Empty Fuel Assembly Locations**

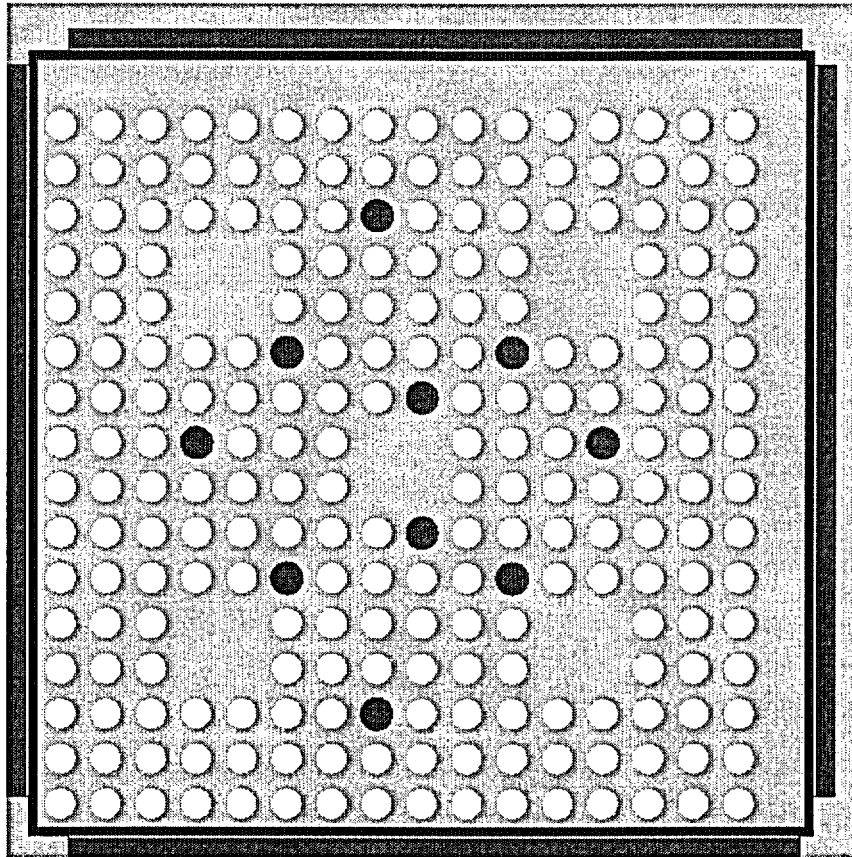
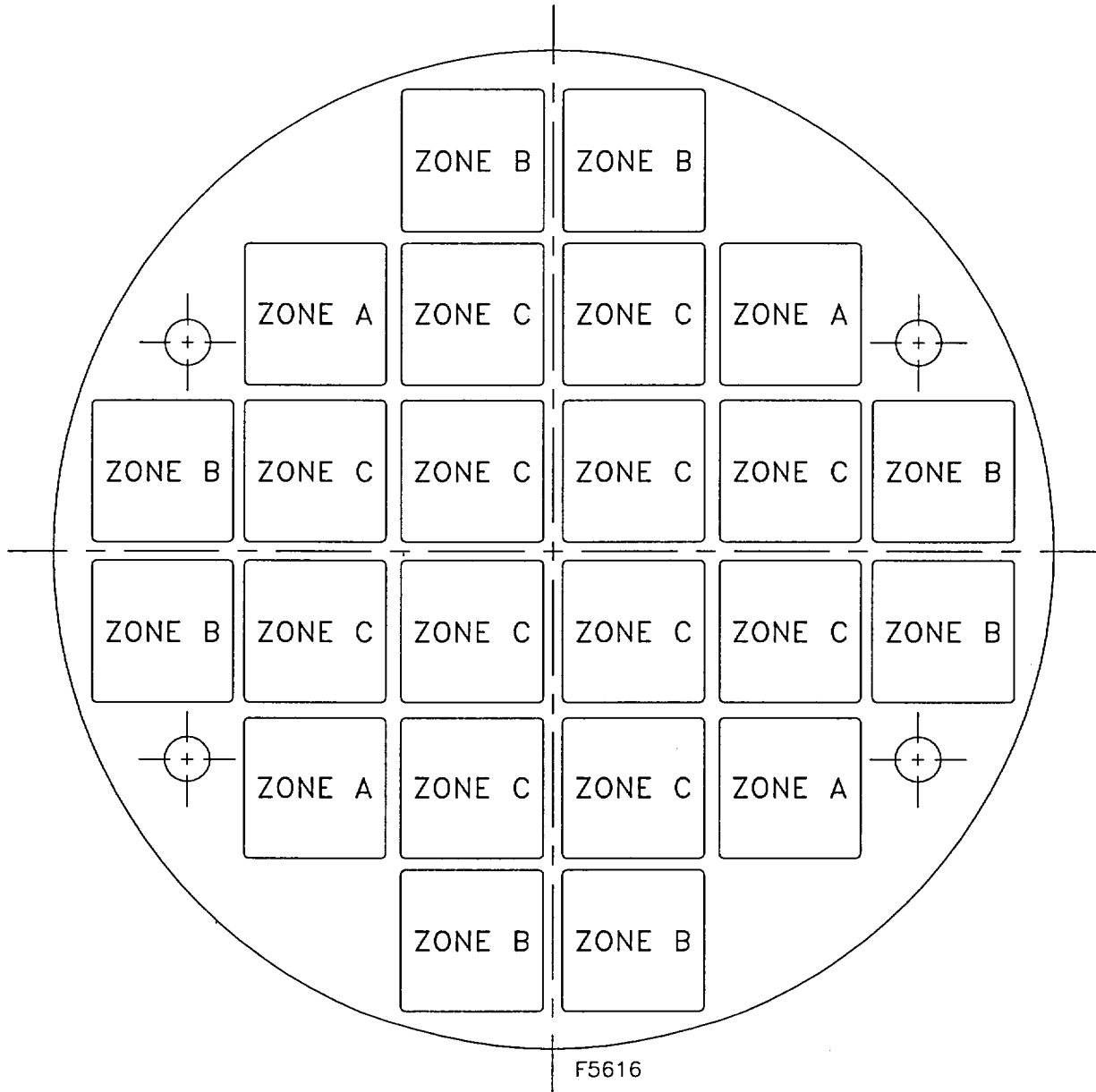


**Figure A.6.4-12**  
**Example of a Reconstituted Fuel Assembly**



1. Locations identified as Zone A are for placement of up to 4 damaged fuel assemblies.
2. Locations identified as Zone B are for placement of up to 8 additional damaged fuel assemblies (Maximum of 12 damaged fuel assemblies allowed, Zones A and B combined).
3. Locations identified as Zone C are for placement of up to 12 intact fuel assemblies, including 4 empty slots in the center as shown in Figure A.2.1-3.
4. Poison Rodlets are to be located in the guide tubes of intact fuel assemblies placed in Zone C only per Table A.2.1-4.

**Figure A.6.4-13**  
**Failed Fuel Cans Positions**

## A.6.5 Critical Benchmark Experiments

The criticality safety analysis presented above used the CSAS25 module of the SCALE system of codes. The CSAS25 control module allows simplified data input to the functional modules BONAMI-S, NITAWL-S, and KENO V.a. These modules process the required cross-section data and calculate the  $k_{\text{eff}}$  of the system. BONAMI-S performs resonance self-shielding calculations for nuclides that have Bondarenko data associated with their cross sections. NITAWL-S applies a Nordheim resonance self-shielding correction to nuclides having resonance parameters. Finally, KENO V.a calculates the effective neutron multiplication ( $k_{\text{eff}}$ ) of a 3-D system.

The analysis uses the fresh fuel assumption for criticality analysis. The analysis employed the 44-group ENDF/B-V cross-section library because it has a small bias, as determined by the 121 benchmark calculations described in Chapter 6 of the FSAR for the 24PT1-DSC. The USL Method 1 (USL-1) was determined using the results of these 121 benchmark calculations.

The benchmark problems used to perform this verification are representative of benchmark arrays of commercial light water reactor (LWR) fuels with the following characteristics:

- water moderation
- boron neutron absorbers
- unirradiated light water reactor type fuel (no fission products or “burnup credit”) near room temperature (vs. reactor operating temperature)
- close reflection
- Uranium Oxide

The 121 uranium oxide experiments were chosen to model a wide range of uranium enrichments, fuel pin pitches, assembly separation, concentration of soluble boron and control elements in order to test the codes ability to accurately calculate  $k_{\text{eff}}$ . These experiments are discussed in detail in Chapter 6. The Run ID referred to in the following sub-sections are identical to those used in Chapter 6.

### A.6.5.1 Benchmark Experiments and Applicability

A summary of all of the pertinent parameters for each experiment is included in Table A.6.5-1 along with the results of each run. The best correlation is observed for fuel assembly separation distance with a correlation of 0.68. All other parameters show much lower correlation ratios, indicating no real correlation. All parameters were evaluated for trends and to determine the most conservative USL.

The USL is calculated in accordance to NUREG/CR-6361 [A6.6]. USL applies a statistical calculation of the bias and its uncertainty plus an administrative margin (0.05) to the linear fit of

results of the experimental benchmark data. The basis for the administrative margin is from NUREG-1536 [A6.13]. Results from the USL evaluation are taken from Chapter 6 and reproduced in Table A.6.5-2.

The criticality evaluation used the same cross section set, fuel materials and similar material/geometry options that were used in the 121 benchmark calculations as shown in Table A.6.5-1. The modeling techniques and the applicable parameters listed in Table A.6.5-2 for the actual criticality evaluations fall within the range of those addressed by the benchmarks in Table A.6.5-1.

#### A.6.5.2 Results of the Benchmark Calculations

The results from the comparisons of physical parameters of each of the fuel assembly types to the applicable USL value are presented in Table A.6.5-3. The minimum value of the USL was determined to be 0.9411 based on comparisons to the limiting assembly parameters as shown in Table A.6.5-2.

**Table A.6.5-1  
Benchmarking Results**

| Run ID               | U Enrich.<br>Wt. % | Pitch<br>(cm) | H <sub>2</sub> O/fuel<br>volume | Separation<br>of<br>assemblies<br>(cm) | AEG <sup>(1)</sup> | k <sub>eff</sub> | 1σ     |
|----------------------|--------------------|---------------|---------------------------------|--|--------------------|------------------|--------|
| B1645SO1             | 2.46               | 1.41          | 1.015                           | 1.78                                   | 32.8194            | 0.9967           | 0.0009 |
| B1645SO2             | 2.46               | 1.41          | 1.015                           | 1.78                                   | 32.7584            | 1.0002           | 0.0011 |
| BW1231B1             | 4.02               | 1.511         | 1.139                           |  | 31.1427            | 0.9966           | 0.0012 |
| BW1231B2             | 4.02               | 1.511         | 1.139                           |  | 29.8854            | 0.9972           | 0.0009 |
| BW1273M              | 2.46               | 1.511         | 1.376                           |  | 32.2106            | 0.9965           | 0.0009 |
| BW1484A1             | 2.46               | 1.636         | 1.841                           | 1.64                                   | 34.5304            | 0.9962           | 0.0010 |
| BW1484A2             | 2.46               | 1.636         | 1.841                           | 4.92                                   | 35.1629            | 0.9931           | 0.0010 |
| BW1484B1             | 2.46               | 1.636         | 1.841                           |  | 33.9421            | 0.9979           | 0.0010 |
| BW1484B2             | 2.46               | 1.636         | 1.841                           | 1.64                                   | 34.5820            | 0.9955           | 0.0012 |
| BW1484B3             | 2.46               | 1.636         | 1.841                           | 4.92                                   | 35.2609            | 0.9969           | 0.0011 |
| BW1484C1             | 2.46               | 1.636         | 1.841                           | 1.64                                   | 34.6463            | 0.9931           | 0.0011 |
| BW1484C2             | 2.46               | 1.636         | 1.841                           | 1.64                                   | 35.2422            | 0.9939           | 0.0012 |
| BW1484S1             | 2.46               | 1.636         | 1.841                           | 1.64                                   | 34.5105            | 1.0001           | 0.0010 |
| BW1484S2             | 2.46               | 1.636         | 1.841                           | 1.64                                   | 34.5569            | 0.9992           | 0.0010 |
| BW1484SL             | 2.46               | 1.636         | 1.841                           | 6.54                                   | 35.4151            | 0.9935           | 0.0011 |
| BW1645S1             | 2.46               | 1.209         | 0.383                           | 1.78                                   | 30.1040            | 0.9990           | 0.0010 |
| BW1645S2             | 2.46               | 1.209         | 0.383                           | 1.78                                   | 29.9961            | 1.0037           | 0.0011 |
| BW1810A              | 2.46               | 1.636         | 1.841                           |  | 33.9465            | 0.9984           | 0.0008 |
| BW18 <sup>10</sup> B | 2.46               | 1.636         | 1.841                           |  | 33.9631            | 0.9984           | 0.0009 |
| BW1810C              | 2.46               | 1.636         | 1.841                           |  | 33.1569            | 0.9992           | 0.0010 |
| BW1810D              | 2.46               | 1.636         | 1.841                           |  | 33.0821            | 0.9985           | 0.0013 |
| BW1810E              | 2.46               | 1.636         | 1.841                           |  | 33.1600            | 0.9988           | 0.0009 |
| BW1810F              | 2.46               | 1.636         | 1.841                           |  | 33.9556            | 1.0031           | 0.0011 |
| BW1810G              | 2.46               | 1.636         | 1.841                           |  | 32.9409            | 0.9973           | 0.0011 |
| BW1810H              | 2.46               | 1.636         | 1.841                           |  | 32.9420            | 0.9972           | 0.0011 |
| BW1810I              | 2.46               | 1.636         | 1.841                           |  | 33.9655            | 1.0037           | 0.0009 |
| BW1810J              | 2.46               | 1.636         | 1.841                           |  | 33.1403            | 0.9983           | 0.0011 |
| EPRU65               | 2.35               | 1.562         | 1.196                           |  | 33.9106            | 0.9960           | 0.0011 |
| EPRU65B              | 2.35               | 1.562         | 1.196                           |  | 33.4013            | 0.9993           | 0.0012 |
| EPRU75               | 2.35               | 1.905         | 2.408                           |  | 35.8671            | 0.9958           | 0.0010 |
| EPRU75B              | 2.35               | 1.905         | 2.408                           |  | 35.3043            | 0.9996           | 0.0010 |
| EPRU87               | 2.35               | 2.21          | 3.687                           |  | 36.6129            | 1.0007           | 0.0011 |
| EPRU87B              | 2.35               | 2.21          | 3.687                           |  | 36.3499            | 1.0007           | 0.0011 |
| NSE71SQ              | 4.74               | 1.26          | 1.823                           |  | 33.7610            | 0.9979           | 0.0012 |
| NSE71W1              | 4.74               | 1.26          | 1.823                           |  | 34.0129            | 0.9988           | 0.0013 |
| NSE71W2              | 4.74               | 1.26          | 1.823                           |  | 36.3037            | 0.9957           | 0.0010 |
| P2438BA              | 2.35               | 2.032         | 2.918                           | 5.05                                   | 36.2277            | 0.9979           | 0.0013 |

**Table A.6.5-1**  
**Benchmarking Results**  
(continued)

| Run ID   | U Enrich.<br>Wt. % | Pitch<br>(cm) | H <sub>2</sub> O/fuel<br>volume | Separation<br>of<br>assemblies<br>(cm) | AEG <sup>(1)</sup> | k <sub>eff</sub> | 1σ     |
|----------|--------------------|---------------|---------------------------------|--|--------------------|------------------|--------|
| P2438SLG | 2.35               | 2.032         | 2.918                           | 8.39                                   | 36.2889            | 0.9986           | 0.0012 |
| P2438SS  | 2.35               | 2.032         | 2.918                           | 6.88                                   | 36.2705            | 0.9974           | 0.0011 |
| P2438ZR  | 2.35               | 2.032         | 2.918                           | 8.79                                   | 36.2840            | 0.9987           | 0.0010 |
| P2615BA  | 4.31               | 2.54          | 3.883                           | 6.72                                   | 35.7286            | 1.0019           | 0.0014 |
| P2615SS  | 4.31               | 2.54          | 3.883                           | 8.58                                   | 35.7495            | 0.9952           | 0.0015 |
| P2615ZR  | 4.31               | 2.54          | 3.883                           | 10.92                                  | 35.7700            | 0.9977           | 0.0014 |
| P2827L1  | 2.35               | 2.032         | 2.918                           | 13.72                                  | 36.2526            | 1.0057           | 0.0011 |
| P2827L2  | 2.35               | 2.032         | 2.918                           | 11.25                                  | 36.2908            | 0.9999           | 0.0012 |
| P2827L3  | 4.31               | 2.54          | 3.883                           | 20.78                                  | 35.6766            | 1.0092           | 0.0012 |
| P2827L4  | 4.31               | 2.54          | 3.883                           | 19.04                                  | 35.7131            | 1.0073           | 0.0012 |
| P2827SLG | 2.35               | 2.032         | 2.918                           | 8.31                                   | 36.3037            | 0.9957           | 0.0010 |
| P3314BA  | 4.31               | 1.892         | 1.6                             | 2.83                                   | 33.1881            | 0.9988           | 0.0012 |
| P3314BC  | 4.31               | 1.892         | 1.6                             | 2.83                                   | 33.2284            | 0.9992           | 0.0012 |
| P3314BF1 | 4.31               | 1.892         | 1.6                             | 2.83                                   | 33.2505            | 1.0037           | 0.0013 |
| P3314BF2 | 4.31               | 1.892         | 1.6                             | 2.83                                   | 33.2184            | 1.0009           | 0.0013 |
| P3314BS1 | 2.35               | 1.684         | 1.6                             | 3.86                                   | 34.8594            | 0.9956           | 0.0013 |
| P3314BS2 | 2.35               | 1.684         | 1.6                             | 3.46                                   | 34.8356            | 0.9949           | 0.0010 |
| P3314BS3 | 4.31               | 1.892         | 1.6                             | 7.23                                   | 33.4247            | 0.9970           | 0.0013 |
| P3314BS4 | 4.31               | 1.892         | 1.6                             | 6.63                                   | 33.4162            | 0.9998           | 0.0012 |
| P3314SLG | 4.31               | 1.892         | 1.6                             | 2.83                                   | 34.0198            | 0.9974           | 0.0012 |
| P3314SS1 | 4.31               | 1.892         | 1.6                             | 2.83                                   | 33.9601            | 0.9999           | 0.0012 |
| P3314SS2 | 4.31               | 1.892         | 1.6                             | 2.83                                   | 33.7755            | 1.0022           | 0.0012 |
| P3314SS3 | 4.31               | 1.892         | 1.6                             | 2.83                                   | 33.8904            | 0.9992           | 0.0013 |
| P3314SS4 | 4.31               | 1.892         | 1.6                             | 2.83                                   | 33.7625            | 0.9958           | 0.0011 |
| P3314SS5 | 2.35               | 1.684         | 1.6                             | 7.8                                    | 34.9531            | 0.9949           | 0.0013 |
| P3314SS6 | 4.31               | 1.892         | 1.6                             | 10.52                                  | 33.5333            | 1.0020           | 0.0011 |
| P3314W1  | 4.31               | 1.892         | 1.6                             |  | 34.3994            | 1.0024           | 0.0013 |
| P3314W2  | 2.35               | 1.684         | 1.6                             |  | 35.2167            | 0.9969           | 0.0011 |
| P3314ZR  | 4.31               | 1.892         | 1.6                             | 2.83                                   | 33.9954            | 0.9971           | 0.0013 |
| P3602BB  | 4.31               | 1.892         | 1.6                             | 8.3                                    | 33.3221            | 1.0029           | 0.0013 |
| P3602BS1 | 2.35               | 1.684         | 1.6                             | 4.8                                    | 34.7750            | 1.0027           | 0.0012 |
| P3602BS2 | 4.31               | 1.892         | 1.6                             | 9.83                                   | 33.3679            | 1.0039           | 0.0012 |
| P3602N11 | 2.35               | 1.684         | 1.6                             | 8.98                                   | 34.7438            | 1.0023           | 0.0012 |
| P3602N12 | 2.35               | 1.684         | 1.6                             | 9.58                                   | 34.8391            | 1.0030           | 0.0012 |
| P3602N13 | 2.35               | 1.684         | 1.6                             | 9.66                                   | 34.9337            | 1.0013           | 0.0012 |
| P3602N14 | 2.35               | 1.684         | 1.6                             | 8.54                                   | 35.0282            | 0.9974           | 0.0013 |

**Table A.6.5-1**  
**Benchmarking Results**  
(continued)

| Run ID   | U Enrich.<br>Wt. % | Pitch<br>(cm) | H <sub>2</sub> O/fuel<br>volume | Separation<br>of<br>assemblies<br>(cm) | AEG <sup>(1)</sup> | k <sub>eff</sub> | 1σ     |
|----------|--------------------|---------------|---------------------------------|--|--------------------|------------------|--------|
| P3602N21 | 2.35               | 2.032         | 2.918                           | 10.36                                  | 36.2821            | 0.9987           | 0.0011 |
| P3602N22 | 2.35               | 2.032         | 2.918                           | 11.2                                   | 36.1896            | 1.0025           | 0.0011 |
| P3602N31 | 4.31               | 1.892         | 1.6                             | 14.87                                  | 33.2094            | 1.0057           | 0.0013 |
| P3602N32 | 4.31               | 1.892         | 1.6                             | 15.74                                  | 33.3067            | 1.0093           | 0.0012 |
| P3602N33 | 4.31               | 1.892         | 1.6                             | 15.87                                  | 33.4174            | 1.0107           | 0.0012 |
| P3602N34 | 4.31               | 1.892         | 1.6                             | 15.84                                  | 33.4683            | 1.0045           | 0.0013 |
| P3602N35 | 4.31               | 1.892         | 1.6                             | 15.45                                  | 33.5185            | 1.0013           | 0.0012 |
| P3602N36 | 4.31               | 1.892         | 1.6                             | 13.82                                  | 33.5855            | 1.0004           | 0.0014 |
| P3602N41 | 4.31               | 2.54          | 3.883                           | 12.89                                  | 35.5276            | 1.0109           | 0.0013 |
| P3602N42 | 4.31               | 2.54          | 3.883                           | 14.12                                  | 35.6695            | 1.0071           | 0.0014 |
| P3602N43 | 4.31               | 2.54          | 3.883                           | 12.44                                  | 35.7542            | 1.0053           | 0.0015 |
| P3602SS1 | 2.35               | 1.684         | 1.6                             | 8.28                                   | 34.8701            | 1.0025           | 0.0013 |
| P3602SS2 | 4.31               | 1.892         | 1.6                             | 13.75                                  | 33.4202            | 1.0035           | 0.0012 |
| P3926L1  | 2.35               | 1.684         | 1.6                             | 10.06                                  | 34.8519            | 1.0000           | 0.0011 |
| P3926L2  | 2.35               | 1.684         | 1.6                             | 10.11                                  | 34.9324            | 1.0017           | 0.0011 |
| P3926L3  | 2.35               | 1.684         | 1.6                             | 8.5                                    | 35.0641            | 0.9949           | 0.0012 |
| P3926L4  | 4.31               | 1.892         | 1.6                             | 17.74                                  | 33.3243            | 1.0074           | 0.0014 |
| P3926L5  | 4.31               | 1.892         | 1.6                             | 18.18                                  | 33.4074            | 1.0057           | 0.0013 |
| P3926L6  | 4.31               | 1.892         | 1.6                             | 17.43                                  | 33.5246            | 1.0046           | 0.0013 |
| P3926SL1 | 2.35               | 1.684         | 1.6                             | 6.59                                   | 33.4737            | 0.9995           | 0.0012 |
| P3926SL2 | 4.31               | 1.892         | 1.6                             | 12.79                                  | 33.5776            | 1.0007           | 0.0012 |
| P4267B1  | 4.31               | 1.8901        | 1.59                            |  | 31.8075            | 0.9990           | 0.0010 |
| P4267B2  | 4.31               | 0.89          | 1.59                            |  | 31.5323            | 1.0033           | 0.0010 |
| P4267B3  | 4.31               | 1.715         | 1.09                            |  | 30.9905            | 1.0050           | 0.0011 |
| P4267B4  | 4.31               | 1.715         | 1.09                            |  | 30.5061            | 0.9996           | 0.0011 |
| P4267B5  | 4.31               | 1.715         | 1.09                            |  | 30.1011            | 1.0004           | 0.0011 |
| P4267SL1 | 4.31               | 1.89          | 1.59                            |  | 33.4737            | 0.9995           | 0.0012 |
| P4267SL2 | 4.31               | 1.715         | 1.09                            |  | 31.9460            | 0.9988           | 0.0016 |
| P62FT231 | 4.31               | 1.891         | 1.6                             | 5.67                                   | 32.9196            | 1.0012           | 0.0013 |
| P71F14F3 | 4.31               | 1.891         | 1.6                             | 5.19                                   | 32.8237            | 1.0009           | 0.0014 |
| P71F14V3 | 4.31               | 1.891         | 1.6                             | 5.19                                   | 32.8597            | 0.9972           | 0.0014 |
| P71F14V5 | 4.31               | 1.891         | 1.6                             | 5.19                                   | 32.8609            | 0.9993           | 0.0013 |
| P71F214R | 4.31               | 1.891         | 1.6                             | 5.19                                   | 32.8778            | 0.9969           | 0.0012 |
| PAT80L1  | 4.74               | 1.6           | 3.807                           | 2                                      | 35.0253            | 1.0012           | 0.0012 |
| PAT80L2  | 4.74               | 1.6           | 3.807                           | 2                                      | 35.1136            | 0.9993           | 0.0015 |
| PAT80SS1 | 4.74               | 1.6           | 3.807                           | 2                                      | 35.0045            | 0.9988           | 0.0013 |
| PAT80SS2 | 4.74               | 1.6           | 3.807                           | 2                                      | 35.1072            | 0.9960           | 0.0013 |

**Table A.6.5-1**  
**Benchmarking Results**  
 (concluded)

| Run ID      | U Enrich.<br>Wt. % | Pitch<br>(cm) | H <sub>2</sub> O/fuel<br>volume | Separation<br>of<br>assemblies<br>(cm) | AEG <sup>(1)</sup> | k <sub>eff</sub> | 1σ     |
|-------------|--------------------|---------------|---------------------------------|--|--------------------|------------------|--------|
| W3269A      | 5.7                | 1.422         | 1.93                            |  | 33.1480            | 0.9988           | 0.0012 |
| W3269B1     | 3.7                | 1.105         | 1.432                           |  | 32.4055            | 0.9961           | 0.0011 |
| W3269B2     | 3.7                | 1.105         | 1.432                           |  | 32.3921            | 0.9963           | 0.0011 |
| W3269B3     | 3.7                | 1.105         | 1.432                           |  | 32.2363            | 0.9944           | 0.0011 |
| W3269C      | 2.72               | 1.524         | 1.494                           |  | 33.7727            | 0.9989           | 0.0012 |
| W3269SL1    | 2.72               | 1.524         | 1.494                           |  | 33.3850            | 0.9981           | 0.0014 |
| W3269SL2    | 5.7                | 1.422         | 1.93                            |  | 33.0910            | 1.0005           | 0.0013 |
| W3269W1     | 2.72               | 1.524         | 1.494                           |  | 33.5114            | 0.9966           | 0.0014 |
| W3269W2     | 5.7                | 1.422         | 1.93                            |  | 33.1680            | 1.0014           | 0.0014 |
| W3385SL1    | 5.74               | 1.422         | 1.932                           |  | 33.2387            | 1.0009           | 0.0012 |
| W3385SL2    | 5.74               | 2.012         | 5.067                           |  | 35.8818            | 0.9997           | 0.0013 |
| Correlation | 0.31               | 0.39          | 0.16                            | 0.68                                   | -0.03              | N/A              | N/A    |

(1) AEG = Average Energy Group causing fission

**Table A.6.5-2  
USL-1 Results**

| Parameter                                  | Range of Applicability | USL-1  |
|--|------------------------|--------|
| U Enrichment (wt. % <sup>235</sup> U)      | 2.4                    | 0.9423 |
|  | 2.8                    | 0.9429 |
|  | 3.3                    | 0.9434 |
|  | 3.8–5.7                | 0.9437 |
| Fuel Rod Pitch (cm)                        | 0.89                   | 0.9396 |
|  | 1.1                    | 0.9407 |
|  | 1.2                    | 0.9411 |
|  | 1.4                    | 0.9418 |
|  | 1.6                    | 0.9429 |
|  | 1.8–2.6                | 0.9438 |
| Water/Fuel Volume Ratio                    | 0.38                   | 0.9420 |
|  | 1.1                    | 0.9425 |
|  | 1.7                    | 0.9429 |
|  | 2.4–5.1                | 0.9433 |
| Assembly Separation (cm)                   | 1.4                    | 0.9412 |
|  | 1.6                    | 0.9413 |
|  | 4.4                    | 0.9428 |
|  | 7.1–21                 | 0.9442 |
| Average Energy Group Causing Fission (AEG) | 30–32                  | 0.9434 |
|  | 33                     | 0.9433 |
|  | 34                     | 0.9432 |
|  | 35                     | 0.9431 |
|  | 36                     | 0.9430 |
|  | 37                     | 0.9430 |

**Table A.6.5-3**  
**USL Determination for Criticality Analysis**

| <b>Parameter</b>                           | <b>Value from Limiting Analysis</b> | <b>Bounding USL-1</b> |
|--|-------------------------------------|-----------------------|
| U Enrichment (wt. % <sup>235</sup> U)      | 4.2                                 | 0.9437                |
| Fuel Rod Pitch (cm)                        | 1.28524                             | 0.9411                |
| Water/Fuel Ratio                           | 1.663                               | 0.9425                |
| Assembly Separation (cm)                   | 1.80 – 3.07 (value of 1.60 used)    | 0.9413                |
| Average Energy Group Causing Fission (AEG) | 33.6                                | 0.9433                |

## A.6.6 Supplemental Information

### A.6.6.1 References

- [A6.1] Code of Federal Regulations, Title 10, Part 72, "Licensing Requirements for the Independent Storage of Spent Nuclear Fuel and High-Level Radioactive Waste."
- [A6.2] Code of Federal Regulations, Title 10, Part 71, "Packaging and Transportation of Radioactive Material."
- [A6.3] "SCALE, A Modular Code System for Performing Standardized Computer Analyses for Licensing Evaluation", NUREG/CR-0200, Rev. 6 (ORNL/NUREG/CSD-2/R6), Vol. I-III, September 1998.
- [A6.4] ANSI/ANS 57.2, Design Requirements for Light Water Reactor Spent Fuel Storage Facilities at Nuclear Power Plants, 1983.
- [A6.5] ANS/ANSI-8.1, American National Standard for Nuclear Criticality Safety in Operations with Fissionable Materials Outside Reactors, 1983.
- [A6.6] U.S. Nuclear Regulatory Commission, "Criticality Benchmark Guide for Light-Water-Reactor fuel in Transportation and Storage Packages," NUREG/CR-6361, ORNL-TM-13211, March 1997.
- [A6.7] U.S. Nuclear Regulatory Commission, "Recommendations for Preparing the Criticality Safety Evaluation of Transportation Packages," NUREG/CR-5661, ORNL/TM-11936, April 1997.
- [A6.8] Not used.
- [A6.9] J. J. Duderstadt and L. J. Hamilton, "Nuclear Reactor Analysis," John Wiley and Sons, 1976.
- [A6.10] Burn, Reed R., "Boral™ Accelerated Radiation Aging Tests", Nuclear Reactor Laboratory, University of Michigan, Ann Arbor, Michigan, May 9, 1990.
- [A6.11] American National Standards Institute, ANSI N14.5-1997, Leakage Tests on Packages for Shipment of Radioactive Materials.
- [A6.12] Transnuclear, Safety Analysis Report for the NUHOMS® OS197H Transfer Cask.
- [A6.13] Nuclear Regulatory Commission, NUREG 1536, Standard Review Plan for Dry Cask Storage Systems, January 1997.

A.6.6.2 KENO V.a Input Files

## A.7 CONFINEMENT

### A.7.1 Confinement Boundary

Sections of this Chapter have been identified as “No change” due to the addition of 24PT4-DSC to the Advanced NUHOMS<sup>®</sup> system. For these sections, the description or analysis presented in the corresponding sections of the FSAR for the Advanced NUHOMS<sup>®</sup> system with 24PT1-DSC is also applicable to the system with 24PT4-DSC.

The 24PT4-DSC is a high integrity stainless steel welded vessel that provides confinement of radioactive materials, encapsulates the fuel in a helium atmosphere and provides biological shielding during 24PT4-DSC closure, transfer and storage operations. The 24PT4-DSC is designed to maintain confinement of radioactive material within the limits of 10CFR 72.104(a), 10CFR 72.106(b) and 10CFR 20 under normal, off-normal, and credible accident conditions. Chapters A.3, A.4 and A.11 conclude that the design including the helium atmosphere within the 24PT4-DSC will adequately protect the spent fuel cladding against degradation that might otherwise lead to gross ruptures during storage.

The cylindrical shell, the inner cover plates of the top and bottom shield plug assemblies, the vent and siphon block, the vent and siphon cover plates, and associated welds form the pressure retaining confinement boundary for the spent fuel (see Figure A.7.1-1). The outer top cover plate and associated welds function as a redundant welded barrier for confining radioactive material within the 24PT4-DSC. The dimensions and material descriptions for the confinement boundary assemblies and the redundant welded barriers are discussed in Chapter A.1. The components important to safety are identified in Chapter A.2.

#### A.7.1.1 Confinement Vessel

The cylindrical shell to inner bottom cover plate weld is made during fabrication of the 24PT4-DSC and is fully compliant to ASME Section III [A7.1], Subsection NB. The vent and siphon block to shell weld is also made during fabrication. The inner top cover plate to shell closure weld is made after fuel loading. These top closure welds are fully compliant to ASME Code Case N-595-1. Both top plug penetrations (siphon and vent ports) are welded after drying operations are complete.

Stringent design and fabrication requirements ensure that the confinement function of the 24PT4-DSC is maintained. The shell and inner bottom cover plate are pressure tested in accordance with the ASME Code, Section III, Subarticle NB-6300. This pressure test is performed after installation of the inner bottom cover plate and may be performed concurrently with the leak test, provided the requirements of NB-6300 are met.

Following the pressure test, a leak test of the shell assembly, including the inner bottom cover plate, is performed in accordance with ANSI N14.5 [A7.2]. These tests are typically performed at the fabricator. The acceptance criteria for the test is “leaktight” as defined in ANSI N14.5-1997 [A7.2].

The process involved in leak testing the 24PT4-DSC shell assembly involves temporarily sealing the shell top end. The gas filled envelope and evacuated envelope testing methodologies have

the required test sensitivity to demonstrate leaktight construction and are used for leak testing. A helium mass spectrometer is used to detect any leakage as defined in ANSI N14.5 [A7.2].

During final drying and sealing operations of the 24PT4-DSC, the top closure confinement welds are completed to confine radioactive materials within the cavity. The inner top cover plate is welded to the shell using automated welding equipment. Once the 24PT4-DSC has been vacuum dried, backfilled with helium and vent and siphon port penetrations welded, the outer top cover plate is lowered onto the 24PT4-DSC. The outer top cover plate is welded in place using automated welding equipment. The outer top cover plate and associated closure weld to the shell acts as a redundant barrier for confining radioactive material within the 24PT4-DSC throughout its service life.

Leak testing of the 24PT4-DSC top shield plug assembly to shell weld, vent and siphon cover plate and vent/siphon block to shell welds may be performed by evacuating the volume between the top shield plug assembly and outer top cover plate through a test port in the outer top cover plate and monitoring for helium in accordance with the requirements of ANSI N14.5 [A7.2]. Optionally, an outer top cover plate with no test port may be utilized, although, in this case an independent test fixture with a test port would be utilized for the helium leak test. The test port is welded closed following satisfactory completion of the helium leak test.

#### A.7.1.2 Confinement Penetrations

All penetrations in the 24PT4-DSC confinement boundary are welded closed. The 24PT4-DSC is designed and tested to be "leaktight" as described above.

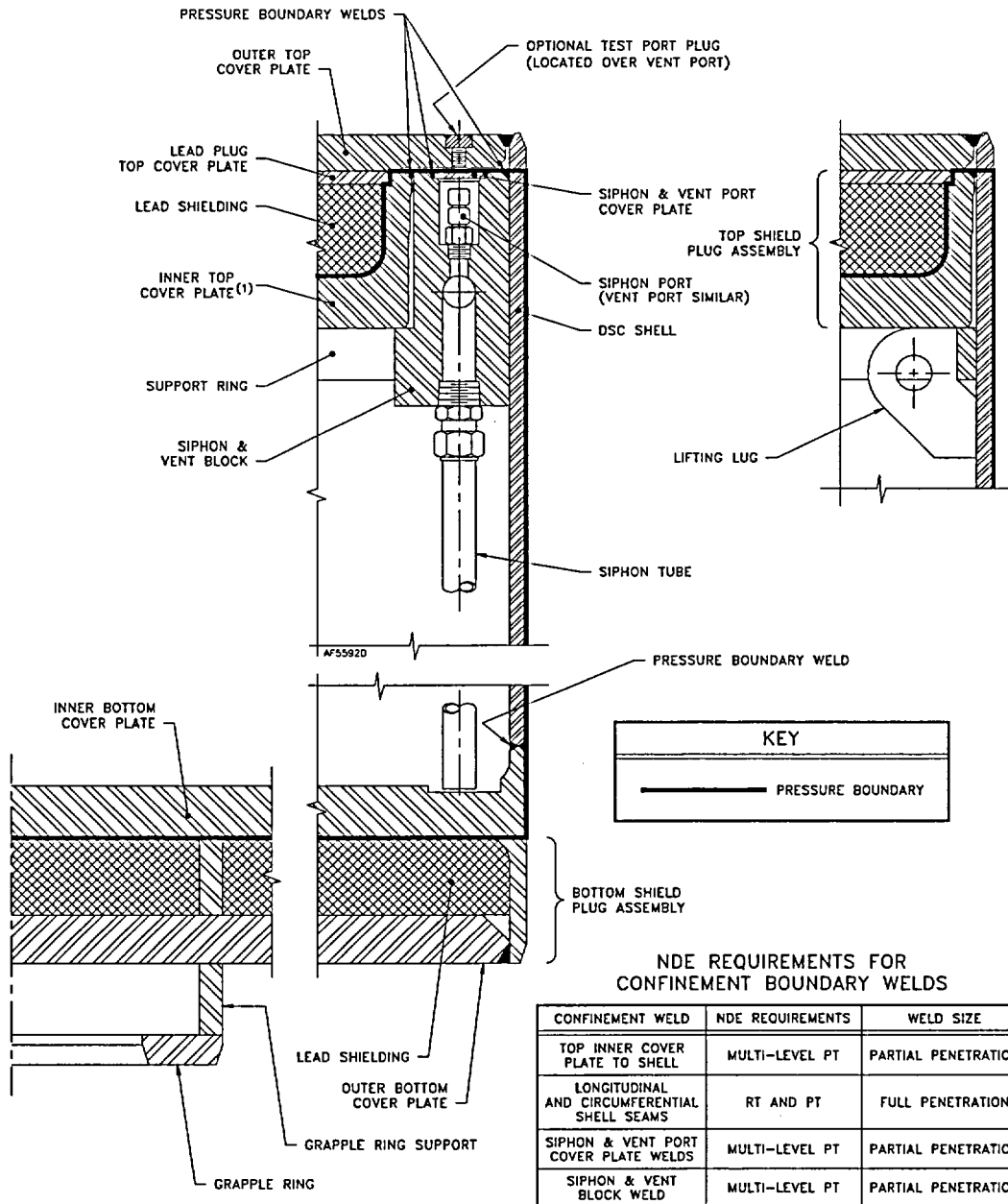
#### A.7.1.3 Seals and Welds

The welds made during fabrication of the 24PT4-DSC that affect the confinement boundary include the weld applied to the inner bottom cover plate and the circumferential and longitudinal seam welds applied to the shell. These welds are examined (radiographic or ultrasonic and liquid penetrant) according to the requirements of Subsection NB of the ASME Code. The vent and siphon block-to-shell weld is also made during fabrication and is liquid penetrant examined in accordance with Subsection NB of the ASME Code.

The welds of the vent and siphon port covers, and the inner top cover plate to shell, completed during closure operations, and the vent and siphon block to shell weld define the confinement boundary at the top end of the 24PT4-DSC. These welds are applied using multiple-layer techniques with multi-level PT in accordance with Subsection NB of the ASME Code and Code Case N-595-1. This effectively eliminates any pinhole leaks which might occur in a single-pass weld, since the chance of pinholes being in alignment on successive weld passes is negligibly small. Figure A.7.1-1 provides a graphic representation of the confinement boundary welds.

#### A.7.1.4 Closure

The 24PT4-DSC is entirely closed by welding and thus, no closure devices are utilized for confinement.



(1) FORGING CONFIGURATION IS SHOWN. MAY BE FABRICATED FROM SEPARATE INNER TOP COVER AND SIDE CASING PLATES.

**NOTE:** Outer top cover plate may use a test plug, or helium leak testing may be performed with a test fixture, which eliminates need for test plug.

**Figure A.7.1-1**  
**24PT4-DSC Confinement Boundary Welds**

A.7.2 Requirements for Normal Conditions of Storage

No change.

A.7.2.1 Release of Radioactive Material

No change.

A.7.2.2 Pressurization of Confinement Vessel

No change.

A.7.3 Confinement Requirements for Hypothetical Accident Conditions

A.7.3.1 Fission Gas Products

No change.

A.7.3.2 Release of Contents

No change.

## A.7.4 Supplemental Data

### A.7.4.1 Confinement Monitoring Capability

No change.

### A.7.4.2 References

- [A7.1] American Society of Mechanical Engineers, Boiler & Pressure Vessel Code, Section III, 1992 Edition with Addenda through 1994, including exceptions allowed by Code Case N-595-1.
- [A7.2] American National Standards Institute, ANSI N14.5-1997, Leakage Tests on Packages for Shipment of Radioactive Materials.
- [A7.3] NRC Spent Fuel Project Office, Interim Staff Guidance, ISG-5, Revision 1, Confinement Evaluation.

## A.8 OPERATING PROCEDURES

Sections of this Chapter have been identified as “No change” due to the addition of 24PT4-DSC to the Advanced NUHOMS® system. For these sections, the description or analysis presented in the corresponding sections of the FSAR for the Advanced NUHOMS® system with 24PT1-DSC is also applicable to the system with 24PT4-DSC.

### A.8.1 Procedures for Loading the 24PT4-DSC and Transfer to the AHSM

No change.

#### A.8.1.1 Narrative Description

The following steps describe the recommended generic operating procedures for the Advanced NUHOMS® System using the 24PT4-DSC. A list of instrumentation used during loading operations is provided in Table 8.1.1. Flowcharts of loading operations are provided in Figure A.8.1-1. A pictorial representation of key phases of this process is provided in Figure 8.1-2.

##### A.8.1.1.1 Transfer Cask and 24PT4-DSC Preparation

1. Prior to placement in dry storage, the candidate fuel assemblies are to be visually examined to ensure that no known or suspected gross cladding breaches exist for assemblies considered to be intact. Pinholes and hairline cracks are acceptable. Visual verification of fuel integrity may also be accomplished in conjunction with existing plant records. The assemblies shall be evaluated (by plant records or other means) to verify that they meet the physical, thermal and radiological criteria specified in Technical Specifications. Failed fuel cans, required for loading damaged fuel assemblies, must replace the DSC guidesleeves at the locations specified for the specific basket configurations within the 24PT4-DSC basket. This must occur prior to lowering the 24PT4-DSC/TC into the spent fuel pool. The location and identification of each failed fuel can shall be verified and documented.
2. Prior to being placed in service, the transfer cask is to be cleaned or decontaminated as necessary to ensure an acceptable surface contamination level.
3. Place the transfer cask in the vertical position in the cask decon area using the cask handling crane and the transfer cask lifting yoke (the design basis and criteria for the yoke is addressed in Chapter 1).
4. Place scaffolding around the cask so that the cask top cover plate and surface of the cask are accessible to personnel.
5. Remove the cask top cover plate and examine the cask cavity for any physical damage and ready the cask for service.

6. Examine the 24PT4-DSC for any physical damage which might have occurred since receipt inspection was performed. The 24PT4-DSC exterior and interior is to be inspected and any loose debris removed.
7. Using a crane, lower the 24PT4-DSC into the cask cavity by the internal lifting lugs and rotate the 24PT4-DSC to match the cask alignment marks.
8. Place the top shield plug assembly onto the 24PT4-DSC. Examine the top shield plug assembly to verify a proper fit.
9. Fill the cask/24PT4-DSC annulus with clean water. Place the inflatable seal into the upper cask liner recess and seal the cask/24PT4-DSC annulus by pressurizing the seal with compressed air.

**NOTE:** A transfer cask/24PT4-DSC annulus pressurization tank filled with water may be connected to the top annulus port of the transfer cask via a hose to provide a positive head above the level of water in the cask/24PT4-DSC annulus. This is an optional arrangement, which provides additional assurance that contaminated water from the fuel pool will not enter the cask/24PT4-DSC annulus, provided a positive head is maintained at all times.

10. Position the cask lifting yoke and engage the cask lifting trunnions and the rigging cables to the 24PT4-DSC top shield plug assembly. Adjust the rigging cables as necessary to obtain even cable tension and a level top shield plug assembly. Remove the top shield plug assembly and place clear of the cask and disconnect from the yoke.
11. Fill the 24PT4-DSC cavity with water from the fuel pool or an equivalent source.
12. Visually inspect the yoke lifting hooks to insure that they are properly positioned and engaged on the cask lifting trunnions.
13. Move the scaffolding away from the cask as necessary. If required for weight limits, drain TC neutron shield.
14. Lift the cask just far enough to allow the weight of the cask to be distributed onto the yoke lifting hooks. Reinspect the lifting hooks to insure that they are properly positioned on the cask trunnions.
15. Optionally, secure a sheet of suitable material to the bottom of the cask to minimize the potential for ground-in contamination within the fuel pool. This step may be done prior to initial placement of the cask in the decontamination area.
16. Prior to the cask being lifted into the fuel pool, the water level in the pool should be adjusted as necessary to accommodate the cask/24PT4-DSC volume. If the water placed in the 24PT4-DSC cavity was obtained from the fuel pool, a level adjustment may not be necessary.

A.8.1.1.2 24PT4-DSC Fuel Loading

1. Lift the cask/24PT4-DSC and position them over the cask loading area of the spent fuel pool in accordance with the plant's 10CFR 50 cask handling procedures.
2. Lower the cask into the fuel pool until the bottom of the cask is at the height of the fuel pool surface. As the cask is lowered into the pool, spray the exterior surface of the cask with demineralized water to minimize surface adhesion of contaminated particles. If the annulus pressurization tank is utilized, ensure it is filled, connected, and the tubing is clear of the cask.

**NOTE:** The introduction of water may dilute fuel pool boron concentration.

3. Place the cask in the location of the fuel pool designated as the cask loading area and in correct orientation.
4. Disengage the lifting yoke from the cask lifting trunnions and move the yoke clear of the cask. Spray the lifting yoke with clean demineralized water as it is raised out of the fuel pool.
5. Prior to loading of fuel assemblies, a loading plan shall be prepared to verify that the canister loading configuration and selected fuel assemblies meet the CofC requirements. The plan shall be independently verified.
6. Prior to insertion of a spent fuel assembly into the 24PT4-DSC, the identity of the assembly shall be verified by two individuals using an underwater video camera. Read and record the fuel assembly identification number from the fuel assembly and check this identification number against the 24PT4-DSC loading plan that indicates which fuel assemblies are acceptable for dry storage.

**NOTE:** If poison rodlets are required for criticality control, they must be present in the assembly prior to insertion into the 24PT4-DSC. The presence and location of poison rodlets shall be verified at the location designated in Technical Specification by two individuals.

7. Move a candidate fuel assembly from a fuel rack in accordance with the plant's 10CFR 50 fuel handling procedures.
8. Position the fuel assembly for insertion into the selected 24PT4-DSC storage cell and load the fuel assembly. Repeat Steps 5 through 7 for each SFA loaded. After the 24PT4-DSC has been fully loaded, independently verify and record the identity and location of each fuel assembly.
9. If damaged assemblies have been loaded in the 24PT4-DSC, install the failed fuel can lids. Tighten the connecting bolts.

10. Connect the top shield plug assembly to the yoke. Position the lifting yoke and the top shield plug assembly and lower the top shield plug assembly onto the 24PT4-DSC.

**CAUTION:** Verify that all the lifting height restrictions specified in the Technical Specifications can be met in the following steps which involve lifting of the transfer cask.

11. Visually verify that the top shield plug assembly is properly seated onto the 24PT4-DSC.
12. Position the lifting yoke and verify that it is properly engaged with the cask trunnions.
13. Raise the transfer cask to the pool surface. Prior to raising the top of the cask above the water surface, stop vertical movement.
14. Inspect the top shield plug assembly to re-verify that it is properly seated onto the 24PT4-DSC. If not, lower the cask and reposition the top shield plug assembly. Repeat Steps 11 to 14 as necessary.
15. Continue to raise the cask from the pool and spray the exposed portion of the cask with water.
16. Drain any excess water from the top of the top shield plug assembly back to the fuel pool.
17. Check the radiation levels at the center of the top shield plug assembly and around the perimeter of the cask.
18. If required, and not done previously, drain neutron shield as required to maintain total weight within plant crane limits, while lifting cask from pool. Lift the cask from the fuel pool. As the cask is raised from the pool, continue to spray the cask with demineralized water. Disconnect annulus pressurization tank from cask.
19. Move the cask with loaded 24PT4-DSC to the cask decon area.

#### A.8.1.1.3 24PT4-DSC Drying and Backfilling

1. Check the radiation levels along the perimeter of the cask. Temporary shielding may be installed as necessary to minimize personnel exposure. Liquid neutron shield, if left unfilled or drained during lift from pool for weight reduction, shall be filled.
2. Place scaffolding around the cask so that any point on the surface of the cask is accessible to personnel.

3. Disengage the rigging cables from the top shield plug assembly. Eyebolts may be removed now or later. Disengage the lifting yoke from the trunnions and move it clear of the cask.
4. Decontaminate the exposed surfaces of the 24PT4-DSC shell perimeter and remove the inflatable cask/24PT4-DSC annulus seal. A neutron shield tank overflow hose may, as an option, be connected to the cask neutron shield.
5. Connect the cask drain line to the cask, open the cask cavity drain port and allow water from the annulus to drain out until the water level is approximately twelve inches below the top edge of the 24PT4-DSC shell. Take swipes around the outer surface of the shell and check for smearable contamination in accordance with Technical Specification limits.
6. Check radiation levels along the surface of the top shield plug assembly. Temporary shielding may be installed as necessary to minimize personnel exposure.
7. Install the automated welding machine onto the top shield plug assembly.
8. Connect the vacuum drying system (VDS) to the 24PT4-DSC and use the liquid pump to remove approximately 60 gallons to the fuel pool. This will lower the water level below the bottom of the top shield plug assembly.
9. Disconnect the VDS from the 24PT4-DSC.
10. Cover the cask/24PT4-DSC annulus to prevent debris and weld splatter from entering the annulus.
11. Continuous hydrogen monitoring during the welding of the top shield plug assembly to the shell is required [A8.1]. Insert a piece of ¼" tygon tube (or equivalent) of sufficient length through the vent port such that it terminates just below the top shield plug assembly. Connect the tube to a hydrogen monitor to allow continuous monitoring of the hydrogen atmosphere in the 24PT4-DSC cavity during welding of the top shield plug assembly. The 24PT4-DSC internal pressure is to be maintained at atmospheric pressure during welding of the top shield plug assembly.
12. Ready the automated welding machine and tack weld the top shield plug assembly to the 24PT4-DSC shell. Verify that the measured hydrogen concentration does not exceed a safety limit of 2.4% [A8.1]. If this limit is exceeded, stop all welding operations and purge the 24PT4-DSC cavity with 2-3 psig helium (or other inert medium) via the ¼" tubing to reduce hydrogen concentration safely below the 2.4% limit. Complete the top shield plug assembly weldment and remove the automated welding machine.
13. Perform dye penetrant weld examination of the top shield plug assembly weld.

14. As an option, place the strongback so that it sits on the top shield plug assembly and is oriented such that:
  - The siphon and vent ports are accessible.
  - The strongback stud holes line up with the cask lid bolt holes.
15. Lubricate the studs and, using a crossing pattern, adjust the strongback studs to snug tight ensuring approximately even pressure on the top shield plug assembly.
16. Connect the VDS to the siphon and vent ports.
17. Install temporary shielding to minimize personnel exposure throughout the subsequent draining/drying and welding operations as required.
18. Engage the helium or air supply and open the valve on the vent port and allow compressed gas to force the water from the 24PT4-DSC cavity through the siphon port.
19. Once the water stops flowing from the 24PT4-DSC, close the siphon port and disengage the gas source.
20. Connect the hose from the vent port and the siphon port to the intake of the vacuum pump. Connect a hose from the discharge side of the VDS to the plant's radioactive waste system or spent fuel pool. Connect the VDS to a helium source.
21. Open the valve on the suction side of the pump, start the VDS and draw a vacuum on the 24PT4-DSC cavity. The cavity pressure should be reduced in steps to approximately 100 torr, 50 torr, 25 torr, 15 torr, 10 torr, 5 torr, and 3 torr. This staged drawdown will verify no ice blockage of the evacuation path. After pumping down to each level, the pump is valved off and the cavity pressure monitored. The cavity pressure will rise as water and other volatiles in the cavity evaporate. When the cavity pressure stabilizes, the pump is valved in to complete the vacuum drying process. It may be necessary to repeat some steps, depending on the rate and extent of the pressure increase. Vacuum drying is complete when the pressure stabilizes for a minimum of 30 minutes at 3 torr or less as specified in the Technical Specifications.

**NOTE:** If air is used as the medium for blowdown in Step 18, the Technical Specifications contain limitations on the duration of vacuum drying as a function of the specific heat load configuration for the DSC. The duration of vacuum during shall be monitored and appropriate corrective actions taken if required vacuum levels are not reached within the time limits. No time limits apply for vacuum drying of the DSC, if helium is used for blowdown in Step 18.

22. Open the valve to the vent port and fill the 24PT4-DSC cavity with helium.

**NOTE:** Helium gas introduced into the 24PT4-DSC shall be welding grade (>99% purity) and Important to Safety.

23. Pressurize the 24PT4-DSC with helium in accordance with Technical Specifications requirements.
24. At Licensee discretion, perform a helium sniff test on the top shield plug assembly and vent/siphon block.
25. If a leak is found, repair the weld in accordance with the Code of Construction. Re-pressurize the 24PT4-DSC and repeat the helium sniff test.
26. Once no leaks are detected, depressurize the 24PT4-DSC cavity by releasing the helium through the VDS to the plant's spent fuel pool or radioactive waste system.
27. Re-evacuate the 24PT4-DSC cavity using the VDS. The cavity pressure should be reduced in steps to approximately 10 torr, 5 torr, and 3 torr. After pumping down to each level, the pump is valved off and the cavity pressure is monitored. When the cavity pressure stabilizes, the pump is valved in to continue the vacuum drying process. Vacuum drying is complete when the pressure stabilizes for a minimum of 30 minutes at 3 torr or less in accordance with the Technical Specifications requirements.

**NOTE:** No time limits for vacuum drying apply since helium is present in the DSC prior to initiating vacuum drying operations per this step.

28. Open the valve on the vent port and allow helium to flow into the cavity to pressurize the 24PT4-DSC in accordance with the limits specified in the Technical Specifications.
29. Close the valves on the helium source.

**NOTE:** If during drying and backfilling the system is inadvertently vented, re-evacuation and backfilling with helium will be required.

#### A.8.1.1.4 24PT4-DSC Sealing Operations

1. Disconnect the VDS from the 24PT4-DSC. Introduce helium behind port covers. Seal weld the prefabricated covers over the vent and siphon ports and perform a dye penetrant weld examination. If installed, remove strongback.
2. Install the automated welding machine onto the outer top cover plate and place the outer top cover plate with the automated welding system onto the 24PT4-DSC. Verify proper fit up of the outer top cover plate.

3. Tack weld the outer top cover plate to the 24PT4-DSC shell. Place the outer top cover plate weld root pass. Perform dye penetrant examination of the root pass weld.
4. Remove the outer top cover plate leak test port plug.
5. Perform a helium leak test of the top shield plug assembly and vent/siphon ports by establishing a vacuum between the top shield plug assembly and outer cover plate. The acceptance criteria for this leak test is defined in Chapters A.7 and the Technical Specifications. If a leak is found, remove outer top cover, repair and retest until acceptance criteria is met.
6. Replace outer top cover plate leak test port plug and seal weld (may be completed after outer top cover plate welding). Perform penetrant testing.
7. Weld out the outer top cover plate to the shell and perform dye penetrant examination on the weld surface.

**NOTE:** Helium leak testing of the primary containment welds may also be performed using a test fixture with an appropriate test port and configuration which maintains a void between the test fixture and the top shield plug assembly, siphon block, and vent and siphon port welds. If this approach is used, the helium leak test would be performed prior to welding of the outer cover plate, which would not have a helium leak test port. Welding of the outer cover plate would be performed in accordance with the steps above without the need to stop and perform a helium sniff test after the root pass as described in Steps 23-25 Section A.8.1.1.3.

8. Open the cask drain port valve and remove the remaining water from the cask/24PT4-DSC annulus.
9. Remove the automated welding machine from the 24PT4-DSC.
10. Rig the cask top cover plate and lower the cover plate onto the cask.
11. Bolt the cask cover plate into place, tightening the bolts to the required torque in a star pattern.

A.8.1.1.5 Transfer Cask Downending and Transport to ISFSI

No change.

A.8.1.1.6 24PT4-DSC Transfer to the AHSM

No change. If a neutron shield overflow system is used, monitor to maintain water inventory in cask.

A.8.1.1.7 Monitoring Operations

No change.

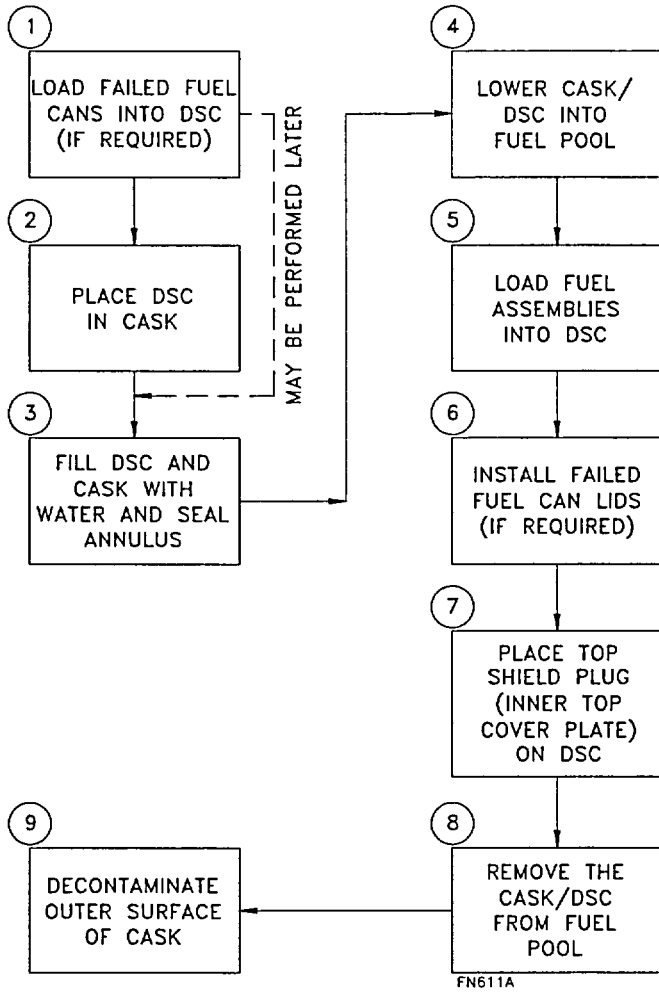


**Figure A.8.1-1  
Advanced NUHOMS® System Loading Operations Flow Chart**

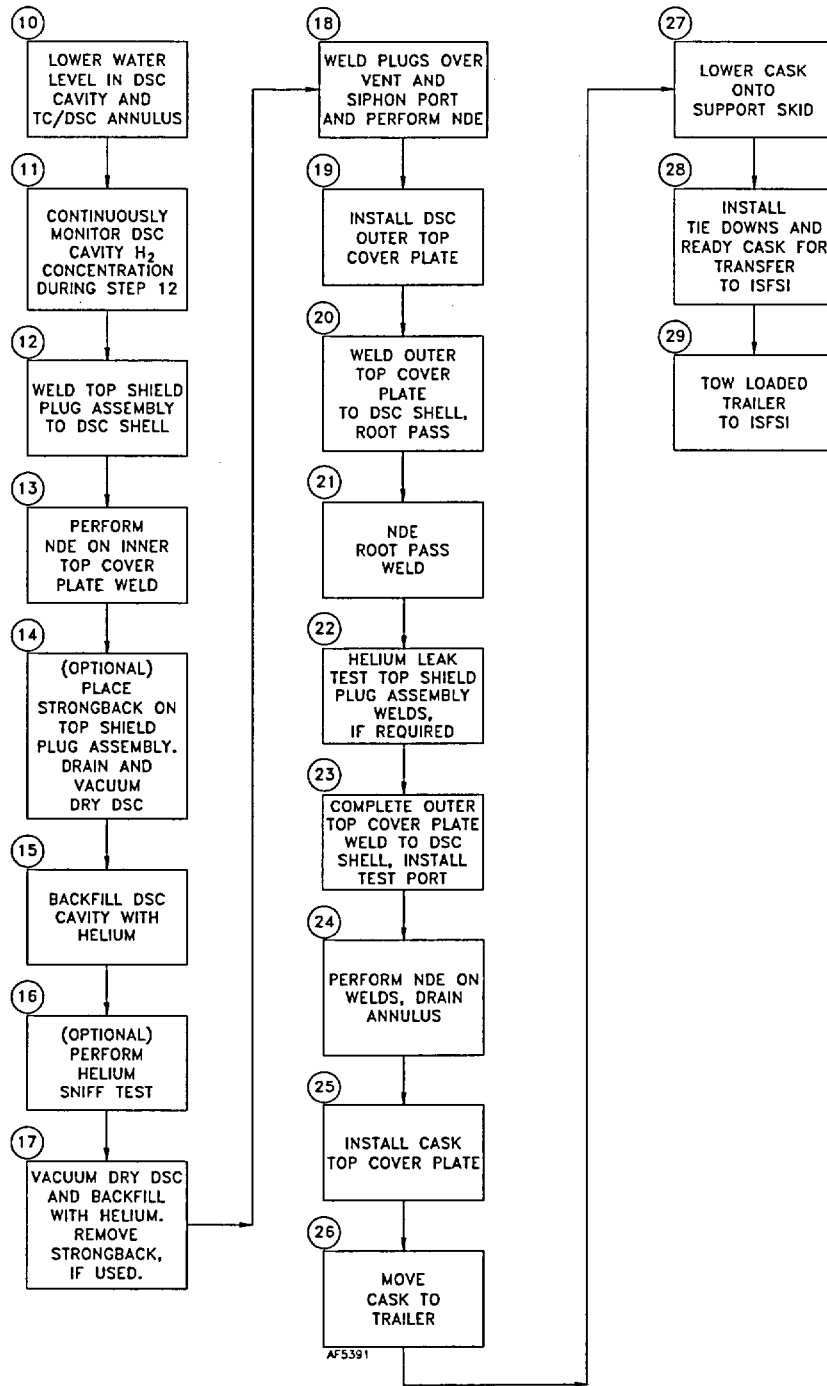


**Figure A.8.1-1**  
**Advanced NUHOMS® System Loading Operations Flow Chart**  
 (continued)

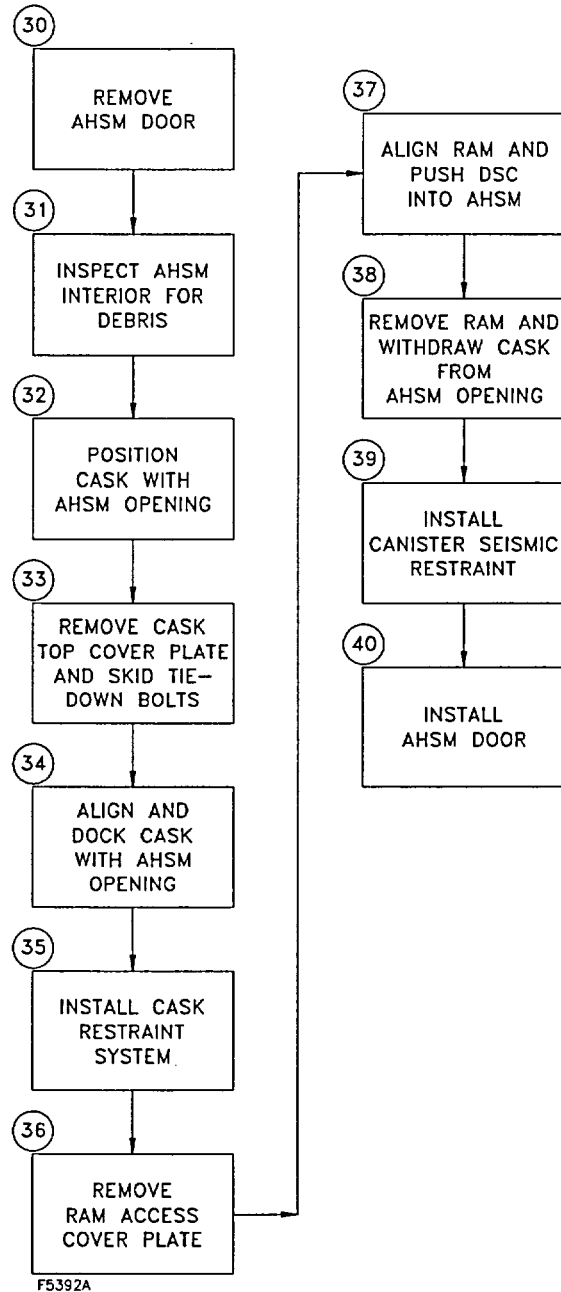


**Figure A.8.1-1**  
**Advanced NUHOMS® System Loading Operations Flow Chart**  
**(concluded)**

## A.8.2 Procedures for Unloading the 24PT4-DSC

The following section outlines the procedures for retrieving the 24PT4-DSC from the AHSM and for removing the fuel assemblies from the 24PT4-DSC. These procedures are provided as a guide and are not intended to be limiting if the licensee determines that alternate means are available to accomplish the same operational objective. A process flow diagram for the Advanced NUHOMS® System retrieval is presented in Figure A.8.2-1.

### A.8.2.1 24PT4-DSC Retrieval from the AHSM

No change.

### A.8.2.2 Removal of Fuel from the 24PT4-DSC

When the 24PT4-DSC has been removed from the AHSM, there are several potential options for off-site shipment of the fuel. These options include, but are not limited to, shipping the 24PT4-DSC with fuel assemblies or removing the fuel from the 24PT4-DSC as described below. It is preferred to ship the 24PT4-DSC intact to a reprocessing facility, monitored retrievable storage facility or permanent geologic repository in a compatible shipping cask, such as the MP197, licensed under 10CFR 71. However, there are several reasons why it may be necessary to remove fuel assemblies from the 24PT4-DSC. These include off-site transport in a transport cask requiring an alternate canister configuration, return of fuel assemblies to a spent fuel pool, or placement of fuel assemblies in a different 24PT4-DSC. Other reasons might include removing fuel assemblies at the end of service life or for inspection following an accident as discussed in Chapter A.12.

If it becomes necessary to remove fuel from the 24PT4-DSC prior to off-site shipment, there are two basic options available at the ISFSI or reactor site. The fuel assemblies could be removed and reloaded into a shipping cask using dry transfer techniques, or if the applicant so desires, the initial fuel loading sequence could be reversed and the plant's spent fuel pool utilized. Procedures for unloading the 24PT4-DSC in a fuel pool are presented here, however wet or dry unloading procedures are essentially identical to those of 24PT4-DSC loading through the weld removal process (beginning of preparation to placement of the transfer cask in the fuel pool). Prior to opening the 24PT4-DSC, the following operations are to be performed.

1. Transport the transfer cask to the cask handling area inside the plant's fuel handling building.
2. Position and ready the trailer for access by the crane.
3. Attach the lifting yoke to the crane hook.
4. Engage the lifting yoke with the trunnions of the transfer cask.
5. Visually inspect the yoke lifting hooks to insure that they are properly aligned and engaged onto the transfer cask trunnions.

6. Lift the transfer cask approximately one inch off the trunnion supports. Visually inspect the yoke lifting hooks to insure that they are properly positioned on the trunnions.
7. Move the crane in a horizontal motion while simultaneously raising the crane hook vertically and lift the transfer cask off the trailer. Move the transfer cask to the cask decontamination area.
8. Lower the transfer cask into the cask decontamination area in the vertical position.
9. Wash the transfer cask to remove any dirt which may have accumulated during the 24PT4-DSC unloading and transfer operations.
10. Place scaffolding around the transfer cask so that any point on the surface of the transfer cask is accessible to handling personnel.
11. Unbolt the transfer cask top cover plate.
12. Connect the rigging cables to the transfer cask top cover plate and lift the cover plate from the transfer cask. Set the transfer cask cover plate aside and disconnect the lid lifting cables.
13. Install temporary shielding to reduce personnel exposure as required. Fill the transfer cask/24PT4-DSC annulus with clean water and seal the annulus.

The process of unloading the 24PT4-DSC is similar to that used for loading. Operations that involve opening the 24PT4-DSC described below are to be carefully controlled in accordance with plant procedures. These operations are to be performed under the site's standard health physics guidelines for welding, grinding, and handling of potentially highly contaminated equipment. These are to include the use of prudent housekeeping measures and monitoring of airborne particulates. Procedures may require personnel to perform the work using respirators or supplied air.

If fuel needs to be removed from the 24PT4-DSC, precautions must be taken for the presence of damaged or oxidized fuel and to prevent radiological exposure to personnel during this operation. If degraded fuel is suspected, additional measures appropriate for the specific conditions are to be planned, reviewed, and implemented to minimize exposures to workers and radiological releases to the environment. A sampling of the atmosphere within the 24PT4-DSC should be taken prior to inspection or removal of fuel.

If the work is performed outside the fuel handling building, a tent may be constructed over the work area which may be kept under a negative pressure to control airborne particulates. Any radioactive gas release will be Kr-85, which is not readily captured. Whether the krypton is vented through the plant stack or allowed to be released directly depends on the plant operating requirements.

Following opening of the 24PT4-DSC, it is to be filled with demineralized or pool water prior to placement in the spent fuel pool to prevent a sudden inrush of pool water. Parameters related to reflooding the 24PT4-DSC cavity are addressed in Chapter A.3. Place transfer cask into the pool. Fuel unloading procedures will be governed by the plant operating license under 10CFR 50. The generic procedures for these operations are as follows:

1. Locate the siphon and vent port using the indications on the top cover plate. Place a portable drill press on top of the 24PT4-DSC. Align the drill over the siphon port.
2. Place an exhaust hood or tent over the 24PT4-DSC, if necessary. The exhaust should be filtered or routed to the site radwaste system.
3. Drill a hole through the top cover plate to expose the siphon port quick connect.
4. Drill a second hole through the top cover plate to expose the vent port quick connect.

**CAUTION:** (a) The water fill rate must be regulated during this reflooding operation to ensure that the 24PT4-DSC vent pressure does not exceed 20 psig.

(b) Provide for continuous hydrogen monitoring of the 24PT4-DSC cavity atmosphere during all subsequent cutting operations to ensure that a safety limit of 2.4% hydrogen concentration is not exceeded. Purge with 2-3 psig helium (or any other inert medium) as necessary to maintain the hydrogen concentration safely below this limit.

5. Obtain a sample of the 24PT4-DSC atmosphere (confirm acceptable hydrogen concentration). Fill the 24PT4-DSC with water from the fuel pool through the siphon port with the vent port open and routed to the plant's off-gas system.
6. Place welding blankets around the transfer cask and scaffolding.
7. Using plasma arc-gouging, a mechanical cutting system or other suitable means, remove the weld from the outer top cover plate and 24PT4-DSC shell. A fire watch should be placed on the scaffolding with the welder, as appropriate. The exhaust system should be operating at all times.
8. The material or waste from the cutting or grinding process should be treated and handled in accordance with the plant's low level waste procedures unless determined otherwise.
9. Remove the top of the tent, if necessary.
10. Remove the exhaust hood, if necessary.
11. Remove the outer top cover plate.

12. Reinstall tent and temporary shielding, as required. Remove the weld from the top shield plug assembly to the shell in the same manner as the outer cover plate. Visually verify that the top shield plug assembly has no remaining weld interferences that would prevent its removal.
13. Clean the transfer cask surface of dirt and any debris which may be on the transfer cask surface as a result of the weld removal operation. Other procedures which are required for the operation of the transfer cask should take place at this point as necessary.
14. Engage the yoke onto the trunnions, install eyebolts into the top shield plug assembly and connect the rigging cables to the eyebolts.
15. Visually inspect the lifting hooks of the yoke to insure that they are properly positioned on the trunnions.
16. The transfer cask should be lifted just far enough to allow the weight of the transfer cask to be distributed onto the yoke lifting hooks. Inspect the lifting hooks to insure that they are properly positioned on the trunnions.
17. Install suitable protective material onto the bottom of the transfer cask to minimize cask contamination, as appropriate. Move the transfer cask to the spent fuel pool.
18. Prior to lowering the transfer cask into the pool, adjust the pool water level, if necessary, to accommodate the volume of water which will be displaced by the transfer cask during the operation.
19. Position the transfer cask over the cask loading area in the spent fuel pool.
20. Lower the transfer cask into the pool. As the transfer cask is being lowered, the exterior surface of the transfer cask should be sprayed with clean demineralized water.
21. Disengage the lifting yoke from the transfer cask and lift the top shield plug assembly from the 24PT4-DSC.
22. Remove the fuel from the 24PT4-DSC and place the fuel into the spent fuel racks. For damaged fuel within failed fuel cans, either the entire failed fuel can may be grappled and removed, or the lids removed and the damaged assemblies removed from the cans.
23. Lower the top shield plug assembly onto the empty 24PT4-DSC. (Optional)
24. Visually verify that the top shield plug assembly is properly positioned. (Optional)
25. Engage the lifting yoke onto the cask trunnions.

26. Visually verify that the yoke lifting hooks are properly engaged with the cask trunnions.
27. Lift the transfer cask by a small amount and verify that the lifting hooks are properly engaged with the trunnions.
28. Lift the transfer cask to the pool surface. If top shield plug is installed, prior to raising the top of the transfer cask above the water surface, stop vertical movement and inspect the top shield plug assembly to ensure that it is properly positioned. If the top shield plug assembly is not properly seated, lower the transfer cask back to the fuel pool and reposition the plug.
29. Spray the exposed portion of the transfer cask with demineralized water.
30. Drain any excess water from the top of the top shield plug assembly into the fuel pool.
31. Lift the transfer cask from the spent fuel pool. As the transfer cask is rising out of the pool, spray the transfer cask with water.
32. Move the transfer cask to the cask decontamination area.
33. Check radiation levels around the perimeter of the transfer cask. The transfer cask exterior surface should be decontaminated, if necessary.
34. Place scaffolding around the transfer cask so that any point along the surface of the transfer cask is easily accessible to personnel.
35. Ready the VDS.
36. Connect the VDS to the vent port with the system open to atmosphere. Also connect the VDS to the siphon port and connect the other end of the system to the liquid pump. The pump discharge should be routed to the plant radwaste system or the spent fuel pool.
37. Open the valves on the vent port and siphon port of the VDS.
38. Activate the liquid pump.
39. Once the water stops flowing, deactivate the pump.
40. Close the valves on the VDS.
41. Disconnect the VDS from the vent and siphon ports.
42. Seal 24PT4-DSC cavity, if required.

43. Decontaminate the 24PT4-DSC, as necessary, and handle in accordance with low-level waste procedures. Alternatively, the 24PT4-DSC may be repaired and recertified for reuse.

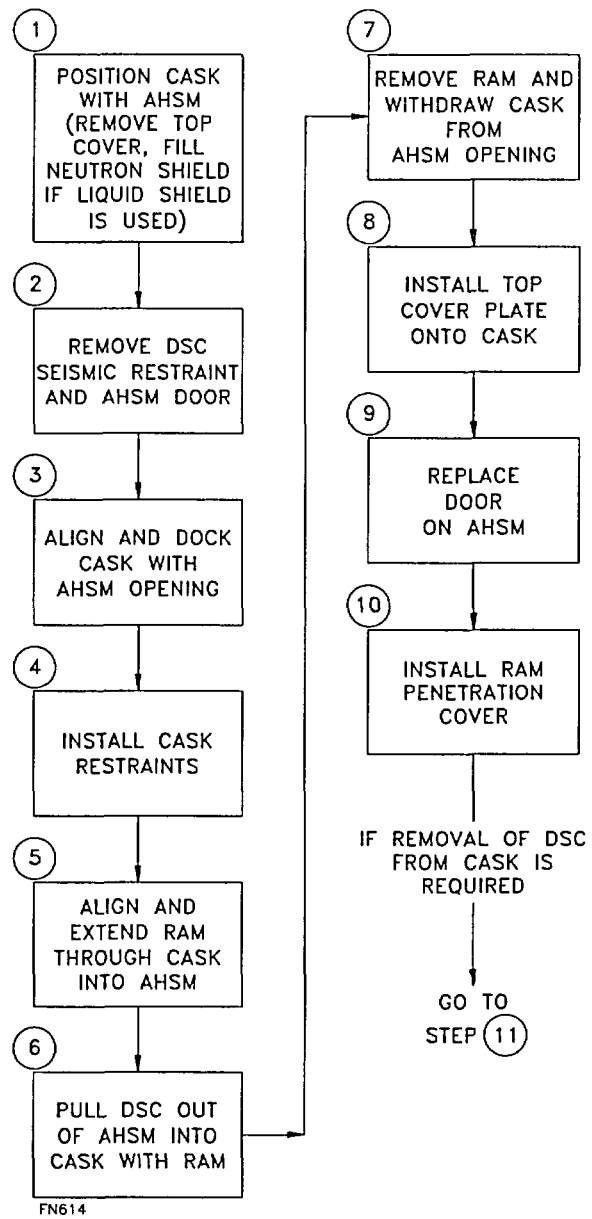


**Figure A.8.2-1**  
**Advanced NUHOMS® System Retrieval Operations Flow Chart**

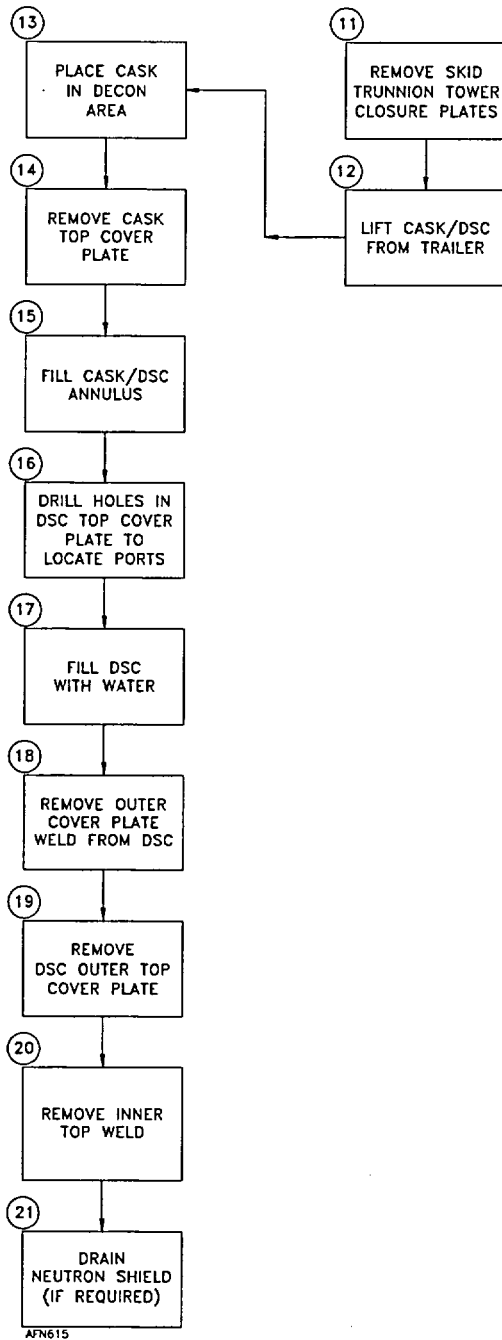


**Figure A.8.2-1**  
**Advanced NUHOMS® System Retrieval Operations Flow Chart**  
**(continued)**

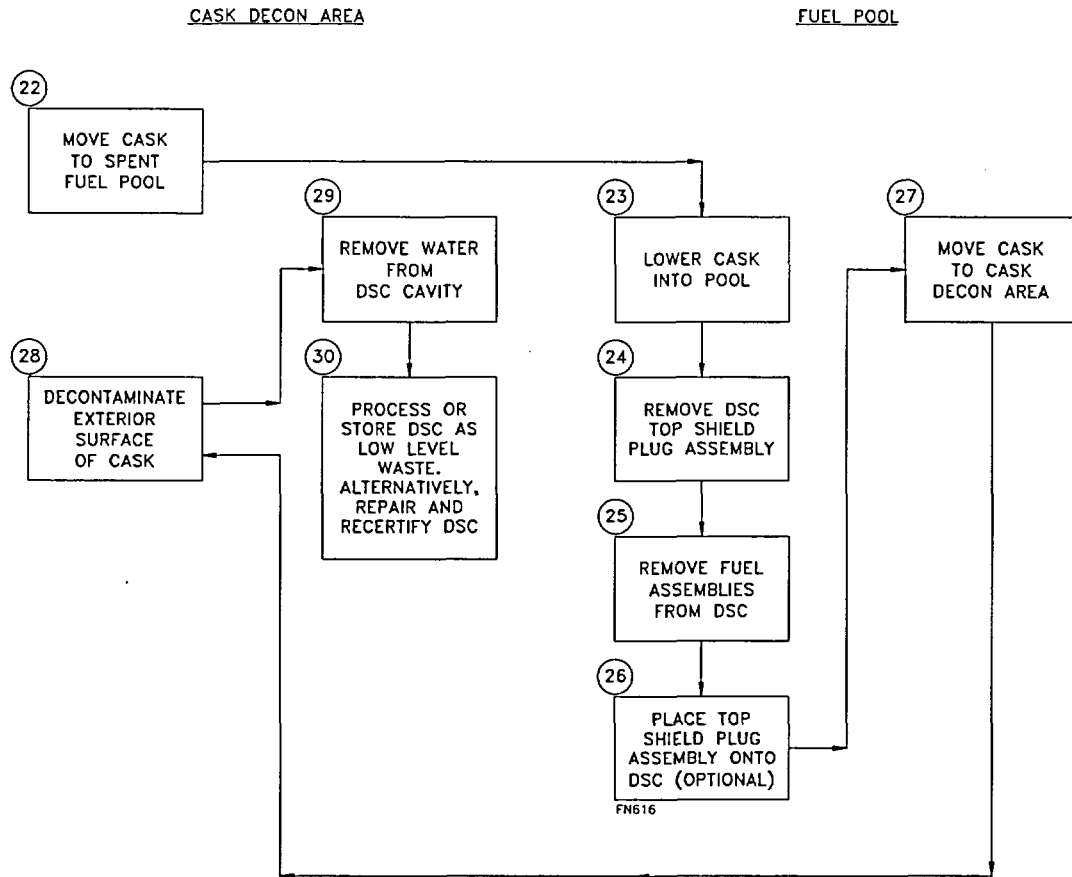


**Figure A.8.2-1**  
**Advanced NUHOMS® System Retrieval Operations Flow Chart**  
**(concluded)**

### A.8.3 Supplemental Information

#### A.8.3.1 Other Operating Systems

No change.

##### A.8.3.1.1 Component/Equipment Spares

No change.

#### A.8.3.2 Operation Support System

No change.

##### A.8.3.2.1 Instrumentation and Control System

No change.

##### A.8.3.2.2 System and Component Spares

No change.

#### A.8.3.3 Control Room and/or Control Areas

No change.

#### A.8.3.4 Analytical Sampling

No change.

#### A.8.3.5 References

[A8.1] U.S. Nuclear Regulatory Commission, Office of the Nuclear Material Safety and Safeguards, "Safety Evaluation of VECTRA Technologies' Response to Nuclear Regulatory Commission Bulletin 96-04 for NUHOMS<sup>®</sup> -24P and NUHOMS<sup>®</sup>-7P Dry Spent Fuel Storage System," November 1997 (Dockets 72-1004, 72-3, 72-4, 72-8, and 72-14).

## A.9 ACCEPTANCE TESTS AND MAINTENANCE PROGRAM

Sections of this Chapter have been identified as “No change” due to the addition of 24PT4-DSC to the Advanced NUHOMS® system. For these sections, the description or analysis presented in the corresponding sections of the FSAR for the Advanced NUHOMS® system with 24PT1-DSC is also applicable to the system with 24PT4-DSC.

### A.9.1 Acceptance Criteria

No change.

#### A.9.1.1 Visual Inspection

No change.

#### A.9.1.2 Structural

No change.

#### A.9.1.3 Leak Tests and Hydrostatic Pressure Tests

24PT4-DSC leakage tests are performed on the confinement system at the fabricator’s facility and during 24PT4-DSC closure operations. These tests are usually performed using the helium mass spectrometer method. Alternative methods are acceptable, provided that the required sensitivity is achieved. The 24PT4-DSC confinement boundary is tested to be “leaktight” as defined in ANSI N14.5 [A9.2]. Personnel performing the leakage tests, both at the fabricator and the loading site, are qualified in accordance with SNT-TC-1A [A9.1].

The 24PT4-DSC shell (longitudinal and circumferential welds and inner bottom cover assembly) is pressure tested in accordance with ASME Code.

#### A.9.1.4 Components

No change.

##### A.9.1.4.1 Valves, Rupture Discs, and Fluid Transport Devices

No change.

##### A.9.1.4.2 Gaskets

No change.

#### A.9.1.4.3 Miscellaneous

No change.

#### A.9.1.5 Shielding Integrity

The analyses performed to ensure shielding integrity over the lifetime of the Advanced NUHOMS® System are presented in Chapter A.5. The gamma and neutron shielding materials used are limited to concrete AHSM components and stainless steel/lead shield plugs in the 24PT4-DSC. The integrity of these shielding materials is ensured by the control of their fabrication in accordance with the appropriate ASME, ASTM or ACI criteria.

External dose rate surveys are performed at loading to ensure that Technical Specification radiation dose limits are not exceeded for each 24PT4-DSC and AHSM.

Details of the shielding materials are discussed in Chapter A.5.

#### A.9.1.6 Thermal Acceptance

No change.

#### A.9.1.7 Neutron Absorber Tests

This section describes the tests, process controls, and measurements relied upon to demonstrate proper fabrication and effectiveness of the neutron absorber sheets.

During fabrication, the neutron absorber sheets used in the 24PT4-DSC are verified to have their minimum total  $^{10}\text{B}$  per unit area (areal density) of the sandwiched material as specified on the drawings in Chapter A.1.

Samples from each sheet of the neutron absorber are retained for testing and record purposes. The minimum  $^{10}\text{B}$  content per unit area and the uniformity of dispersion within a sheet are verified by chemical analysis and/or neutron attenuation testing. All material certifications, lot control records, and test records are maintained to assure material traceability and are part of the maintenance records discussed in Section 9.2.1.4.

Chemical (destructive) testing is the preferred method because the  $^{10}\text{B}$  areal density, which is the primary requirement for the material, can be directly measured. This is done by taking two 1 cm square samples from each end of the rolled product. The size of the 1 cm sample is small compared to the finished sheet size, over 1300 in<sup>2</sup>, so that non-uniformities in  $^{10}\text{B}$  areal density would be readily apparent between the samples. The material on the ends of the rolled product is known to be thinner than the rest of the sheet because of the rolling process. This characteristic of the finished product is confirmed by examination of thickness in four locations on 100% of the sheets. The thinnest of these samples is used for destructive chemical determination of the amount of boron in the sample using written, approved procedures and standard laboratory processes and equipment. Using the area of the sample, and the mass of boron in the sample, the

areal boron density may be calculated. Once the areal boron density is known, the areal  $^{10}\text{B}$  density is calculated using the isotopic assay of the  $\text{B}_4\text{C}$  powder used to manufacture the product. The sample frequency is determined using standard statistical procedures to assure that minimum  $^{10}\text{B}$  areal densities are achieved with a 95/95 confidence level. This assures that the minimum safety requirements for the neutron absorber sheets are met. The neutron absorber sheets are capable of performing their function throughout the service life of the 24PT4-DSC as discussed in Chapter A.6.

Neutron attenuation testing may be performed to augment or replace chemical (destructive) testing as required to demonstrate acceptable minimum areal  $^{10}\text{B}$  loading of the neutron absorber sheets. Neutron transmission measurements may be performed on samples, or completed sheets, using a neutron diffractometer. If used, the neutron transmission measurements shall be performed using written, approved procedures in accordance with applicable portions of ASTM E94 [A9.3], "Guide for Radiographic Testing," ASTM E142 [A9.4], "Method for Controlling Quality of Radiographic Testing", and ASTM E545 [A9.5], "Method for Determining Image Quality in Direct Thermal Neutron Radiographic Examination." Since this type of testing does not measure directly the  $^{10}\text{B}$  areal density of the sheets, the results of neutron attenuation tests shall be demonstrated by calculation to show that the minimum specified  $^{10}\text{B}$  areal densities are achieved with a 95/95 confidence level.

The 95/95 confidence level may be determined by a pre-defined sampling technique and associated criteria for increased sampling as a result of rejection of material in the initial sample. An initial sampling of 100% of the coupons may be employed with a reduced sampling of 50% of the coupons introduced if all coupons in the first 25% of the lot are acceptable. A rejection during reduced inspection will require a return to 100% inspection of the lot.

Alternatively, the 95/95 confidence level may be obtained by a review of test data. A one-sided tolerance limit factor (F) may be applied to the test data (average + F [standard deviation]) to establish the minimum acceptable value required to ensure test results meet the 95/95 confidence level [A9.6], [A9.7], [A9.8] and [A9.9].

#### A.9.1.8 Borated Stainless Steel Poison Rod Tests

This section describes the tests, process controls and measurements relied upon to demonstrate proper fabrication and effectiveness of the borated stainless steel poison rods.

During fabrication, the borated stainless steel poison rods used in the 24PT4-DSC are verified to have a minimum boron content of 1.75% . The minimum weight percent boron is verified by chemical analysis. All material certifications, control records and test records are maintained to assure material traceability and are part of the maintenance records in Section 9.2.1.4.

Chemical testing is the preferred method because the boron can be directly measured. This is done by cask or heat analysis in accordance with ASTM A751 [A9.14]. A representative sample taken from each heat is obtained during the pouring of the steel which is analyzed for the elements. The sample frequency is determined to assure that the minimum 1.75 wt% boron is achieved for all heats.

#### A.9.1.9 Tests for B<sub>4</sub>C Encapsulated in Stainless Steel Tubes

The physical requirements for B<sub>4</sub>C encapsulated in stainless steel tubes are listed in Chapter A.2 which specifies the minimum linear B<sub>4</sub>C content of 0.70 g/cm. This minimum B<sub>4</sub>C content specification is consistent with the criticality analysis presented in Chapter A.6 using 64% credit for the <sup>10</sup>B content.

Pellets or powder representing each powder lot shall be tested per ASTM C751 [A9.14] or ASTM C750 (Type 2) [A9.15] (or equivalent). Density and diameter shall be measured to verify conformance to the specification requirements.

Deviations from the specified dimensions or density may be accepted, so long as the resulting minimum B<sub>4</sub>C mass per unit length is maintained.

#### Justification for Durability of B<sub>4</sub>C Pellets:

B<sub>4</sub>C is essentially inert and will not be attacked even by hot hydrofluoric or nitric acids [A9.10]. It is insoluble in water [A9.11], resistant to steam at temperatures of 200 to 300°C [A9.12] and has a melting point of 2450°C [A9.12]. Mechanically, B<sub>4</sub>C is extremely hard (Mohs hardness of 9.3 vs. 10 for diamond) and is used in abrasion- and wear-resistant applications and in bullet-proof tiles. It has a compressive strength of 398,000 psi. The B<sub>4</sub>C pellets are sealed within the stainless steel tube. With this configuration there is nothing that could cause the material to degrade. In the unlikely event that a pellet were to crack or break, the total mass would be confined by the steel to the same dimensions.

The irradiation-induced swelling is due to neutron capture by the <sup>10</sup>B isotope. Using data from [A9.13] and by determining the neutron absorption in the B<sub>4</sub>C (<sup>10</sup>B capture) from the shielding analyses, the swelling is determined to be negligible ~ 0.00002%. Finally, according to [A9.13], the first intergranular cracks do not start to appear until fluences are 5.5 orders of magnitude greater than those calculated for 50 year operation.

## A.9.2 Pre-Operational Testing and Maintenance Program

No change.

### A.9.2.1 Subsystems Maintenance

#### A.9.2.1.1 Inspection (Transfer Cask Only)

The following sections discuss typical subsystem maintenance requirements that are applicable to the TC systems. Detailed requirements for these systems can be found in their associated SARs.

##### A.9.2.1.1.1 Routine Inspection

No change.

##### A.9.2.1.1.2 Annual Inspection

No change.

##### A.9.2.1.2 Pre-Operational Tests

No change.

##### A.9.2.1.2.1 Pre-Operational Test Discussion

No change.

##### A.9.2.1.3 Repair, Replacement, and Maintenance

No change.

##### A.9.2.1.4 Maintenance of Records

No change.

##### A.9.2.1.5 Maintenance of Thermal Monitoring System

No change.

### A.9.2.2 Valves, Rupture Discs, and Gaskets on Confinement Vessel

No change.

A.9.3 Training Program

No change.

A.9.3.1 Program Description

A.9.3.1.1 Training for Operations Personnel

No change.

A.9.3.1.2 Training for Maintenance Personnel

No change.

A.9.3.1.3 Training for Health Physics Personnel

No change.

A.9.3.1.4 Training for Security Personnel

No change.

A.9.3.2 Retraining Program

No change.

A.9.3.3 Administration and Records

No change.

#### A.9.4 Supplemental Information

##### A.9.4.1 References

- [A9.1] SNT-TC-1A, "American Society for Nondestructive Testing, Personnel Qualification and Certification in Nondestructive Testing," 1984.
- [A9.2] ANSI N14.5-1997, "American National Standard for Leakage Tests on Packages for Shipment of Radioactive Materials", February 1998.
- [A9.3] ASTM E94, "Guide for Radiographic Testing", 1993.
- [A9.4] ASTM E142, "Method for Controlling Quality of Radiographic Testing", 1992.
- [A9.5] ASTM E545, "Method for Determining Image Quality in Direct Thermal Neutron Radiographic Examination", 1991.
- [A9.6] Hahn, G. J., Statistical Intervals for a Normal Population, Part I," Journal of Quality Technology, Vol. 2, No. 3, July 1970.
- [A9.7] Hahn, G. J., Statistical Intervals for a Normal Population, Part II," Journal of Quality Technology, Vol. 2, No. 4, October 1970.
- [A9.8] Owen, D. B., "A Survey of Properties and Applications of the Noncentral t-Distribution," Technometrics, Vol. 10, No. 3, August 1968.
- [A9.9] "SCR607, Factors for One-Sided Tolerance Limits and for Variables Sampling Plans," U.S. Department of Energy, Sandia Corporation, March 1963.
- [A9.10] The Merck Index, 9<sup>th</sup> edition, Merck & Co., 1976.
- [A9.11] Grant (ed.), Hackh's Chemical Dictionary, 4<sup>th</sup> edition, McGraw-Hill, 1969.
- [A9.12] Lipp, A., "Boron Carbide: Production, Properties, Application," Reprint from Technische Rundschau, Nos. 14, 28, 33 (1995) and 7 (1966).
- [A9.13] Stoto, T. et al., "Swelling and Microcracking of Boron Carbide Subjected to Fast Neutron Irradiations," Journal of Applied Physics, Vol. 68, No.7, October 1, 1990, pp. 3198-3206.
- [A9.14] ASTM C751, "Standard Specification for Nuclear-Grade Boron Carbide Pellets."
- [A9.15] ASTM C750, "Standard Specification for Nuclear-Grade Boron Carbide Powder."

## A.10 RADIATION PROTECTION

Sections of this Chapter have been identified as “No change” due to the addition of 24PT4-DSC to the Advanced NUHOMS<sup>®</sup> system. For these sections, the description or analysis presented in the corresponding sections of the FSAR for the Advanced NUHOMS<sup>®</sup> system with 24PT1-DSC is also applicable to the system with 24PT4-DSC.

### A.10.1 Ensuring that Occupational Radiation Exposures Are as Low as Reasonably Achievable (ALARA)

No change.

## A.10.2 Radiation Protection Design Features

### A.10.2.1 Advanced NUHOMS® System Design Features

The Advanced NUHOMS® System has design features which ensure a high degree of integrity for the confinement of radioactive materials and reduction of direct radiation exposures to ALARA. These features are described below:

- The 24PT4-DSCs are loaded, sealed and leak tested prior to transfer to the ISFSI.
- The fuel will not be unloaded nor will the 24PT4-DSCs be opened at the ISFSI unless the ISFSI is specifically licensed for these purposes.
- The fuel is stored in a dry inert environment inside the 24PT4-DSCs so that no radioactive liquid is available for leakage.
- The 24PT4-DSCs are sealed and tested leaktight with a helium atmosphere to prevent oxidation of the fuel. The leaktight design features are described in Chapter A.7.
- The 24PT4-DSCs are heavily shielded to reduce external dose rates. The shielding design features are discussed in Chapter A.5.
- No radioactive material will be discharged during storage since the 24PT4-DSC is designed, fabricated and tested to be leaktight.

Geometric attenuation, enhanced by air and ground dispersion, provides additional shielding for distant locations at restricted area and site boundaries. However, the contribution of the sky shine dose rate must be considered for distant locations. The total dose rate estimation, including sky shine, is provided in the following section.

### A.10.2.2 Radiation Dose Rates

Calculated dose rates in the immediate vicinity of the Advanced NUHOMS® System are presented in Chapter A.5, which provides a detailed description of source term configuration, analysis model and expected dose rates. Dose rates for longer distances (off site doses) are presented in this section for the design basis fuel load.

The Monte-Carlo computer code MCNP [A10.1] is used to calculate the dose rates at the required locations around the AHSM.

The assumptions used to generate the geometry of the AHSM and shield walls for the MCNP runs are summarized below.

- A single AHSM is modeled as a box enveloping the AHSM and 3 foot shield walls on the back and two sides. Source particles are then started on the surfaces of the box. A discussion of the source assumptions is provided below.

- The AHSM slab is modeled as a concrete slab, approximately 108 feet by 84 feet by 3 feet thick. The remaining volume below ground level is modeled as soil.
- AHSM interiors are filled with air. Most particles that enter the AHSM will therefore pass through unhindered.
- The "universe" is a sphere surrounding the AHSM. The radius of this sphere is more than 10 mean free paths (gamma) greater than that of the outermost detector.

The assumptions used to generate the AHSM surface sources for the MCNP runs are summarized below.

- The AHSM surface sources are generated using the AHSM surface dose rates calculated in Chapter A.5.
- The AHSM is assumed to be filled with a canister containing 24 design basis fuel assemblies (see Chapter A.5).

The assumptions used for the MCNP computer runs are summarized below:

- Source particles are generated on the AHSM with initial directions following a cosine distribution. Radiation fluxes outside thick shields such as the AHSM walls and roof tend to have forward peaked angular distributions that are reasonably approximated by a cosine function. Vents through shielding regions such as the AHSM vents tend to collimate particles such that a semi-isotropic assumption is not appropriate.
- Point detectors are used for all of the dose rates on the four sides of the AHSM. All detectors have been placed three feet above ground level.

Source information required by MCNP includes gamma-ray and neutron spectra for the AHSM, total gamma-ray and neutron activities for each AHSM face and total gamma-ray and neutron activities for the entire AHSM. The neutron and gamma-ray spectra are determined using a 1-D ANISN run through the AHSM roof using the "in-core" design basis fuel source from Chapter A.5. Table A.10.2-9 provides the material and region thicknesses used in the ANISN model. The AHSM spectra as determined from ANISN are normalized to a one mrem/hour source using the flux-to-dose-factors [A10.4] in Table A.10.2-6 and Table A.10.2-7 and converted to a current by dividing by two. These normalized currents are then input in the MCNP ERG source variable.

The probability of a particle being born on a given surface is proportional to the total activity of that surface. The activity of each surface is determined by multiplying the sum of the normalized group currents, calculated above, by the average surface dose rate and by the area of the surface. This calculation is performed for the roof, sides and front of the AHSM. The sum of the surface activities is then input as the tally multiplier for each of the MCNP tallies to properly normalize the results to the total source strength.

Gamma-ray spectrum calculations for the AHSM are shown in Table A.10.2-6. The group fluxes on the AHSM roof are taken from the ANISN run. The dose rate contribution from each

group is the product of the flux and the flux-to-dose factor [A10.4]. The "MCNP Input Current" column of Table A.10.2-6 is simply half the roof flux in each group, divided by the total dose rate and represents the roof current normalized to one mrem per hour. The total current for a one mrem/hr average surface dose rate is then  $4.139 \times 10^2 \text{ } \gamma/\text{cm}^2 \cdot \text{s}$ . Similar calculations for neutrons are shown in Table A.10.2-7. The total neutron current for a one mrem/hr average surface dose rate is  $2.898 \times 10^1 \text{ n/cm}^2 \cdot \text{s}$ .

The AHSM modeled in MCNP is approximated by a box that envelops the individual AHSM and shield walls. The dimensions of the box also include the width of the AHSM end and back shield walls. As is discussed above, the total activity of each face of the box is calculated by multiplying the flux per mrem/hr by the average dose rate of the face and by the area of the face. The dimensions of an AHSM are:

|   |            |
|---|------------|
| AHSM Width (without End Shield Wall).....           | 101 inches |
| End Shield Wall Thickness .....                     | 36 inches  |
| AHSM Height.....                                    | 247 inches |
| Depth (Front-to-Back) (with Rear Shield Wall) ..... | 235 inches |

The source area of the front and back is,

$$\begin{aligned}
 A_{front / back} &= [(247)(101 + 2(36))](2.54)^2 \\
 &= 275,683 \text{ cm}^2
 \end{aligned}
 \tag{1}$$

The total gamma activity for the front is  $2.458 \times 10^8 \text{ } \gamma/\text{s}$  and the total neutron activity is  $1.111 \times 10^6 \text{ n/s}$ . The total gamma activity for the back is  $9.710 \times 10^6 \text{ } \gamma/\text{s}$  and the total neutron activity is  $8.389 \times 10^3 \text{ n/s}$ .

The source area of the roof is,

$$\begin{aligned}
 A_{roof} &= [(235 + 36)(101 + 2(36))](2.54)^2 \\
 &= 302,470 \text{ cm}^2
 \end{aligned}
 \tag{2}$$

The total gamma activity for the array roof is  $5.934 \times 10^7 \text{ } \gamma/\text{s}$  and the total neutron activity is  $1.368 \times 10^4 \text{ n/s}$ .

The source area of the side is,

$$\begin{aligned}
 A_{side} &= [(235 + 36)(247)](2.54)^2 \\
 &= 431,851 \text{ cm}^2
 \end{aligned}
 \tag{3}$$

The total gamma activity for each side is  $5.523 \times 10^7 \text{ } \gamma/\text{s}$  and the total neutron activity is  $1.327 \times 10^5 \text{ n/s}$ .

The AHSM surface activities are summarized in Table A.10.2-8.

24PT4-DSC dose rates were calculated for distances of 6.1 meters (20 feet) to 600 meters from a single AHSM at the front, side and back of the AHSM. The results of the single AHSM analyses (with 3-foot shield walls on sides and back of module, as described in Chapter A.1) are presented in Table A.10.2-1, Table A.10.2-2 and Table A.10.2-3. The total annual dose (direct + sky shine) as a function of distance from the surfaces of the AHSM for a single AHSM is shown in Figure A.10.2-1.

### A.10.2.3 AHSM Dose Rates

An array of 2x10 modules (back-to-back) is also considered. In this case, the rear shield walls are removed and the end shield walls are present only on the outermost modules. The dimensions for the 2x10 array are provided in the following list:

|   |            |
|---|------------|
| AHSM Width (without the End Shield Wall) .....                          | 101 inches |
| End Side Shield Wall Thickness.....                                     | 36 inches  |
| AHSM Height .....   | 247 inches |
| Depth (Front-to-Front of Back-to-Back Module) (without Rear Wall) ..... | 470 Inches |

The source area of the “front” and “front” is,

$$\begin{aligned}
 A_{front / front} &= [(247)((10)(101) + 2(36))](2.54)^2 \\
 &= 1,724,216 \text{ cm}^2
 \end{aligned}
 \tag{4}$$

Therefore, the total gamma activity for the array front is  $1.537 \times 10^9$   $\gamma/s$  and the total neutron activity is  $6.946 \times 10^6$  n/s. For the back-to-back array the total gamma and neutron activity on the front is the same on the back.

The source area of the roof is,

$$\begin{aligned}
 A_{roof} &= [(470)((101)(10) + 2(36))](2.54)^2 \\
 &= 3,280,897 \text{ cm}^2
 \end{aligned}
 \tag{5}$$

Therefore, the total gamma activity for the array roof is then  $6.436 \times 10^8$   $\gamma/s$  and the total neutron activity is  $1.483 \times 10^5$  n/s.

The source area of the side is,

$$\begin{aligned}
 A_{side} &= [(470)(247)](2.54)^2 \\
 &= 748,966 \text{ cm}^2
 \end{aligned}
 \tag{6}$$

Finally, the total gamma activity for each side is then  $9.578 \times 10^7$   $\gamma/s$  and the total neutron activity is  $2.301 \times 10^5$  n/s. The total activities for the 2x10 array are summarized in Table A.10.2-8.

Table A.10.2-4, Table A.10.2-5, and Figure A.10.2-2 provide dose rates for the 2x10 array.

For a single AHSM containing design basis fuel, a minimum distance of approximately 60 meters is necessary to meet the 10CFR 72.104 [A10.2] limit of 25 mrem per year, assuming an exposure of 8,760 hours per year from the front of the AHSM (AHSM doses are highest at the front of the AHSM due to radiation through the air inlet opening). For a 2 x 10 array without any site specific shielding, a distance of approximately 150 meters from the front and back of the AHSMs is required to ensure doses are less than the 10CFR 72.104 limits. A distance of approximately 30 meters is required to meet these limits from the side of the single AHSM. A distance of approximately 60 meters is required to meet these limits from the side of a 2 x 10 array of AHSMs.

#### A.10.2.4 ISFSI Array

The dose rates from a typical ISFSI are evaluated by the licensee in a 10CFR 72.212 evaluation to address the site-specific ISFSI layout and its time phased installation.

Dose rates at the site boundary will depend on specific ISFSI parameters such as storage array configuration, number of stored 24PT4-DSCs, characteristics of stored fuel, fuel loading patterns, site geography, etc. Berms, walls, removable shields or preferential loading of "cooler" fuel in the outer cells of the 24PT4-DSC may be used to keep the site boundary dose rate within the 10CFR 72.104 limits. Shields located within ten feet of the perimeter of the ISFSI modules or attached to the modules must be analyzed to confirm that they do not adversely impact the design basis of the AHSM. Shields attached to the AHSM must be evaluated for their potential impact on all normal, off-normal and accident scenarios to ensure that they do not introduce an unreviewed safety question as part of the site analysis performed as required by 10CFR 72.104 and 10CFR 72.212.

**Table A.10.2-1  
MCNP Front Detector Dose Rate Results for a Single AHSM**

| Distance (meters) | Gamma Dose Rate (mrem/hr) | Gamma MCNP 1 $\sigma$ error | Neutron Dose Rate (mrem/hr) | Neutron MCNP 1 $\sigma$ error | Total Dose Rate (mrem/hr) | Combined MCNP 1 $\sigma$ error |
|-------------------|---------------------------|-----------------------------|-----------------------------|-------------------------------|---------------------------|--------------------------------|
| 6.1               | 2.07E-01                  | 0.13%                       | 1.67E-02                    | 0.59%                         | 2.23E-01                  | 0.13%                          |
| 10                | 9.13E-02                  | 0.15%                       | 7.28E-03                    | 0.74%                         | 9.86E-02                  | 0.15%                          |
| 20                | 2.47E-02                  | 0.27%                       | 1.97E-03                    | 1.74%                         | 2.66E-02                  | 0.28%                          |
| 30                | 1.08E-02                  | 0.28%                       | 8.26E-04                    | 1.32%                         | 1.16E-02                  | 0.28%                          |
| 40                | 5.84E-03                  | 0.39%                       | 4.49E-04                    | 2.07%                         | 6.29E-03                  | 0.39%                          |
| 50                | 3.63E-03                  | 0.48%                       | 3.14E-04                    | 6.03%                         | 3.94E-03                  | 0.65%                          |
| 60                | 2.40E-03                  | 0.50%                       | 1.92E-04                    | 5.47%                         | 2.59E-03                  | 0.62%                          |
| 70                | 1.69E-03                  | 0.51%                       | 1.35E-04                    | 4.57%                         | 1.83E-03                  | 0.58%                          |
| 80                | 1.25E-03                  | 0.64%                       | 9.44E-05                    | 3.08%                         | 1.35E-03                  | 0.63%                          |
| 90                | 9.66E-04                  | 1.08%                       | 7.78E-05                    | 7.18%                         | 1.04E-03                  | 1.13%                          |
| 100               | 7.36E-04                  | 0.69%                       | 5.37E-05                    | 3.93%                         | 7.90E-04                  | 0.70%                          |
| 200               | 1.26E-04                  | 3.73%                       | 9.99E-06                    | 13.90%                        | 1.36E-04                  | 3.60%                          |
| 300               | 3.25E-05                  | 1.82%                       | 2.77E-06                    | 10.86%                        | 3.53E-05                  | 1.88%                          |
| 400               | 1.26E-05                  | 6.40%                       | 1.68E-06                    | 45.77%                        | 1.43E-05                  | 7.81%                          |
| 500               | 4.70E-06                  | 3.27%                       | 5.51E-07                    | 21.84%                        | 5.25E-06                  | 3.72%                          |
| 600               | 1.93E-06                  | 2.62%                       | 1.84E-07                    | 12.37%                        | 2.11E-06                  | 2.62%                          |

| Distance (meters) | Total Dose Rate (mrem/yr) | Combined MCNP 1 $\sigma$ error |
|-------------------|---------------------------|--------------------------------|
| 6.1               | 1957                      | 0.13%                          |
| 10                | 863                       | 0.15%                          |
| 20                | 233                       | 0.28%                          |
| 30                | 102                       | 0.28%                          |
| 40                | 55                        | 0.39%                          |
| 50                | 35                        | 0.65%                          |
| 60                | 23                        | 0.62%                          |
| 70                | 16                        | 0.58%                          |
| 80                | 12                        | 0.63%                          |
| 90                | 9.1                       | 1.13%                          |
| 100               | 6.9                       | 0.70%                          |
| 200               | 1.2                       | 3.60%                          |
| 300               | 0.31                      | 1.88%                          |
| 400               | 0.12                      | 7.81%                          |
| 500               | 0.046                     | 3.72%                          |
| 600               | 0.018                     | 2.62%                          |

**Table A.10.2-2  
MCNP Side Detector Dose Rate Results for a Single AHSM**

| Distance (meters) | Gamma Dose Rate (mrem/hr) | Gamma MCNP 1 $\sigma$ error | Neutron Dose Rate (mrem/hr) | Neutron MCNP 1 $\sigma$ error | Total Dose Rate (mrem/hr) | Combined MCNP 1 $\sigma$ error |
|-------------------|---------------------------|-----------------------------|-----------------------------|-------------------------------|---------------------------|--------------------------------|
| 6.1               | 4.53E-02                  | 0.14%                       | 2.48E-03                    | 0.61%                         | 4.77E-02                  | 0.14%                          |
| 10                | 2.12E-02                  | 0.20%                       | 1.24E-03                    | 0.90%                         | 2.25E-02                  | 0.20%                          |
| 20                | 6.18E-03                  | 0.34%                       | 4.14E-04                    | 2.58%                         | 6.60E-03                  | 0.36%                          |
| 30                | 2.84E-03                  | 0.48%                       | 2.16E-04                    | 2.62%                         | 3.06E-03                  | 0.48%                          |
| 40                | 1.63E-03                  | 0.84%                       | 1.28E-04                    | 2.99%                         | 1.75E-03                  | 0.81%                          |
| 50                | 1.04E-03                  | 0.84%                       | 9.30E-05                    | 16.75%                        | 1.13E-03                  | 1.58%                          |
| 60                | 7.17E-04                  | 0.72%                       | 5.55E-05                    | 2.74%                         | 7.72E-04                  | 0.70%                          |
| 70                | 5.22E-04                  | 1.04%                       | 4.32E-05                    | 4.66%                         | 5.65E-04                  | 1.02%                          |
| 80                | 3.92E-04                  | 1.67%                       | 3.26E-05                    | 3.69%                         | 4.25E-04                  | 1.57%                          |
| 90                | 3.07E-04                  | 1.13%                       | 2.51E-05                    | 4.46%                         | 3.32E-04                  | 1.10%                          |
| 100               | 2.36E-04                  | 0.95%                       | 1.98E-05                    | 5.10%                         | 2.56E-04                  | 0.96%                          |
| 200               | 4.74E-05                  | 5.75%                       | 3.81E-06                    | 5.85%                         | 5.12E-05                  | 5.34%                          |
| 300               | 1.40E-05                  | 8.54%                       | 1.41E-06                    | 14.28%                        | 1.54E-05                  | 7.87%                          |
| 400               | 4.07E-06                  | 3.99%                       | 4.20E-07                    | 3.39%                         | 4.49E-06                  | 3.63%                          |
| 500               | 1.60E-06                  | 3.87%                       | 2.77E-07                    | 14.49%                        | 1.88E-06                  | 3.93%                          |
| 600               | 9.28E-07                  | 25.79%                      | 7.38E-08                    | 4.54%                         | 1.00E-06                  | 23.89%                         |

| Distance (meters) | Total Dose Rate (mrem/yr) | Combined MCNP 1 $\sigma$ error |
|-------------------|---------------------------|--------------------------------|
| 6.1               | 418                       | 0.14%                          |
| 10                | 197                       | 0.20%                          |
| 20                | 58                        | 0.36%                          |
| 30                | 27                        | 0.48%                          |
| 40                | 15                        | 0.81%                          |
| 50                | 10                        | 1.58%                          |
| 60                | 7                         | 0.70%                          |
| 70                | 5                         | 1.02%                          |
| 80                | 4                         | 1.57%                          |
| 90                | 2.9                       | 1.10%                          |
| 100               | 2.2                       | 0.96%                          |
| 200               | 0.4                       | 5.34%                          |
| 300               | 0.14                      | 7.87%                          |
| 400               | 0.04                      | 3.63%                          |
| 500               | 0.016                     | 3.93%                          |
| 600               | 0.009                     | 23.89%                         |

**Table A.10.2-3  
MCNP Back Detector Dose Rate Results for a Single AHSM**

| Distance (meters) | Gamma Dose Rate (mrem/hr) | Gamma MCNP 1 $\sigma$ error | Neutron Dose Rate (mrem/hr) | Neutron MCNP 1 $\sigma$ error | Total Dose Rate (mrem/hr) | Combined MCNP 1 $\sigma$ error |
|-------------------|---------------------------|-----------------------------|-----------------------------|-------------------------------|---------------------------|--------------------------------|
| 6.1               | 9.76E-03                  | 0.21%                       | 5.17E-04                    | 1.87%                         | 1.03E-02                  | 0.22%                          |
| 10                | 4.74E-03                  | 0.30%                       | 3.39E-04                    | 3.16%                         | 5.08E-03                  | 0.35%                          |
| 20                | 1.58E-03                  | 0.43%                       | 1.55E-04                    | 4.03%                         | 1.74E-03                  | 0.53%                          |
| 30                | 8.07E-04                  | 0.56%                       | 8.93E-05                    | 4.85%                         | 8.96E-04                  | 0.70%                          |
| 40                | 5.12E-04                  | 1.30%                       | 6.57E-05                    | 7.23%                         | 5.78E-04                  | 1.42%                          |
| 50                | 3.47E-04                  | 1.02%                       | 4.09E-05                    | 5.96%                         | 3.88E-04                  | 1.11%                          |
| 60                | 2.54E-04                  | 1.25%                       | 3.47E-05                    | 15.93%                        | 2.89E-04                  | 2.21%                          |
| 70                | 1.92E-04                  | 1.67%                       | 2.21E-05                    | 6.55%                         | 2.14E-04                  | 1.64%                          |
| 80                | 1.52E-04                  | 1.55%                       | 1.74E-05                    | 9.59%                         | 1.70E-04                  | 1.70%                          |
| 90                | 1.21E-04                  | 1.52%                       | 1.58E-05                    | 13.45%                        | 1.36E-04                  | 2.06%                          |
| 100               | 9.54E-05                  | 1.57%                       | 1.00E-05                    | 4.40%                         | 1.05E-04                  | 1.48%                          |
| 200               | 1.77E-05                  | 2.11%                       | 3.53E-06                    | 38.62%                        | 2.12E-05                  | 6.67%                          |
| 300               | 5.52E-06                  | 9.95%                       | 8.00E-07                    | 12.11%                        | 6.32E-06                  | 8.82%                          |
| 400               | 1.72E-06                  | 4.98%                       | 2.41E-07                    | 4.91%                         | 1.96E-06                  | 4.41%                          |
| 500               | 5.70E-07                  | 2.85%                       | 1.19E-07                    | 10.12%                        | 6.89E-07                  | 2.93%                          |
| 600               | 2.53E-07                  | 8.10%                       | 3.93E-08                    | 5.69%                         | 2.92E-07                  | 7.05%                          |

| Distance (meters) | Total Dose Rate (mrem/yr) | Combined MCNP 1 $\sigma$ error |
|-------------------|---------------------------|--------------------------------|
| 6.1               | 90.3                      | 0.22%                          |
| 10                | 44.5                      | 0.35%                          |
| 20                | 15.3                      | 0.53%                          |
| 30                | 7.85                      | 0.70%                          |
| 40                | 5.07                      | 1.42%                          |
| 50                | 3.40                      | 1.11%                          |
| 60                | 2.53                      | 2.21%                          |
| 70                | 1.88                      | 1.64%                          |
| 80                | 1.49                      | 1.70%                          |
| 90                | 1.19                      | 2.06%                          |
| 100               | 0.92                      | 1.48%                          |
| 200               | 0.19                      | 6.67%                          |
| 300               | 5.54E-02                  | 8.82%                          |
| 400               | 1.72E-02                  | 4.41%                          |
| 500               | 6.04E-03                  | 2.93%                          |
| 600               | 2.56E-03                  | 7.05%                          |

**Table A.10.2-4  
MCNP Front Detector Dose Rate Results for a 2x10 ISFSI**

| Distance (meters) | Gamma Dose Rate (mrem/hr) | Gamma MCNP 1 $\sigma$ error | Neutron Dose Rate (mrem/hr) | Neutron MCNP 1 $\sigma$ error | Total Dose Rate (mrem/hr) | Combined MCNP 1 $\sigma$ error |
|-------------------|---------------------------|-----------------------------|-----------------------------|-------------------------------|---------------------------|--------------------------------|
| 6.1               | 5.95E-01                  | 0.16%                       | 4.95E-02                    | 0.52%                         | 6.44E-01                  | 0.15%                          |
| 10                | 3.55E-01                  | 0.21%                       | 2.88E-02                    | 0.62%                         | 3.84E-01                  | 0.20%                          |
| 20                | 1.29E-01                  | 0.26%                       | 1.03E-02                    | 0.89%                         | 1.39E-01                  | 0.25%                          |
| 30                | 6.16E-02                  | 0.38%                       | 4.93E-03                    | 1.03%                         | 6.66E-02                  | 0.36%                          |
| 40                | 3.53E-02                  | 0.76%                       | 2.88E-03                    | 1.82%                         | 3.82E-02                  | 0.72%                          |
| 50                | 2.21E-02                  | 0.57%                       | 1.83E-03                    | 2.78%                         | 2.40E-02                  | 0.57%                          |
| 60                | 1.50E-02                  | 0.58%                       | 1.21E-03                    | 2.12%                         | 1.62E-02                  | 0.56%                          |
| 70                | 1.08E-02                  | 1.54%                       | 8.91E-04                    | 2.43%                         | 1.17E-02                  | 1.43%                          |
| 80                | 7.91E-03                  | 0.74%                       | 6.38E-04                    | 2.60%                         | 8.55E-03                  | 0.71%                          |
| 90                | 5.97E-03                  | 0.63%                       | 4.73E-04                    | 2.48%                         | 6.45E-03                  | 0.61%                          |
| 100               | 4.68E-03                  | 0.78%                       | 3.91E-04                    | 3.14%                         | 5.07E-03                  | 0.76%                          |
| 200               | 7.67E-04                  | 1.50%                       | 8.90E-05                    | 20.55%                        | 8.56E-04                  | 2.52%                          |
| 300               | 2.11E-04                  | 2.80%                       | 2.14E-05                    | 9.58%                         | 2.32E-04                  | 2.69%                          |
| 400               | 8.54E-05                  | 19.13%                      | 8.21E-06                    | 10.23%                        | 9.36E-05                  | 17.48%                         |
| 500               | 2.73E-05                  | 1.73%                       | 3.23E-06                    | 10.58%                        | 3.06E-05                  | 1.91%                          |
| 600               | 1.21E-05                  | 2.17%                       | 1.69E-06                    | 17.57%                        | 1.38E-05                  | 2.87%                          |

| Distance (meters) | Total Dose Rate (mrem/yr) | Combined MCNP 1 $\sigma$ error |
|-------------------|---------------------------|--------------------------------|
| 6.1               | 5644                      | 0.15%                          |
| 10                | 3362                      | 0.20%                          |
| 20                | 1221                      | 0.25%                          |
| 30                | 583                       | 0.36%                          |
| 40                | 335                       | 0.72%                          |
| 50                | 210                       | 0.57%                          |
| 60                | 142                       | 0.56%                          |
| 70                | 103                       | 1.43%                          |
| 80                | 75                        | 0.71%                          |
| 90                | 56                        | 0.61%                          |
| 100               | 44                        | 0.76%                          |
| 200               | 7.5                       | 2.52%                          |
| 300               | 2.0                       | 2.69%                          |
| 400               | 0.82                      | 17.48%                         |
| 500               | 0.27                      | 1.91%                          |
| 600               | 0.12                      | 2.87%                          |

**Table A.10.2-5  
MCNP Side Detector Dose Rate Results for a 2x10 ISFSI**

| Distance (meters) | Gamma Dose Rate (mrem/hr) | Gamma MCNP 1 $\sigma$ error | Neutron Dose Rate (mrem/hr) | Neutron MCNP 1 $\sigma$ error | Total Dose Rate (mrem/hr) | Combined MCNP 1 $\sigma$ error |
|-------------------|---------------------------|-----------------------------|-----------------------------|-------------------------------|---------------------------|--------------------------------|
| 6.1               | 7.26E-02                  | 0.22%                       | 5.56E-03                    | 1.36%                         | 7.81E-02                  | 0.23%                          |
| 10                | 3.94E-02                  | 0.34%                       | 3.54E-03                    | 2.12%                         | 4.29E-02                  | 0.36%                          |
| 20                | 1.41E-02                  | 0.37%                       | 1.73E-03                    | 4.39%                         | 1.58E-02                  | 0.58%                          |
| 30                | 7.55E-03                  | 0.58%                       | 1.02E-03                    | 3.80%                         | 8.57E-03                  | 0.68%                          |
| 40                | 4.83E-03                  | 0.70%                       | 6.77E-04                    | 2.91%                         | 5.50E-03                  | 0.71%                          |
| 50                | 3.38E-03                  | 0.81%                       | 4.89E-04                    | 5.22%                         | 3.87E-03                  | 0.97%                          |
| 60                | 2.52E-03                  | 1.18%                       | 3.60E-04                    | 3.58%                         | 2.88E-03                  | 1.13%                          |
| 70                | 1.94E-03                  | 1.22%                       | 2.75E-04                    | 3.64%                         | 2.21E-03                  | 1.16%                          |
| 80                | 1.54E-03                  | 1.06%                       | 2.38E-04                    | 9.88%                         | 1.78E-03                  | 1.61%                          |
| 90                | 1.28E-03                  | 1.44%                       | 1.92E-04                    | 5.82%                         | 1.47E-03                  | 1.46%                          |
| 100               | 1.04E-03                  | 1.61%                       | 1.61E-04                    | 8.20%                         | 1.20E-03                  | 1.78%                          |
| 200               | 2.12E-04                  | 1.71%                       | 2.96E-05                    | 4.94%                         | 2.42E-04                  | 1.62%                          |
| 300               | 6.43E-05                  | 5.23%                       | 1.28E-05                    | 28.81%                        | 7.70E-05                  | 6.47%                          |
| 400               | 2.40E-05                  | 6.12%                       | 4.31E-06                    | 18.24%                        | 2.83E-05                  | 5.89%                          |
| 500               | 7.70E-06                  | 3.19%                       | 1.78E-06                    | 11.38%                        | 9.48E-06                  | 3.36%                          |
| 600               | 3.41E-06                  | 9.46%                       | 7.01E-07                    | 4.60%                         | 4.11E-06                  | 7.88%                          |

| Distance (meters) | Total Dose Rate (mrem/yr) | Combined MCNP 1 $\sigma$ error |
|-------------------|---------------------------|--------------------------------|
| 6.1               | 684                       | 0.23%                          |
| 10                | 376                       | 0.36%                          |
| 20                | 139                       | 0.58%                          |
| 30                | 75                        | 0.68%                          |
| 40                | 48                        | 0.71%                          |
| 50                | 34                        | 0.97%                          |
| 60                | 25                        | 1.13%                          |
| 70                | 19                        | 1.16%                          |
| 80                | 15.6                      | 1.61%                          |
| 90                | 12.9                      | 1.46%                          |
| 100               | 10.5                      | 1.78%                          |
| 200               | 2.1                       | 1.62%                          |
| 300               | 0.67                      | 6.47%                          |
| 400               | 0.25                      | 5.89%                          |
| 500               | 0.083                     | 3.36%                          |
| 600               | 0.036                     | 7.88%                          |

**Table A.10.2-6  
AHSM Gamma-Ray Spectrum Calculation Results**

| CASK-81 Group Number | E <sub>upper</sub> (MeV) | E <sub>mean</sub> (MeV) | Flux-Dose ANSI/ANS-6.1.1-1977 (mrem/hr)/(γ/cm <sup>2</sup> -sec) | Roof Flux (γ/cm <sup>2</sup> -sec) | Dose Rate (mrem/hr) | MCNP Input Current (γ/cm <sup>2</sup> -sec per mrem/hr) |
|----------------------|--------------------------|-------------------------|--|------------------------------------|---------------------|---|
| 23                   | 10                       | 9                       | 8.772E-03  | 1.23E-02                           | 1.08E-04            | 7.824E-02   |
| 24                   | 8                        | 7.25                    | 7.479E-03  | 6.65E-02                           | 4.97E-04            | 4.244E-01   |
| 25                   | 6.5                      | 5.75                    | 6.375E-03  | 1.01E-01                           | 6.42E-04            | 6.424E-01   |
| 26                   | 5                        | 4.5                     | 5.414E-03  | 1.01E-01                           | 5.48E-04            | 6.454E-01   |
| 27                   | 4                        | 3.5                     | 4.622E-03  | 2.56E-01                           | 1.18E-03            | 1.635E+00   |
| 28                   | 3                        | 2.75                    | 3.960E-03  | 3.12E-01                           | 1.24E-03            | 1.992E+00   |
| 29                   | 2.5                      | 2.25                    | 3.469E-03  | 1.95E+00                           | 6.78E-03            | 1.247E+01   |
| 30                   | 2                        | 1.83                    | 3.019E-03  | 1.69E+00                           | 5.10E-03            | 1.077E+01   |
| 31                   | 1.66                     | 1.495                   | 2.628E-03  | 3.18E+00                           | 8.37E-03            | 2.031E+01   |
| 32                   | 1.33                     | 1.165                   | 2.205E-03  | 5.06E+00                           | 1.12E-02            | 3.230E+01   |
| 33                   | 1                        | 0.9                     | 1.833E-03  | 4.21E+00                           | 7.71E-03            | 2.683E+01   |
| 34                   | 0.8                      | 0.7                     | 1.523E-03  | 5.68E+00                           | 8.65E-03            | 3.625E+01   |
| 35                   | 0.6                      | 0.5                     | 1.173E-03  | 8.23E+00                           | 9.65E-03            | 5.252E+01   |
| 36                   | 0.4                      | 0.35                    | 8.759E-04  | 5.33E+00                           | 4.67E-03            | 3.403E+01   |
| 37                   | 0.3                      | 0.25                    | 6.306E-04  | 7.09E+00                           | 4.47E-03            | 4.526E+01   |
| 38                   | 0.2                      | 0.15                    | 3.834E-04  | 1.56E+01                           | 5.97E-03            | 9.928E+01   |
| 39                   | 0.1                      | 0.08                    | 2.669E-04  | 5.99E+00                           | 1.60E-03            | 3.823E+01   |
| 40                   | 0.05                     | 0.03                    | 9.348E-04  | 3.29E-02                           | 3.07E-05            | 2.096E-01   |
|                      |                          |                         | Totals   | 6.49E+01                           | 7.84E-02            | 4.139E+02   |

**Table A.10.2-7  
AHSM Neutron Spectrum Calculations**

| CASK-81<br>Group<br>Number | $E_{upper}$<br>(MeV) | $E_{mean}$<br>(MeV) | Flux-Dose<br>ANSI/ANS-<br>6.1.1-1977<br>(mrem/hr)/<br>(n/cm <sup>2</sup> -sec) | Roof Flux<br>(n/cm <sup>2</sup> -sec) | Dose Rate<br>(mrem/hr) | MCNP Input<br>Current<br>(n/cm <sup>2</sup> -sec per<br>mrem/hr) |
|----------------------------|----------------------|---------------------|--|---------------------------------------|------------------------|--|
| 1                          | 1.49E+01             | 1.36E+01            | 1.945E-01  | 3.45E-07                              | 6.70E-08               | 1.794E-04  |
| 2                          | 1.22E+01             | 1.11E+01            | 1.597E-01  | 2.28E-06                              | 3.64E-07               | 1.186E-03  |
| 3                          | 1.00E+01             | 9.09E+00            | 1.471E-01  | 8.89E-06                              | 1.31E-06               | 4.630E-03  |
| 4                          | 8.18E+00             | 7.27E+00            | 1.477E-01  | 9.18E-05                              | 1.36E-05               | 4.776E-02  |
| 5                          | 6.36E+00             | 5.66E+00            | 1.534E-01  | 2.37E-04                              | 3.63E-05               | 1.231E-01  |
| 6                          | 4.96E+00             | 4.51E+00            | 1.506E-01  | 1.98E-04                              | 2.98E-05               | 1.029E-01  |
| 7                          | 4.06E+00             | 3.54E+00            | 1.389E-01  | 2.20E-04                              | 3.06E-05               | 1.147E-01  |
| 8                          | 3.01E+00             | 2.74E+00            | 1.284E-01  | 4.64E-04                              | 5.97E-05               | 2.418E-01  |
| 9                          | 2.46E+00             | 2.41E+00            | 1.253E-01  | 5.15E-04                              | 6.45E-05               | 2.678E-01  |
| 10                         | 2.35E+00             | 2.09E+00            | 1.263E-01  | 7.98E-04                              | 1.01E-04               | 4.156E-01  |
| 11                         | 1.83E+00             | 1.47E+00            | 1.289E-01  | 1.22E-03                              | 1.57E-04               | 6.358E-01  |
| 12                         | 1.11E+00             | 8.30E-01            | 1.169E-01  | 1.26E-03                              | 1.47E-04               | 6.539E-01  |
| 13                         | 5.50E-01             | 3.31E-01            | 6.521E-02  | 1.81E-03                              | 1.18E-04               | 9.437E-01  |
| 14                         | 1.11E-01             | 5.72E-02            | 9.188E-03  | 2.76E-03                              | 2.53E-05               | 1.436E+00  |
| 15                         | 3.35E-03             | 1.97E-03            | 3.713E-03  | 1.25E-03                              | 4.64E-06               | 6.501E-01  |
| 16                         | 5.83E-04             | 3.42E-04            | 4.009E-03  | 1.55E-03                              | 6.22E-06               | 8.080E-01  |
| 17                         | 1.01E-04             | 6.50E-05            | 4.295E-03  | 1.29E-03                              | 5.52E-06               | 6.689E-01  |
| 18                         | 2.90E-05             | 1.96E-05            | 4.476E-03  | 9.21E-04                              | 4.12E-06               | 4.792E-01  |
| 19                         | 1.01E-05             | 6.58E-06            | 4.567E-03  | 1.23E-03                              | 5.62E-06               | 6.402E-01  |
| 20                         | 3.06E-06             | 2.09E-06            | 4.536E-03  | 1.09E-03                              | 4.92E-06               | 5.648E-01  |
| 21                         | 1.12E-06             | 7.67E-07            | 4.370E-03  | 1.13E-03                              | 4.95E-06               | 5.898E-01  |
| 22                         | 4.14E-07             | 2.12E-07            | 3.714E-03  | 3.76E-02                              | 1.40E-04               | 1.959E+01  |
|                            |                      |                     | Totals   | 5.57E-02                              | 9.61E-04               | 2.898E+01  |

**Table A.10.2-8**  
**Summary of AHSM Surface Activities**  
**Single AHSM**

| Source | Area (cm <sup>2</sup> ) | Neutron Activity (neutrons/sec) | Gamma-Ray Activity (γ/sec) |
|--------|-------------------------|---------------------------------|----------------------------|
| Roof   | 302,470.4               | 1.368x10 <sup>4</sup>           | 5.934x10 <sup>7</sup>      |
| Front  | 275,683.3               | 1.111x10 <sup>6</sup>           | 2.458x10 <sup>8</sup>      |
| Back   | 275,683.3               | 8.389x10 <sup>3</sup>           | 9.710x10 <sup>6</sup>      |
| Side 1 | 431,850.7               | 1.327x10 <sup>5</sup>           | 5.523x10 <sup>7</sup>      |
| Side 2 | 431,850.7               | 1.327x10 <sup>5</sup>           | 5.523x10 <sup>7</sup>      |
| Total  |                         | 1.398x10 <sup>6</sup>           | 4.253x10 <sup>8</sup>      |

**2x10 Back-to-Back Array**

| Source  | Area (cm <sup>2</sup> ) | Neutron Activity (neutrons/sec) | Gamma-Ray Activity (γ/sec) |
|---------|-------------------------|---------------------------------|----------------------------|
| Roof    | 3,280,896.7             | 1.483x10 <sup>5</sup>           | 6.436x10 <sup>8</sup>      |
| Front 1 | 1,724,215.9             | 6.946x10 <sup>6</sup>           | 1.537x10 <sup>9</sup>      |
| Front 2 | 1,724,215.9             | 6.946x10 <sup>6</sup>           | 1.537x10 <sup>9</sup>      |
| Side 1  | 748,966.2               | 2.301x10 <sup>5</sup>           | 9.578x10 <sup>7</sup>      |
| Side 2  | 748,966.2               | 2.301x10 <sup>5</sup>           | 9.578x10 <sup>7</sup>      |
| Total   |                         | 1.450x10 <sup>7</sup>           | 3.909x10 <sup>9</sup>      |

**Table A.10.2-9**  
**ANISN Model Details**

| Region                     | Material        | Outer Radius (cm) | Thickness (cm) | Thickness (in)       |
|----------------------------|-----------------|-------------------|----------------|----------------------|
| Source Region              | In-Core         | 71.71             | 71.71          | 28.23                |
| Gap between fuel/basket    | Air             | 84.38             | 12.67          | 4.99                 |
| Canister Wall              | Stainless Steel | 85.33             | 0.95           | 0.37                 |
| Gap between 24PT4-DSC/AHSM | Air             | 156.58            | 71.25          | 28.05                |
| Roof                       | Concrete        | 304.80            | 148.22         | 58.35 <sup>(1)</sup> |

(1) Reduced from 5 feet to partially account for horizontal vent in roof.

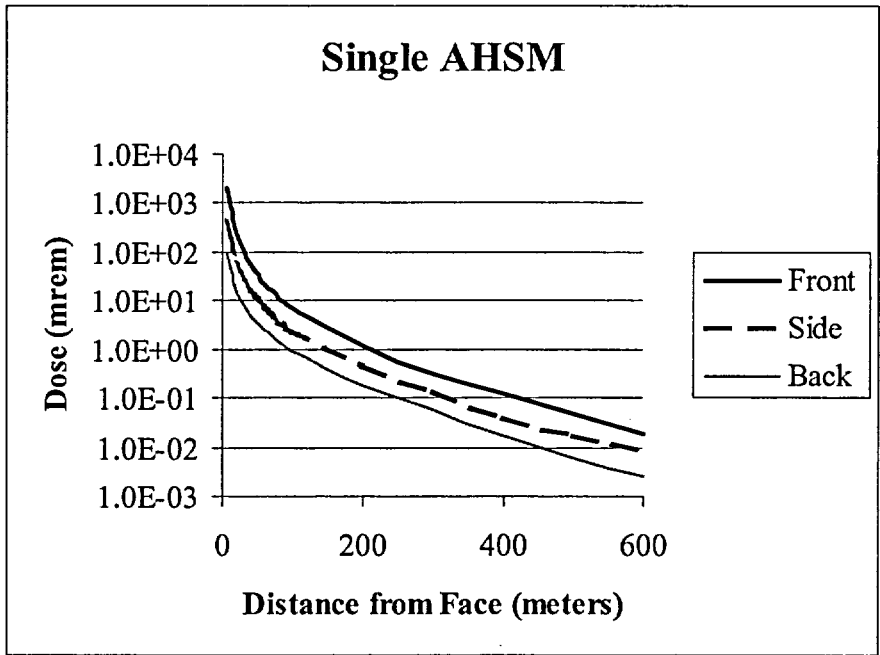


**Figure A.10.2-1**  
**Annual Exposure from a Single AHSM as a Function of Distance**

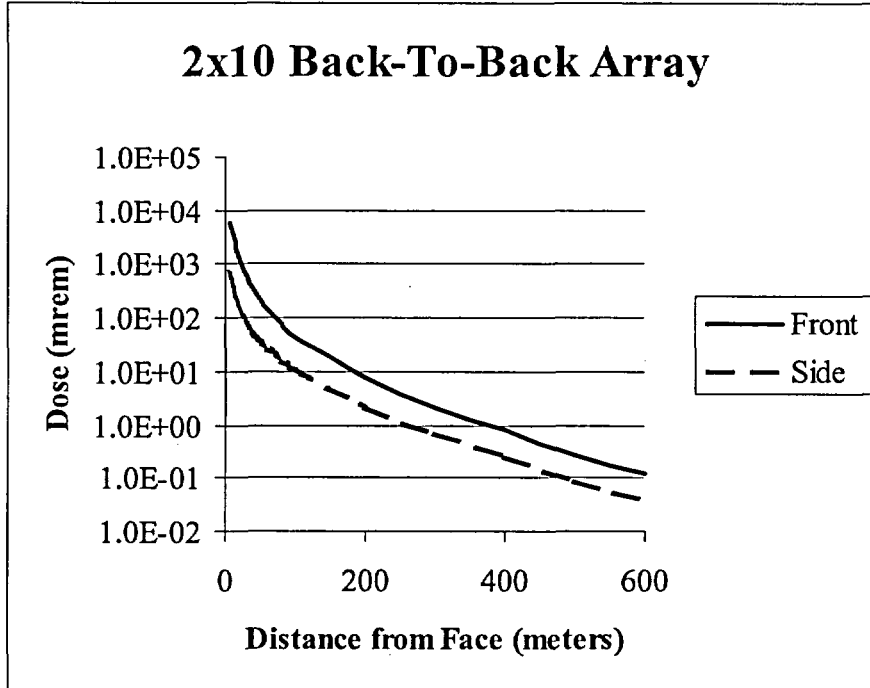


**Figure A.10.2-2**  
**Annual Exposure from a 2x10 AHSM Array as a Function of Distance**

### A.10.3 Estimated Onsite and Offsite Dose Assessment

This section provides estimates of occupational and off-site doses for typical ISFSI configurations.

Assumed annual occupancy times, including the anticipated maximum total hours per year for any individual and total person-hours per year for all personnel for each radiation area during normal operation and anticipated operational occurrences, will be evaluated by the licensee in a 10CFR 72.212 evaluation to address the site specific ISFSI layout, inspection, and maintenance requirements. In addition, the estimated annual collective person rem doses associated with loading operations will be addressed by the licensee in a 10CFR 72.212 evaluation.

#### A.10.3.1 Occupational Exposures

##### A.10.3.1.1 24PT4-DSC Loading, Transfer and Storage Operations

Table A.10.3-1 shows the estimated occupational exposures to ISFSI personnel during loading, transfer, and storage of the 24PT4-DSC (time and manpower may vary depending on individual ISFSI practices). The assumed task times and number of personnel required, and total resultant doses are listed in this table. These estimates are based on actual NUHOMS<sup>®</sup> System operating experience. Temporary shielding can be used by the licensee to maintain doses ALARA.

Licensees may elect to use different equipment and/or different procedures than assumed in the evaluation. Unique steps are sometimes necessary at the individual site to load the canister, complete closure operations and place the canister in the AHSM. Specifically, the licensee may choose to modify the sequence of operations in order to achieve reduced dose rates for a larger number of steps, with the end result of reduced total exposure. The only requirement is that the licensee practice ALARA with respect to the total exposure received for a loading campaign. These estimated durations, person-loading and dose rates are not limits.

The average distance for a given operation takes into account that the operator may be in contact with the transfer cask, but this duration will be limited. For draining activities, vacuum drying, and leak testing, the attachment of fittings will take place closer to the cask than the operation of the pump and vacuum drying system. For decontamination activities, although operators could be near the cask for some activities, other parts of the operation could be performed from farther away. For this reason, 1 foot or 3 feet is an appropriate average distance for these operations.

The operator's hands may be in a high dose rate location momentarily, for example when connecting couplings or vacuum fittings at the ports. This does not translate into a whole-body dose, and therefore, these localized streaming effects are not considered here.

For operations near the top end of the 24PT4-DSC, most of the work will take place around the perimeter (top edge of 24PT4-DSC/Transfer cask) and a smaller portion will take place directly over the shield plug.

The areas of highest operational dose (potential streaming paths) are the front of a loaded AHSM at the air inlet vent, at the cask side surface with a dry 24PT4-DSC (outer cover plate welding, transfer operations) and at the cask/DSC annulus. Operating procedures and personnel training minimize personnel exposure in these areas. The guidance of Reg. Guide 8.34 [A10.3] is to be employed in defining the on-site occupational dose and monitoring requirements.

#### A.10.3.1.2 24PT4-DSC Retrieval Operations

Occupational exposures to ISFSI personnel during 24PT4-DSC retrieval are similar to those exposures calculated for 24PT4-DSC insertion. Dose rates for retrieval operations will be lower than those for insertion operations due to radioactive decay of the spent fuel inside the AHSM. Therefore, the dose rates for 24PT4-DSC retrieval are bounded by the dose rates calculated for insertion.

#### A.10.3.1.3 24PT4-DSC Fuel Unloading Operations

The process of unloading the 24PT4-DSC is similar to that used for loading the 24PT4-DSC. The identical ALARA procedures utilized for loading should also be applied to unloading.

Occupational exposures to plant personnel are bounded by those exposures calculated for 24PT4-DSC loading.

#### A.10.3.1.4 Maintenance Operations

The dose rate for surveillance activities is obtained from Table A.10.2-1, Table A.10.2-2 and Table A.10.2-3 for AHSM 20 foot dose rates at the front of an AHSM. The 20 foot dose rate is a conservative estimate for surveillance activities. The AHSM surface dose rate provided in Chapter A.5 is a conservative estimate for thermocouple maintenance activities including calibration and repair. The surface dose rate calculated in Chapter A.5 also provides a conservative estimate of a dose rate at 3 feet from the AHSM which may be encountered during operations associated with removal of debris from AHSM vents.

The ISFSI licensee will evaluate the additional dose to station personnel from ISFSI operations, based on the particular storage configuration and site personnel requirements.

#### A.10.3.1.5 Doses During ISFSI Array Expansion

ISFSI expansion should be planned to eliminate the need for entry into a module adjacent to a loaded module. The reduction in shielding between the side of an array with an installed shield wall (4-feet of concrete, consisting of 1-foot end wall and 3-foot shield wall) versus shielding between the inside of an empty module and an adjacent loaded module (2-feet of concrete) is very significant. Pre-planning to limit entry into a module when it is not separated from a loaded module by at least one empty module (4-feet of concrete) is recommended. Similarly, during array expansion, when the shield wall is removed, personnel access to the area should be controlled. For a module separated from a loaded AHSM by an empty module, the resulting dose will be less than that specified for the side dose rate of an array with an installed shield wall. See Chapter A.5 for estimated AHSM side dose rates for this operation.

### A.10.3.2 Public Exposure

The only off-site dose to the public from the ISFSI is from direct and skyshine radiation at or beyond the controlled area of the ISFSI (as defined by 10CFR 72.106). Figure A.10.2-1 and Table A.10.2-1, Table A.10.2-2 and Table A.10.2-3 show the radiation dose rates in the vicinity of a single AHSM. Dose rates in the vicinity of a 2 x 10 array are provided in Figure A.10.2-2 and Table A.10.2-4 and Table A.10.2-5. The collective off-site dose is a function of the number and arrangement of the AHSMs on the ISFSI, the proximity of the ISFSI to the site boundary and other plant considerations to be addressed by the licensee in accordance with 10CFR 72.212.

Each cask user or general licensee must perform a site-specific analysis as required by 10CFR 72.212(b) to demonstrate compliance with 10CFR 72.104(a) for normal operations and anticipated occurrences. The general licensee may consider site-specific conditions, such as actual distances to the nearest real person, topography, array configurations, characteristics of stored fuel, and use of engineered features, such as berms, walls or additional shield blocks, in their analysis of public doses. The site-specific analysis must also include the doses received from other fuel cycle activities (e.g., reactor operations) in the region.

**Table A.10.3-1**  
**Advanced NUHOMS® System Operations Estimated Time for Occupational Dose**  
**Calculations**

(for information only)

|   | Number of Workers | Completion Time (hours) | Dose (Person-mrem) |
|---|-------------------|-------------------------|--------------------|
| <b>LOCATION: AUXILIARY BUILDING AND FUEL POOL</b>   |                   |                         |                    |
| Prepare the 24PT4-DSC and transfer cask for service   | 2                 | 4.0                     | 0                  |
| Place the 24PT4-DSC into the transfer cask  | 3                 | 1.0                     | 6                  |
| Fill the Cask/24PT4-DSC annulus with uncontaminated water and seal                                | 2                 | 2.0                     | 8                  |
| Fill the 24PT4-DSC cavity with borated water  | 1                 | 0.5                     | 1                  |
| Place the cask containing the 24PT4-DSC in the fuel pool  | 5                 | 1.0                     | 10                 |
| Verify and load the candidate fuel assemblies into the 24PT4-DSC (including failed fuel can lids) | 3                 | 8.0                     | 48                 |
| Place the top shield plug assembly on the 24PT4-DSC and place the cask/DSC in the decon area      | 5                 | 2.0                     | 20                 |
| <b>LOCATION: CASK DECON AREA</b>  |                   |                         |                    |
| Decontaminate the outer surface of the cask   | 7                 | 1.0                     | 712                |
| Drain water above shield plug   | 3                 | 0.3                     | 76                 |
| Set-up welding machine  | 2                 | 3.3                     | 155                |
| Weld the top shield plug assembly to the shell and perform NDE (PT)                               | 3                 | 6                       | 152                |
| Prepare VDS for removal of water from the 24PT4-DSC cavity  | 1                 | 0.02                    | 3                  |
| Operate the VDS and remove water  | 1                 | 0.5                     | 1                  |
| Vacuum dry and backfill the 24PT4-DSC with helium   | 2                 | 2.0                     | 8                  |
| Seal weld the pre-fabricated plugs to the vent and siphon port and perform NDE (PT)               | 2                 | 1.5                     | 579                |
| Prelim. helium leak test the top shield plug assembly weld  | 2                 | 1.0                     | 4                  |
| Fit-up the outer top cover plate  | 2                 | 2                       | 502                |
| Weld the outer top cover plate to the shell and perform NDE (PT)                                  | 7                 | 17.5                    | 364                |

**Table A.10.3-1**  
**Advanced NUHOMS® System Operations Estimated Time for Occupational Dose**  
**Calculations**

(for information only)

(concluded)

|  | Number of Workers | Completion Time (hours) | Dose (Person-mrem) |
|--|-------------------|-------------------------|--------------------|
| <b>LOCATION: REACTOR /FUEL BUILDING BAY</b>                          |                   |                         |                    |
| Helium leak test the inner top cover plate weld                      | 2                 | 1.0                     | 4                  |
| Weld helium leak test vent port plug and NDE weld                    | 2                 | 0.75                    | 290                |
| Drain the cask/24PT4-DSC annulus                                     | 2                 | 0.25                    | 24                 |
| Install the transfer cask top cover plate                            | 2                 | 1.0                     | 95                 |
| <b>LOCATION: REACTOR /FUEL BUILDING BAY</b>                          |                   |                         |                    |
| Place the cask onto the skid and trailer                             | 2                 | 0.5                     | 332                |
| Secure the cask to the skid  | 2                 | 0.25                    | 281                |
| <b>LOCATION: ISFSI SITE</b>  |                   |                         |                    |
| Remove the cask top cover plate                                      | 2                 | 0.5                     | 24                 |
| Align and dock the cask with the AHSM                                | 4                 | 0.5                     | 196                |
| Insert 24PT4-DSC into AHSM   | 4                 | 0.5                     | 153                |
| Lift the ram back onto the trailer and undock the cask from the AHSM | 2                 | 0.25                    | 23                 |
| Install the AHSM door  | 2                 | 0.5                     | 2                  |
| Adjust 24PT4-DSC seismic restraint                                   | 6                 | 1.08                    | 197                |
| <b>TOTAL</b>   | <b>N/A</b>        | <b>60.7</b>             | <b>4270</b>        |

## A.10.4 Supplemental Information

### A.10.4.1 References

- [A10.1] MCNP 4C2- Monte Carlo N-Particle Transport Code System”, CCC-701, Oak Ridge National Laboratory, RSICC Computer Code Collection, June 2001.
- [A10.2] Title 10 Code of Federal Regulations Part 72, Licensing Requirements for the Independent Storage of Spent Nuclear Fuel and High-Level Radioactive Waste.
- [A10.3] U.S. Nuclear Regulatory Commission, Regulatory Guide 8.34, Monitoring Criteria and Methods to Calculate Occupational Radiation Doses, July 1992.
- [A10.4] American Nuclear Society, “American National Standard Neutron and Gamma-Ray Flux-to-Dose Rate Factors”. ANSI/ANS-6.1.1-1977, American Nuclear Society, La Grange Park, Illinois, March 1977.

## A.11 ACCIDENT ANALYSES

Sections of this Chapter have been identified as “No change” due to the addition of 24PT4-DSC to the Advanced NUHOMS<sup>®</sup> system. For these sections, the description or analysis presented in the corresponding sections of the FSAR for the Advanced NUHOMS<sup>®</sup> system with 24PT1-DSC is also applicable to the system with 24PT4-DSC.

This Chapter describes the postulated off-normal and accident events that might occur during storage of the 24PT4-DSC in an AHSM at an ISFSI. In addition, this Chapter also addresses the potential causes of these events, their detection and consequences, and the corrective course of action to be taken by ISFSI personnel. Accident analyses demonstrate that the functional integrity of the system is maintained by:

1. Maintaining sub-criticality within margins defined in Chapter A.6
2. Maintaining confinement boundary integrity
3. Ensuring fuel retrievability and
4. Maintaining doses within 10CFR 72.106 limits (<5 rem).

The Accident Dose Calculations sections report the expected doses resulting from the postulated event in terms of whole body doses only. The leaktight canister design and the maintenance of confinement boundary integrity under all credible off-normal and accident scenarios ensures no radiation leakage from the 24PT4-DSC, thereby limiting dose consequences to direct and scattered radiation doses without any associated inhalation or ingestion doses.

### A.11.1 Off-Normal Operations

Off-normal operations are design events of the second type (Design Event II) as defined in ANSI/ANS 57.9 [A.11.1]. Design Event II conditions consist of that set of events that, although not occurring regularly, can be expected to occur with moderate frequency, or on the order of once during a calendar year of ISFSI operation.

For the Advanced NUHOMS<sup>®</sup> System, off-normal events could occur during fuel loading, trailer towing, 24PT4-DSC transfer and other operational events. The two off-normal events, which bound the range of off-normal conditions, are:

1. A “jammed” 24PT4-DSC during loading or unloading from the AHSM
2. The extreme ambient temperatures of -40°F (winter) and +117°F (summer)

These two events envelope the range of expected off-normal structural loads and temperatures acting on the Advanced NUHOMS<sup>®</sup> System.

#### A.11.1.1 Off-Normal Transfer Loads

No change.

#### A.11.1.2 Extreme Ambient Temperatures

No change.

##### A.11.1.2.1 Postulated Cause of the Event

No change.

##### A.11.1.2.2 Detection of Event

No change.

##### A.11.1.2.3 Analysis of Effects and Consequences

Thermal analysis of the Advanced NUHOMS<sup>®</sup> System with the 24PT4-DSC and CE 16x16 fuel for extreme ambient conditions is presented in Chapter A.4. The effects of extreme ambient temperatures on the 24PT4-DSC system are discussed in Chapter A.3.

##### A.11.1.2.4 Corrective Actions

Install transfer cask solar shield on the OS197H transfer cask if the ambient temperature exceeds 100°F as required in the Technical Specifications. As shown in the analyses described in Chapters A.3 and A.4, the extreme ambient temperatures analyzed do not adversely impact operation of the Advanced NUHOMS<sup>®</sup> System.

A.11.1.3 Radiological Impact from Off-Normal Operations

No change.

## A.11.2 Postulated Accidents

The discussion in Section 11.2 for the 24PT1-DSC applies to 24PT4-DSC. References to Chapter 3 sections and tables apply to the corresponding section/tables presented/referenced in Chapter A.3, as appropriate.

### A.11.2.1 Earthquake

The discussion in Section 11.2.1 for the 24PT1-DSC is applicable to the 24PT4-DSC. The LS-DYNA AHSM non-linear seismic stability analyses and analyses results presented in Section 11.2.1.2.1 for the 24PT1-DSC loaded inside the AHSM, are applicable to the 24PT4-DSC. The LS-DYNA models used for the stability/sliding analyses are based on a total model weight of 1,601 kips. This total weight represents a model consisting of 3 AHSMs, each loaded with a 24PT1-DSC that weights approximately 82,000 lbs. The 24PT4-DSC weighs approximately 85,000 lbs. This weight difference represents a weight increase in the LS-DYNA model of less than 1.0%  $((1,601+(3*3))/1,601)$ . This weight difference is considered to have a negligible effect on the sliding and rocking response estimates reported in Section 11.2.1.2.1. Therefore, the results reported in Section 11.2.1.2.1 apply to AHSMs loaded with 24PT4-DSCs.

The seismic stress evaluations for the AHSM presented in Sections 3.6 and 11.2.1 for the 24PT1-DSC are based on a conservative bounding weight of 85,000 lbs. Thus, the analyses results presented in those sections of the SAR are applicable to the AHSM loaded with a 24PT4-DSC.

### A.11.2.2 Tornado Wind Pressure and Tornado Missiles

The discussion in Section 11.2.2 for the 24PT1-DSC is applicable to the 24PT4-DSC. The AHSM overturning, sliding, and missile impact evaluations presented in Sections 11.2.2.2.1 and 11.2.2.2.2 are bounding for the 24PT4-DSC because the stabilizing moment against overturning and the force required to slide the AHSM are based on the slightly lower weight of the 24PT1-DSC.

### A.11.2.3 Flood

The discussion in Section 11.2.3 for the 24PT1-DSC is applicable to the 24PT4-DSC. Analyses results for the 24PT4-DSC are presented in Chapter A.3. The AHSM overturning and sliding, evaluations presented in Sections 11.2.3.2.1.1 and 11.2.3.2.2 are bounding for the 24PT4-DSC because the stabilizing moment against overturning and the force required to slide the AHSM are based on the on the slightly lower weight of the 24PT1-DSC.

The analyses results for the 24PT4-DSC due to flooding pressure are presented in Chapter A.3.

### A.11.2.4 Fire/Explosion

The discussion in Section 11.2.4 for the 24PT1-DSC is applicable to the 24PT4 –DSC, with the exception that a specific evaluation of the hypothetical fire event has been performed for the 24PT4-DSC and the results are presented in Chapter A.4.

### A.11.2.5 Accidental Drop of the 24PT4-DSC Inside the Transfer Cask

#### A.11.2.5.1 Cause of Accident

This section addresses the structural integrity of the 24PT4-DSC shell and internal basket assemblies when subjected to postulated cask drop accident conditions. Drops are postulated for the 24PT4-DSC when positioned inside the transfer cask and cannot occur once the 24PT4-DSC is transferred into the AHSM.

##### A.11.2.5.1.1 Cask and Transfer Operation

No change.

##### A.11.2.5.1.2 24PT1-DSC Drop Accident Scenarios

No change.

##### A.11.2.5.1.3 Transfer Cask Drop Surface Conditions

No change.

#### A.11.2.5.2 Accident Analysis

The stress analyses of the 24PT4-DSC resulting from the postulated drop scenarios are summarized in Section A.3.6.

##### A.11.2.5.3 Accident Dose Calculations

The accidental transfer cask drop scenarios do not impact the transfer cask/24PT4-DSC confinement boundary. The transfer cask lead shielding is not reduced by these drops. The transfer cask neutron shield, however, may be damaged in an accidental drop.

The following dose rates were determined using the MCNP transfer cask model described in Chapter A.5 with the neutron shield eliminated and with dose rates calculated at the applicable distances. The average dose rate at the transfer cask surface with the loss of the neutron shield is 1796 mrem/hr (862 mrem/hr gamma and 934 mrem/hr neutron). The only potential off-site dose consequences would be additional direct and air scattered radiation if the accident were to occur sufficiently close to the site boundary. It is assumed that eight hours would be required to either recover the neutron shield or to add temporary shielding while arranging recovery operations. As a result, it is estimated that on-site workers at an average distance of fifteen feet would receive an additional dose of 1.6 rem (198 mrem/hr for 8 hours).

Off-site individuals at a distance of 2000 feet would receive an additional dose of 0.18 mrem for the assumed eight hour exposure ( $2.29 \times 10^{-2}$  mrem/hr for 8 hours). Comparing to the annual dose for 600 meters from Figure A.10.2-1 (0.018 mrem, front of a single AHSM), this dose is approximately 10 times the normal annual dose. Extrapolating from Figure A.10.2-1 and assuming that this ratio is valid for other distances, the accident dose from a damaged cask is

approximately 69 mrem at 100 meters (6.9x10). This increase is well within the limits of 10CFR 72.106 for an accident condition (5000 mrem at the nearest boundary, which must be no less than 100 meters from the ISFSI). Also, this does not preclude handling operations for recovery of the transfer cask and its contents. Water bags or other neutron absorbing material could be wrapped around the transfer cask to reduce the surface dose rate to an acceptable level for recovery operations, thus minimizing exposure of personnel in the vicinity. The actual local and off-site dose rates, recovery time and operations needed to retrieve the cask, and the required actions to be performed following the event, depend upon the severity of the event, site characteristics, and the resultant cask and trailer/skid damage.

#### A.11.2.5.4 Corrective Actions

No change.

#### A.11.2.6 Lightning

No change.

#### A.11.2.7 Blockage of Air Inlet and Outlet Openings

Analyses results for the 24PT4-DSC are presented in Chapter A.3 and A.4. References to bounding Chapter 11 analyses correspond to the pertinent Chapter A.11 section.

#### A.11.2.8 Accidental Pressurization of the 24PT4-DSC

Analysis results for the 24PT4-DSC are presented in Chapter A.4.

#### A.11.2.9 Burial

No change.

References to bounding Chapter 11 analysis correspond to the pertinent Chapter A.11 section.

#### A.11.2.10 Inadvertent Loading of a Newly Discharged Fuel Assembly

##### A.11.2.10.1 Cause of Accident

The fuel assemblies to be loaded must meet the cooling time established in the fuel qualification table before the heat generation decays to a level allowing storage in the 24PT4-DSC. This accident scenario postulates the inadvertent loading of an assembly with a higher heat load or enrichment, than allowed for a particular 24PT4-DSC Zone.

In order to preclude this accident from going undetected, and to ensure that appropriate corrective actions can take place prior to the sealing of the 24PT4-DSC, a final verification of the assemblies loaded into the 24PT4-DSC and a comparison with fuel management records is required to assure that the correct assemblies are loaded.

These administrative controls and the records associated with them is included in the procedures described in Chapter A.8.

Appropriate and sufficient actions are taken to ensure than an erroneously loaded fuel assembly does not remain undetected. In particular the storage of a fuel assembly with a heat generation in excess of the specified maximum is not considered credible in view of the multiple administrative controls. There is no thermal or shielding analysis impact since the improperly loaded 24PT4-DSC will not be removed from the fuel pool due to independent review.

Although this event is not considered credible, the following evaluation is provided of the consequences of inadvertently loading spent fuel assemblies not allowed by SAR Chapter A.12.

A significant increase in dose rate due to the misloading scenario would be identified as abnormal by Health Physics surveys during the fuel loading and storage scenario.

The possibility of a spent fuel assembly, with a heat generation rate or enrichment greater than specified for a particular zone in a 24PT4-DSC loading configuration, being erroneously selected for storage in a 24PT4-DSC has been considered. The cause of this accident is postulated to be an error during the loading operations, e.g., wrong assembly picked by the fuel handling crane, or a failure in the administrative controls governing the fuel handling operations.

#### A.11.2.10.2 Accident Analysis

The worst-case consequences of a higher-than-allowed heat load for a fuel assembly would be damage to the fuel cladding and possible reduction in structural capacity of 24PT4-DSC basket components due to the elevated temperature. Such damage would not impact the 24PT4-DSC confinement/pressure boundary. By maintaining 24PT4-DSC pressure boundary integrity, the consequences of this damage will be mitigated by the lack of water in an in-service 24PT4-DSC. The lack of moderation ensures that subcriticality will be maintained after the 24PT4-DSC is sealed. During fuel loading operations, the presence of borated water, which is not credited in the criticality analysis, will compensate for the potential increase in reactivity due to fuel and/or basket damage.

The consequences of a higher-than-allowed enrichment would be an increase in reactivity which would be compensated for by the lack of moderation due to 24PT4-DSC confinement/pressure boundary integrity during storage conditions, and the presence of borated water during fuel loading conditions.

#### A.11.2.10.3 Accident Dose Calculations

A significant increase in dose rate due to the misloading scenario would be identified as abnormal by Health Physics surveys during the fuel loading and storage scenario.

#### A.11.2.10.4 Corrective Actions

If it has been determined that a fuel assembly which is outside the bounds of the design basis has been loaded, removal of the assembly or a detailed analysis of its impact must be performed.

### A.11.3 Supplemental Information

#### A.11.3.1 References

- [A.11.1] American National Standards Institute, American Nuclear Society, ANSI/ANS-57.9-1984, Design Criteria for an Independent Spent Fuel Storage Installation (Dry Storage Type), 1984.

A.12 CONDITIONS FOR CASK USE: OPERATING CONTROLS AND LIMITS OR  
TECHNICAL SPECIFICATIONS

Attachment B of this application provides the suggested changes to the Technical Specifications due to the addition of 24PT4-DSC to the Advanced NUHOMS<sup>®</sup> system.

### A.13 QUALITY ASSURANCE

No change to this section due to the addition of 24PT4-DSC to the Advanced NUHOMS® system. See Chapter 13 of the FSAR.

## A.14 DECOMMISSIONING

### A.14.1 Decommissioning Considerations

The Advanced NUHOMS<sup>®</sup> System design features include inherent ease and simplicity for decommissioning by providing easily decontaminable surfaces and isolating the external surfaces of the 24PT4-DSC from contact with the fuel pool. At the end of its service life, the 24PT4-DSC decommissioning could be performed by one of the options listed below:

- Option 1, the 24PT4-DSC, including stored spent fuel, could be shipped to either a monitored retrievable storage system (MRS) or a geological repository for final disposal, or
- Option 2, the spent fuel could be removed from the 24PT4-DSC (either at the ISFSI site or at another off site location) and shipped in an NRC approved transportation cask.

The first option requires that the Part 72 24PT4-DSC (i.e., designed for storage) be upgraded to current Part 71 regulations. An amendment to the MP197 CoC [A14.2] will be initiated to allow for transport of the 24PT4-DSC using the MP197 cask.

The first option does not require any decommissioning of the 24PT4-DSC. No residual contamination is expected to be left behind on the concrete AHSM. The AHSM, fence, and peripheral utility structures will require no decontamination or special handling after the last 24PT4-DSC is removed. The AHSM, fence, and peripheral utility structures could be demolished and recycled with normal construction techniques.

The second option would require decontamination of the 24PT4-DSC and transfer cask (if applicable). The sources of contamination in the interior of the 24PT4-DSC or transfer cask would be the primary contamination left from the spent fuel pool water; or crud, hot particles and fines from the spent fuel pins. This contamination could be removed with a high pressure water spray. If further surface decontamination of the 24PT4-DSC or transfer cask is necessary, electro-polishing or chemical etching can be used to clean the contaminated surface. After decontamination, the 24PT4-DSC and/or transfer cask could be cut up for scrap, partially scrapped, or refurbished for reuse. Any activated metal would be shipped as low level radioactive waste to a disposal facility.

A review of cask activation analyses previously performed for similar systems (TN-32 cask [A14.4] and NUHOMS<sup>®</sup> site license storage system) indicates that the levels of activation of the 24PT4-DSC, AHSM and transfer cask would be orders of magnitude below the specific activity of the isotopes listed in Tables 1 and 2 of 10CFR 61.55 [A14.3]. A detailed analysis is not considered necessary based on the significant margins determined from these analyses. A comparison of the source terms for this application to those referenced above including the activation analysis summary for the above applications is provided below:

### Comparison of Source Terms for Activation Analyses

| Source Term                    | 24PT4-DSC              | TN-32 (Metal Cask)   | NUHOMS® Site License HSM |
|--------------------------------|------------------------|----------------------|--------------------------|
| $\gamma$ ( $\gamma$ /sec/assy) | $7.501 \times 10^{15}$ | $5.3 \times 10^{15}$ | $1.53 \times 10^{15}$    |
| n (n/sec/assy)                 | $3.696 \times 10^8$    | $3.3 \times 10^8$    | $2.23 \times 10^8$       |

### TN 32 and NUHOMS® Site License HSM Activation Analysis Results

| Nuclide           | Activity Ci/m <sup>3</sup> |                      |                       |                   |
|-------------------|----------------------------|----------------------|-----------------------|-------------------|
|                   | HSM Concrete               | HSM Steel            | TN-32                 | 10CFR 61.55 Limit |
| H-3               |                            |                      | $8.3 \times 10^{-11}$ | 40                |
| C-14              |                            |                      | $2.3 \times 10^{-10}$ | 8                 |
| Co-60             | $4.4 \times 10^{-5}$       | $8.1 \times 10^{-2}$ | $7.7 \times 10^{-6}$  | 700               |
| Ni-59             | $1.4 \times 10^{-10}$      | $3.1 \times 10^{-6}$ | $2.5 \times 10^{-6}$  | 220               |
| Ni-63             | $8.3 \times 10^{-8}$       | $3.2 \times 10^{-4}$ | $3.4 \times 10^{-4}$  | 3.5               |
| Nb-94             |                            | $3.9 \times 10^{-8}$ |                       | 0.2               |
| <5 year half life | $4.6 \times 10^{-3}$       | $2.0 \times 10^{-1}$ | $2.3 \times 10^{-2}$  | 700               |

Following surface decontamination, the radiation levels in the 24PT4-DSC or transfer cask due to activation will be below the acceptable limits of Regulatory Guide 1.86 [A14.1]. The activation levels of the 24PT4-DSC or transfer cask materials will be far below the specific activity limits for both short and long lived nuclides for Class A waste. A detailed evaluation will be performed at the time of decommissioning to determine the appropriate mode of disposal, should refurbishment not be elected.

The procedure for decommissioning a 24PT4-DSC or transfer cask not being returned to service is summarized below:

- Remove fuel in accordance with the unloading procedures of Chapter A.8.
- Survey interior of 24PT4-DSC or transfer cask. Wash down the inside of the 24PT4-DSC or transfer cask. Pump out and filter contaminated water and cleaning agent. Survey interior of 24PT4-DSC or transfer cask again, decontaminate as required. It is expected that surface contamination will be minimal. If so, dispose of the 24PT4-DSC or transfer cask body as scrap metal. If unable to decontaminate to acceptable levels, the 24PT4-DSC and/or transfer cask body can be disposed of as low level radioactive waste.

- Decontaminate the top shield plug assembly and top cover plate until able to dispose of as scrap metal. If unable to achieve acceptable levels, dispose of them as low level radioactive waste.

The fuel unloading and decontamination steps for 24PT4-DSC, AHSM, or cask refurbishment are as outlined for the scrap choices, discussed above. However, the only pieces discarded are components damaged by unloading or that are considered to be difficult to decontaminate. Following a comprehensive survey to confirm continued 24PT4-DSC, AHSM or transfer cask functionality within design basis, the components will be eligible for returning to spent fuel storage service.

The volume of waste material produced incidental to ISFSI decommissioning is expected to be limited to that necessary to accomplish surface decontamination of the 24PT4-DSCs, if the spent fuel elements are removed. No chemical or mixed waste is anticipated. The licensee is responsible for the disposal of any waste generated by decontamination. Furthermore, it is estimated that the 24PT4-DSC materials will be slightly activated as a result of their long term exposure to the relatively small neutron flux emanating from the spent fuel, and that the resultant activation level will be well below the allowable limits for general release as noncontrolled material. Therefore, it is anticipated that the 24PT4-DSCs may be decommissioned from nuclear service by surface decontamination alone. This activity could be performed at the utility, or other suitable facility.

A detailed decommissioning plan will be submitted prior to the commencement of decommissioning activities. The costs of decommissioning the ISFSI are expected to represent a small and negligible fraction of the cost of decommissioning a nuclear power station.

## A.14.2 Supplemental Informational

### A.14.2.1 References

- [A14.1] Regulatory Guide 1.86, "Termination of Operating Licenses for Nuclear Reactors."
- [A14.2] Certificate of Compliance No. 9302 for the NUHOMS<sup>®</sup> MP197 Transport Packaging, Revision 0, July 2002, (US NRC Docket No. 71-9302).
- [A14.3] U.S. Nuclear Regulatory Commission, Title 10 Code of Federal Regulations, Part 61, "Licensing Requirements for Land Disposal or Radioactive Waste."
- [A14.4] Safety Analysis Report for the TN-32 Cask, Docket 72-1021, Revision 0, January 2000.